ISTANBUL TECHNICAL UNIVERSITY ★ GRADUATE SCHOOL

DEVELOPMENT OF ZEOLITE-BASED ADSORBENTS FOR DEEP DESULFURIZATION OF LIQUEFIED PETROLEUM GAS

Ph.D. THESIS

Betül BULUT

Department of Materials Science and Engineering

Materials Science and Engineering Programme

JANUARY 2023

ISTANBUL TECHNICAL UNIVERSITY ★ GRADUATE SCHOOL

DEVELOPMENT OF ZEOLITE-BASED ADSORBENTS FOR DEEP DESULFURIZATION OF LIQUEFIED PETROLEUM GAS

Ph.D. THESIS

Betül BULUT
(521132001)

Department of Materials Science and Engineering

Materials Science and Engineering Programme

Thesis Advisor: Prof. Dr. Ş. Birgül TANTEKİN-ERSOLMAZ

JANUARY 2023

İSTANBUL TEKNİK ÜNİVERSİTESİ ★ LİSANSÜSTÜ EĞİTİM ENSTİTÜSÜ

SIVILAŞTIRILMIŞ PETROL GAZININ KÜKÜRTTEN ARINDIRILMASI İÇİN ZEOLİT ESASLI ADSORBANLARIN GELİŞTİRİLMESİ

DOKTORA TEZİ

Betül BULUT
(521132001)

Malzeme Bilimi ve Mühendisliği Anabilim Dalı

Malzeme Bilimi ve Mühendisliği Programı

Tez Danışmanı: Prof. Dr. Ş. Birgül TANTEKİN-ERSOLMAZ

OCAK 2023

Betül BULUT, a Ph.D. of ITU Graduate School student ID 521132001, successfully defended the dissertation entitled "DEVELOPMENT OF ZEOLITE-BASED ADSORBENTS FOR DEEP DESULFURIZATION OF LIQUEFIED PETROLEUM GAS", which she prepared after fulfilling the requirements specified in the associated legislations, before the jury whose signatures are below.

Thesis Advisor :	**Prof. Dr. Ş. Birgül TANTEKİN ERSOLMAZ** Istanbul Technical University	.....
Jury Members :	**Prof. Dr. Hüsnü ATAKÜL** Istanbul Technical University	.....
	Prof. Dr. A. Erhan AKSOYLU Boğaziçi University	.....
	Prof. Dr. Alper UZUN Koç University	.....
	Doç. Dr. Alper SARIOĞLAN Istanbul Technical University	.....

Date of Submission : 05.12.2022
Date of Defense : 18.01.2023

To my lovely family,

FOREWORD

I would like to extend my deepest respect and thanks to my advisor Prof. Dr. Ş. Birgül TANTEKİN-ERSOLMAZ, who I have had the opportunity to work with for many years, for her patience, support, and guidance through my development. She always shared her knowledge and experience with her positive suggestions and criticisms throughout my thesis. I have learned so much about research and life at every moment that I was with her. I hope to carry her support with me to my future career.

I wish to express special gratitude to Prof. Dr. Hüsnü ATAKÜL and Prof. Dr. A. Erhan AKSOYLU for their helpful feedback on my research during our progress meetings. They contributed a lot to my development with their educational and productive guidance. I would also like to thank Prof. Dr. Mustafa ÜRGEN for supporting Raman analysis and Prof. Dr. Servet TİMUR for supporting XRF analysis, which contributed to the technical interpretation of my studies. I have to thank Cansu YILDIRIM, who is always willing to help me, for her support through my characterization analyzes.

I have to express my special thanks to AYGAZ Research and Development Center, which supported me by providing all the opportunities and possibilities for my doctoral thesis. Additionally, I thank my colleagues from AYGAZ Company for their motivation and contribution to my experimental studies by mind-expanding discussions and technical support.

Finally, I would like to express my deepest gratitude to my very precious FAMILY, who always gave me their unconditional love and support during this long journey as well as throughout my life. I would like to thank them for encouraging me grow into the woman I am today and for all privilege they have provided for me in my life.

December 2022

Betül BULUT
(Chemical Engineer)

TABLE OF CONTENTS

Page

ABBREVIATIONS

AA : Activated alumina
AC : Activated carbon
ADS : Adsorptive desulfurization
BET : Brunaeur, Emmert and Teller
BDS : Biodesulfurization
Bmim : 1-Butyl-3-methylimidazolium
BT : Benzothiophene
CFCs : Chlorofluorocarbons
COFs : Covalent organic frameworks
COS : Carbonyl sulfide
DBT : Dibenzothiophene
DESs : Deep eutectic solvents
4,6-DMDBT : 4,6-Dimethyldibenzothiophene
DMDS : Dimethyl disulfide
DMS : Dimethyl sulfide
2,5-DMT : 2,5-dimethylthiophene
DPS : Diphenyl sulphide
EDS : Extractive desulfurization
EDX : Energy dispersive x-ray
EM : Ethyl mercaptan
EPA : Environmental Protection Agency
EU : European Union
FT-IR : Fourier transform infrared
GC : Gas chromatography
GO : Graphite oxide
HDS : Hydrodesulfurization
HSAB : Hard and soft acids and bases
ICP : Inductively coupled plasma
ILs : Ionic liquids
LHSV : Liquid hourly space velocity
LPG : Liquefied petroleum gas
LPIE : Liquid phase ion-exchange
MOFs : Metal organic frameworks
3-MT : 3-methylthiophene
ODS : Oxidative desulfurization
PM : Particulate matter
SEM : Scanning electron microscopy
S-M : Sulfur-Metal
SO_x : Sulfur oxides
TP : Thiophene
WHO : World Health Organization
XRD : X-ray diffraction
XPS : X-ray photoelectron spectroscopy
XRF : X-ray fluorescence

SYMBOLS

C	**:** Intercept related to the boundary layer thickness
C_o	**:** Initial sulfur concentration
C_e	**:** Equilibrium sulfur concentration
C_S	**:** Breakthrough sulfur concentration
k_1	**:** Pseudo-first-order rate constant
k_2	**:** Pseudo-second-order rate constant
k_i	**:** Intraparticle diffusion rate constant
K_F	**:** Freundlich constant
K_L	**:** Langmuir constant
m	**:** Weight of the adsorbent
n	**:** Freundlich constant related to the intensity
q	**:** Sulfur adsorption capacity
q_e	**:** Equilibrium capacity
q_m	**:** Maximum capacity
q_t	**:** Sulfur adsorption capacity at time t
R	**:** Desulfurization efficiency
R_L	**:** Separation factor
R^2	**:** Regression coefficient
V	**:** LPG volume
V_p	**:** Purified LPG volume at the breakthrough point

LIST OF TABLES

Page

LIST OF FIGURES

Page

DEVELOPMENT OF ZEOLITE-BASED ADSORBENTS FOR DEEP DESULFURIZATION OF LIQUEFIED PETROLEUM GAS

SUMMARY

Air pollution has become one of the major problems facing humanity. A significant part of air pollution is originated from transportation sector. Organic sulfur compounds present in transportation fuels are converted to sulfur oxides (SO_x) during combustion, which cause smog, global warming, and acid rain. Also, stringent sulfur regulations imposed on fuels have been mandated worlwide. Thus, the urgent need for deep desulfurization methods, such as adsorption, is required.

Understanding the factors that affect the sulfur removal performance of adsorbents is important for both adsorbent and fuel industries. Most commercial desulfurization adsorbents are derived from zeolites due to their relatively high performance and low cost. Desulfurization adsorbents are expected to have the properties like high sulfur adsorption capacity, selectivity, thermal stability, regenerability and economical advantage. The effectiveness of zeolites to adsorb organic sulfur compounds in the fuels has been strongly influenced by the structural, textural and chemical properties of the adsorbent. On the other hand, the type of sulfur compound plays an important role in the overall capacity since different adsorption mechanisms are effective for each compound. Therefore, zeolites used in desulfurization should be developed to be suitable on a target-based seperation.

The sulfur adsorption capacity and selectivity of zeolites are continuing to be explored in depth as new materials and methods are developed. According to the investigations on adsorptive desulfurization from fuels, sulfur removal performance of zeolites can be enhanced by ion-exchange method which increases the number of active sites for adsorption. A fundamental understanding of ion-exchange process and its effects on capacity is needed to design high performance desulfurization adsorbents. Considering the difficulties associated with industrial applications, studies should be evaluated by using real fuels to model adsorption system and optimize the parameters.

In this thesis, the adsorptive removal of dimethyl disulfide (DMDS) and thiophene (TP) from real liquefied petroleum gas (LPG) over zeolites was studied. NaX and NaY type zeolites were modified using Cu^{2+}, Zn^{2+} and Cu^{2+}-Zn^{2+} ions by liquid phase ion-exchange (LPIE) method in order to improve their adsorption capacity and selectivity. The adsorbents were characterized to investigate their surface area, crystal structure, surface acidity, ion-exchange rate, and adsorption mechanism. The desulfurization performances of zeolites were tested and compared in both static and dynamic adsorption conditions. Then, the best performing adsorbent, Cu-Y, was investigated in detail to understand the effects of calcination temperature, concentration of $Cu(NO_3)_2$ solution, initial sulfur concentration, competitive adsorption between sulfur compounds and LPG flow rate. Cu-Y zeolite was characterized for its chemical

composition, crystal structure, auto-thermal reduction of copper species, surface acidity, adsorption mechanism, textural properties and surface morphology to reveal performance-structure relationships. Furthermore, the equilibrium isotherms and kinetics for both DMDS and TP adsorption over zeolites in real LPG were also investigated for the first time in the literature.

Results indicate that ion-exchange process enhances the DMDS and TP removal performance of the zeolites in the order of Cu > CuZn > Zn. Among the all prepared zeolites, Cu-Y ion-exchanged with 7 wt.% Cu^{2+} and calcined at 550 ℃ displays the highest sulfur removal capacity in both static and dynamic tests. It is clear that the calcination temperature has great influence on adsorption capacity since the auto-reduction of Cu^{2+} ions into Cu^{+} improves mainly the Lewis acid sites of the zeolites that enhance the sulfur adsorption. Mechanistic investigation shows that DMDS is attached to Cu-Y via direct sulfur-metal (S-M) interaction while both direct S-M interaction and π-complexation contributed in TP adsorption onto zeolite. According to the characterization results, textural, structural and chemical properties directly affect the adsorption performance. The adsorption of both DMDS and TP on the adsorbents appears to fit Langmuir isotherm and the pseudo-second-order kinetic models. Furthermore, Cu-Y has good thermal stability and can be reused efficiently up to 3 cycles that makes it highly beneficial and economical for deep desulfurization of LPG in industrial applications.

SIVILAŞTIRILMIŞ PETROL GAZININ KÜKÜRTTEN ARINDIRILMASI İÇİN ZEOLİT ESASLI ADSORBANLARIN GELİŞTİRİLMESİ

ÖZET

Son yıllarda hava kirliliği insanlığın karşılaştığı en ciddi sorunlardan biri haline gelmiştir. Hava kirliliğinin önemli bir kısmı ise ulaşım sektöründen kaynaklanmaktadır. Yakıtlarda bulunan organik kükürt bileşikleri, yanma sırasında kükürt oksitlere (SO_x) dönüşmekte ve bu da küresel ısınma ve asit yağmurları gibi çevresel problemlere neden olmaktadır. Ayrıca, dünya genelinde yakıtlar için katı kükürt düzenlemeleri getirilmiştir. Bu nedenle, adsorpsiyon gibi derin kükürt giderme yöntemlerine acilen ihtiyaç duyulmaktadır.

Adsorbanların kükürt giderme performansını etkileyen faktörlerin anlaşılması hem adsorban hem de yakıt endüstrileri için oldukça önemlidir. Ticari kükürt giderme adsorbanı olarak, verimleri ve nispeten düşük maliyetleri nedeniyle çoğunlukla zeolit esaslı malzemeler tercih edilmektedir. Kükürt giderme adsorbanlarının yüksek kükürt adsorpsiyon kapasitesi, seçicilik, termal kararlılık, yenilenebilirlik ve ekonomiklik gibi özelliklere sahip olması beklenmektedir. Zeolitlerin yakıtlardaki organik kükürt bileşiklerini giderme performansı; adsorbanın yapısal, dokusal ve kimyasal özelliklerinden etkilenmektedir. Diğer yandan, her bileşiğin giderilmesinde farklı adsorpsiyon mekanizmaları etkili olduğundan, kükürt bileşiğinin türü toplam kapasitenin belirlenmesinde önemli bir rol oynamaktadır. Bu nedenle kükürt gidermede kullanılan zeolitlerin hedef bazlı ayırmaya uygun olarak geliştirilmesi gerekmektedir.

Yeni malzemeler ve yöntemler geliştirildikçe zeolitlerin kükürt adsorpsiyon kapasitesi ve seçiciliği detaylıca araştırılmaktadır. Yakıtlardan adsorpsiyonla kükürt giderilmesi üzerine yapılan araştırmalara göre, zeolitlerin kükürt giderme performansı, adsorpsiyon için gerekli olan aktif bölgelerin sayısını artıran iyon değiştirme yöntemiyle iyileştirilebilmektedir. Yüksek performanslı kükürt giderme adsorbanlarının geliştirilebilmesi için, iyon değişim prosesinin ve bunun adsorpsiyon kapasitesi üzerindeki etkilerinin anlaşılması gerekmektedir. Endüstriyel ölçekli uygulamalar ile ilgili zorluklar göz önüne alındığında, adsorpsiyon sisteminin gerçek yakıt kullanarak modellenmesi ve parametrelerin optimize edilmesi önemlidir.

Bu tez çalışmasında, NaX ve NaY zeolitleri kullanılarak sıvılaştırılmış petrol gazından (LPG) dimetil disülfit (DMDS) ve tiyofen (TP) bileşiklerinin adsorpsiyonla uzaklaştırılması incelenmiştir. Zeolitler adsorpsiyon kapasitelerinin ve seçiciliklerinin iyileştirilmesi amacıyla sıvı faz iyon değişimi yöntemi ile modifiye edilmiştir. İlk kısımda, NaX ve NaY zeolitlerinin yapısına Cu^{2+}, Zn^{2+} ve Cu^{2+}-Zn^{2+} iyonlarının yüklenmesiyle Cu-X, CuZn-X, Zn-X, Cu-Y, CuZn-Y ve Zn-Y zeolitleri hazırlanmıştır. Adsorbanların kristal yapıları, yüzey alanları, yüzey asitlikleri, iyon değişim kapasiteleri ve adsorpsiyon mekanizmaları karakterize edilmiş ve kükürt giderme performansları hem statik hem de dinamik adsorpsiyon koşulları altında test edilmiştir. Statik deneylerde, orijinal ve modifiye edilmiş zeolitlerin adsorpsiyon

performansları, ticari Cu-BTC adsorbanı ile karşılaştırılmıştır. Modifiye edilmiş zeolitler kullanılarak, LPG'den DMDS ve TP giderimi için adsorpsiyon izotermleri ve kinetiği de literatürde ilk kez incelenmiştir.

İyon değişimi çalışmaları, daha düşük Si/Al oranına sahip NaX zeolitinin, iyon tipinden bağımsız olarak NaY zeolitinden daha yüksek bir iyon değişim kapasitesi sergilediğini ortaya koymuştur. Her iki zeolit de Zn^{2+} iyonuna kıyasla Cu^{2+} iyonuna karşı daha yüksek ilgiye sahiptir. Bununla birlikte, Cu^{2+}-Zn^{2+} çözeltisi ile yapılan iyon değişiminde, iyonların yarışmalı adsorpsiyonundan dolayı zeolitlerin iyon değişim kapasitesi azalmıştır. Karakterizasyon sonuçları, modifikasyon işleminin zeolitlerin kristal yapısında herhangi bir bozulmaya neden olmadığını göstermiştir, bu da iyonların zeolitlerin yapısında başarılı bir şekilde dağıldığını göstermektedir. Statik ve dinamik performans analiz sonuçlarında, modifiye edilen zeolitlerin DMDS ve TP giderme kapasitelerinin, Cu > CuZn > Zn sırasına göre arttığı görülmüştür. Hazırlanan zeolitler arasında statik ve dinamik kükürt giderme testlerinde Cu-Y en yüksek kükürt giderimi kapasitesini göstermiştir. Cu-Y zeoliti, maliyet-performans avantajıyla Cu-BTC'ye güçlü bir alternatif olduğunu kanıtlamıştır. Diğer yandan, Cu-Y zeoliti için 2.8 mg/L (5 ppm) kopma noktasında elde edilen DMDS (50.3 mg S/g) ve TP (19.4 mg S/g) adsorpsiyon kapasitelerinin orijinal NaY zeolitine kıyasla, sırasıyla %45 ve %25 daha yüksek olduğu görülmüştür.

Adsorpsiyon performansı ile zeolitlerin asidik özellikleri arasındaki ilişki, adsorbanların yüzey asidik bölgelerinin türü ve miktarı araştırılarak belirlenmiştir. Sonuçlar, bakır iyonlarının esas olarak zeolitlerin Lewis asit bölgelerini artırdığını ve bunun da kükürt adsorpsiyonunu iyileştirdiğini ortaya koymuştur. Kükürt molekülleri ve adsorban arasındaki etkileşimi incelemek için yapılan analizler, Cu-X ve Cu-Y adsorbanların DMDS bileşiğini doğrudan kükürt-metal etkileşimi ile bağladığını, TP adsorpsiyonunda ise hem doğrudan kükürt-metal etkileşimi hem de π-kompleksasyonunun rol oynadığını göstermiştir. Cu-Y zeolitinin LPG'den kükürt giderimi için umut verici bir adsorban olduğu görülmüştür ancak performansını iyileştirmek için daha detaylı çalışmalar gerekmektedir.

İkinci kısımda, bir önceki bölümde seçilmiş olan Cu-Y zeoliti üzerinde daha detaylı çalışmalar yapılmıştır. Cu-Y zeolitinin performansını iyileştirmek için modifikasyon parametrelerinin optimizasyonu, performans analizi ve adsorpsiyon mekanizması ile ilgili detaylı araştırmalar yapılmıştır. Kalsinasyon sıcaklığı, metal konsantrasyonu ve başlangıç kükürt konsantrasyonunun kükürt giderme üzerindeki etkileri statik adsorpsiyon yöntemi ile belirlenmiştir. Ayrıca, Cu-Y zeolitinin yapısında bulunan bakır iyonlarının termal indirgenmesi, DMDS ve TP bileşiklerinin giderilmesindeki denge izotermal adsorpsiyonu ve kinetiği sistematik olarak incelenmiştir. Hazırlanan zeolitlerin yapısal karakterizasyonu yapılmış ve performans ile ilişkileri ortaya konulmuştur.

Ağırlıkça %7 Cu^{2+} yüklenen ve 550 °C'de kalsine edilen Cu-Y zeoliti en yüksek denge kükürt adsorpsiyon kapasitesini göstermiştir. Orijinal NaY zeoliti ile karşılaştırıldığında, Cu-Y zeoliti DMDS (54.8 mg S/g) ve TP (22.4 mg S/g) giderimi için sırasıyla %91 ve %62 daha yüksek denge kapasiteleri göstermiştir. Performans analizinin sonuçları, kalsinasyon sıcaklığının adsorpsiyon kapasitesi üzerinde büyük etkisi olduğunu ortaya koymuştur. Yüksek sıcaklıkta ve N_2 akışı altında kalsinasyon işlemi yapıldığında aktif Cu^{+} iyonlarının oluştuğu ve sıcaklık arttıkça Cu^{2+} iyonlarının termal indirgenmesinin arttığı görülmüştür.

Modifikasyon işleminden sonra zeolitin yüzey alanı, gözenek hacmi ve gözenek boyutunda azalma meydana gelmiştir. Metal iyon konsantrasyonunun artmasıyla yüzey alanı, gözenek çapı ve gözenek hacmindeki düşüşün arttığı görülmüştür. Yüzey görüntüleri, modifikasyon sırasında bakır iyonlarının zeolit yapısında başarılı bir şekilde dağıldığını göstermiştir. Ancak belirli bir miktarın üzerindeki metal yüklemesi, zeolit yapısındaki bazı bölgelerde topaklanmalara neden olmuş ve büyük partikül sayısını bir miktar artırmıştır. Adsorpsiyon izoterm çalışmaları ise, DMDS ve TP'nin Cu-Y üzerinde adsorplanmasının Langmuir modeline çok iyi bir şekilde uyduğunu göstermiştir. Yapılan kinetik çalışmalar adsorpsiyon işleminde hız belirleyici adımın kimyasal adsorpsiyon olabileceği varsayımına dayanan, psödo ikinci dereceden modele uyduğunu ve birden fazla adım tarafından kontrol edildiğini göstermiştir. Bu bölümde yapılan çalışmalar, Cu-Y zeolitinin denge adsorpsiyon performansının modifikasyon koşulları değiştirilerek iyileştirilebileceğini kanıtlamıştır. Ancak endüstriyel adsorpsiyon uygulamalarını anlayabilmek için dinamik sistem üzerine daha fazla araştırma yapmaya ihtiyaç vardır. Çünkü dinamik sistemde çalışmak ve prosesi endüstriyel ölçeğe taşımak daha kolay ve ekonomik olacaktır.

LPG'nin adsorpsiyon yoluyla kükürtten arındırılması için daha iyi performansa, fiziksel özelliklere ve maliyet avatajına sahip yeni adsorbanların geliştirilmesine ihtiyaç vardır. Ayrıca LPG'nin zeolit esaslı adsorbanlar kullanılarak kükürtten arındırılması konusunda sistematik ve detaylı bir çalışma bulunmamaktadır. Bu alandaki boşluğu kapatmak amacıyla adsorban ve adsorbat arasındaki etkileşimler, performans-yapı ilişkileri ve adsorbanın dinamik sistemdeki tam potansiyelini belirleyebilmek için rejenere edilebilirliği incelenmiştir. Son kısımda, kükürt giderme verimliliğini artırmak için adsorban hazırlama ve dinamik sistem parametrelerinin optimizasyonu detaylı olarak çalışılmıştır. Bu nedenle kalsinasyon sıcaklığının, $Cu(NO_3)_2$ çözeltisinin konsantrasyonunun, başlangıç kükürt konsantrasyonunun, kükürt bileşikleri arasındaki yarışmalı adsorpsiyonun ve LPG akış hızının performans üzerindeki etkisi incelenmiştir. Cu-Y zeolitinin kimyasal bileşimi, kristal yapısı, yüzey asitliği, adsorpsiyon mekanizması, yapısal özellikleri ve yüzey morfolojisi analiz edilerek belirlenmiştir.

Ağırlıkça %7 Cu^{2+} yüklenen (%70 iyon değişim oranı) ve 550 ℃'de kalsine edilen Cu-Y zeoliti, dinamik deneylerde en iyi kükürt giderme kapasitesini sergilemiştir. Cu-Y zeoliti DMDS (75.4 mg S/g adsorban) ve TP (27.6 mg S/g adsorban) gidermede orijinal NaY zeolitinden sırasıyla %117 ve %78 daha yüksek performans göstermiştir.

Adsorpsiyon mekanizmasını belirlemek için ayrıntılı bir karakterizasyon yapılmıştır. Sonuçlar, Cu-Y'nin DMDS'yi doğrudan kükürt-metal (S-M) etkileşimi ile bağladığını, TP adsorpsiyonunda ise hem doğrudan S-M etkileşimi hem de π-kompleksasyonunun etkili olduğunu göstermiştir. Kükürt adsorpsiyonundan sonra Cu-Y'de karakteristik Cu-S, C-S ve S-S bağlarının kurulduğu görülmüştür. Asitlik analizi, kalsinasyon sıcaklığı arttıkça kükürt bileşiklerinin adsorpsiyonuna katkıda bulunan Lewis asit bölgelerinin sayısının arttığını göstermiştir. Diğer yandan, 550 ℃ üzerindeki kalsinasyon sıcaklıkları zeolitin hem bağıl kristalliğini hem de performansını düşürmüştür. Rejenerasyon işlemi; yüzey alanı, gözenek hacmi ve gözenek çapının azalmasına ve zeolit yapısında bazı bölgelerde topaklanmaya neden olmuş ve bunların sonucunda adsorpsiyon kapasitesinde düşüş meydana gelmiştir. Bununla birlikte, Cu-Y zeolitinin iyi bir termal kararlılığa sahip olduğu ve 3 çevrime kadar rejenere edilerek verimli bir şekilde yeniden kullanılabileceği görülmüştür.

Sonuç olarak, bu çalışmada gerçek LPG'den kükürt gideriminde kullanılabilecek yüksek seçicilik, yüksek kapasite ve yenilenebilirlik özelliklerine sahip Cu-Y adsorbanı başarılı bir şekilde geliştirilmiş ve endüstriyel ölçekli uygulamalar için yüksek potansiyele sahip olduğunu kanıtlamıştır.

1. INTRODUCTION

Despite all the efforts spent globally, ever increasing environmental pollution is one of the serious problems facing humanity. According to the World Health Organization (WHO) report, about 3 million people die each year due to the ambient air pollution [1]. There are different air pollutants caused by industrial processes, transportation emissions, domestic usages, and aerosols. A significant part of air pollution is caused from transportation sector. Petroleum-derived transportation fuels contain considerable amounts of sulfur compounds. During the combustion of sulfur-rich fuels, sulfur oxides (SO_x) are released to the atmosphere, which have become one of the serious environmental concerns such as smog, global warming, and acid rain [2]. It is necessary to remove sulfur from petroleum fuels to protect the environment and human health. Therefore, there is a pressing need for clean fuels all over the world.

Among petroleum-derived fuels used in transportation, liquefied petroleum gas (LPG) is the best choice as a clean and environmentally friendly fuel since it causes less emissions than the others. Nevertheless, LPG may contain different sulfur compounds depending on its supplying source. It is essential to reduce the sulfur level of fuel in order to prevent catalyst poisoning in LPG vehicles and improve air quality. Consequently, it is virtually impossible to reduce air pollution without implementing pollution prevention measures in the fuels used in transportation sector. European Union (EU) regulations introduced different emission limits for diesel, gasoline and LPG powered vehicles. The emissions originated from fossil fuels are among the main targets of current environmental regulations. “Sulfur-free” (≤ 10 ppm S) diesel and gasoline fuels became mandatory from 2009 on [3]. In addition, fuel quality as it relates to emissions is regulated by Environmental Protection Agency (EPA) in the United States. For on-road vehicles, ultra-low sulfur diesel with maximum of 15 ppm sulfur has been norm since 2006 [4] whereas gasoline is allowed to an average of 10 ppm sulfur beginning in 2017 [5]. As for LPG (autogas), the sulfur limit value is reduced to 30 ppm by 2021 according to the EN 589 standard [6]. These limits are expected to decrease further in the coming years.

Different methods including hydrodesulfurization (HDS) [7-9], oxidative desulfurization (ODS) [10, 11], biodesulfurization (BDS) [12, 13], extractive desulfurization (EDS) [14, 15] and adsorptive desulfurization (ADS) [16-18] have been investigated for sulfur removal from fuels. ADS is defined as an effective and safe method with its practical operation, energy-saving, economical and environmentally friendly nature. Also, the conventional methods are insufficient to remove aromatic sulfur compounds. Thanks to high-capacity and selective adsorbents, low sulfur limits can be provided by adsorptive desulfurization. Hence, ADS technology is regarded as one of the most efficient and promising method to meet strict regulations on sulfur emission.

Considering Turkey's LPG supply channels, LPG with very low sulfur level can generally be obtained from the Mediterranean and Norway regions. The high freight costs and long lead times of LPG procured from these regions increase the time and cost of LPG supply. With the development of high performance, economical and environmentally friendly desulfurization adsorbents, procurement cost and thus the import cost paid abroad will be reduced. Therefore, new and innovative contributions will be made to the adsorbent technology and the energy sector. Thanks to the participation of the refinery sector in this issue, both domestic refinery products and more environmentally friendly products will be offered to the Turkish market.

In recent years, application of ADS method to hydrocarbon fuels in order to meet low sulfur limits has been investigated by researchers. There are numerous studies about adsorptive desulfurization from gasoline, diesel, and jet fuels, whereas there are only a few studies done on sulfur removal from LPG in spite of the growing use of this cleanest conventional fuel. While there are limited studies on adsorption of aliphatic sulfur compounds from LPG, the removal of thiophene from LPG over zeolites has not been reported yet. In addition, systematic and detailed research on the adsorption mechanisms, isotherms and kinetics for both type of sulfur compounds in LPG over zeolites is needed.

In this chapter, an overview of the desulfurization techniques, fundamentals of adsorption, adsorptive desulfurization mechanisms and industrial perspective is provided. As a clean alternative, LPG is presented followed by theory and methods employed for adsorptive desulfurization. Finally, the research objectives and organization of dissertation is clarified.

1.1 LPG: A Clean Alternative

Liquefied petroleum gas (LPG) is basically a mixture of propane and butane hydrocarbons, which exists in the gaseous state under ambient conditions but can be stored as liquid phase under approximately 7 bar pressure. LPG mainly comprises low-boiling hydrocarbons; propane, n-butane, iso-butane, and to a lesser extent propylene or butylene. LPG is predominantly composed of propane; however, its composition and constituents can vary depending on the production method, the region it was produced in or destined for sale in [19]. LPG is a colorless and odorless gas unless it contains sulfur compounds. It does not have a toxic feature but can be suffocating due to the decrease of oxygen level during leaks. LPG also produces less air pollutants than most other fuels and helps to reduce the carbon emissions which are the big contributor of global warming and cause serious health hazards [20]. Thanks to its strong supply prospects, LPG is cheaper than other conventional fuels. Furthermore, its environmental advantages make it by far the most affordable transport fuel option for citizens because it benefits from a favorable tax framework.

LPG is commonly produced as a by-product of natural gas and oil extraction (66%) and via crude oil refining (34%) [21]. Depending on the soil types of the region where the crude oil and natural gas are extracted, the type and amount of sulfur compounds in LPG vary. The structures and properties of the sulfur compounds commonly exist in LPG are shown in Table 1.1 [22]. Although there are many kinds of sulfur components in the content of LPG, when the leakage occurs from the tank or tube where LPG is stored, sufficient stimulating odor may not occur. Since the odor intensity emitted by these sulfur compounds is different, not every sulfur compound is used as odorant in LPG leaks. Mercaptan derivatives, which have pungent odor, are generally added externally to increase the odor intensity so that leaked LPG can be noticed. Apart from this, sulfur compounds should be removed to produce low sulfur LPG as a clean fuel and sulfur free LPG as an aerosol propellant.

Table 1.1 : The most common sulfur compounds in LPG [22].

Sulfur Compound	Boiling Point (°C)	Density (kg/m^3)	Molecular Weight (kg/kmol)	Molecular Structure
Hydrogen Sulfide	-60.3	1539	34.08	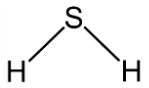
Ethyl Mercaptane	35	845.3	62.14	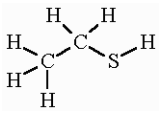
Methyl Mercaptan	6	1999	48.11	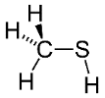
Carbonyl Sulfide	-50	2510	60.07	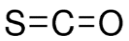
Dimethyl Sulfide	37	846	62.14	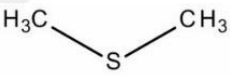
Dimethyl Disulfide	110	1060	94.20	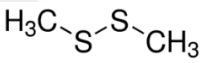
tert-Butyl Mercaptan	63.7	794.3	90.19	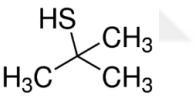
4,6-dimethyl dibenzothiophene	365	1182	212.31	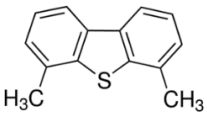
Benzothiophene	221	1150	134.2	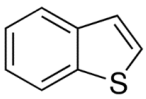
Dibenzothiophene	332	1252	184.26	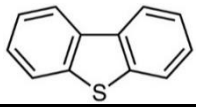

1.2 Industrial Perspective

LPG is an all-rounded energy source and widely used in different industrial applications. It offers versatile benefits due to its global availability, affordability, environmental benefits, transportation flexibility and diverse applications. LPG is an exceptional fuel and plays a crucial role in the transition to a safer, sustainable, and competitive energy model.

LPG is generally used in cooking, heating, vehicles, and as an aerosol propellant replacing Chlorofluorocarbons (CFCs) which cause damage to the ozone layer. LPG can be used as a feedstock in petrochemical industry; as an alternative fuel to natural gas in residential and industrial applications and as an alternative to diesel and gasoline for automotive fuel, especially thanks to its cost advantage.

Achieving net-zero carbon emissions is very important for many countries around the world to comply with the Paris climate agreement. However, the effects of climate change and global warming have become much more urgent in recent years. Europe's goal is to become the world's first net-zero emissions continent by 2050, and the EU has recently set a target in law to reduce emissions by 55% by 2030, compared to 1990 levels [23]. Therefore, adequate supply and reasonable cost of fossil-based fuels inevitably encourage their production, while renewable energy still attracts considerable attention [24]. Among the fossil-based transportation fuels, LPG is cleaner and more economic choice than others. Thus, the use of LPG, a low-carbon fuel, is important at the transition point to the 2030 targets. Due to its environmentally friendly nature, LPG causes less carbon emissions, but it still contains some sulfur compounds depending on the production method and source.

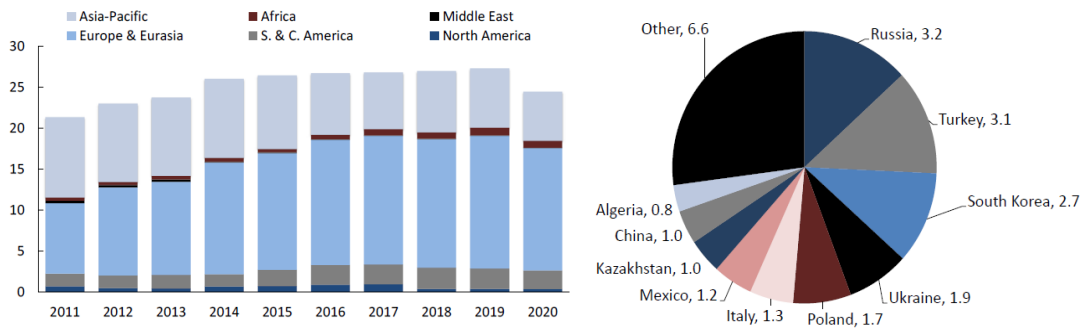

(a) (b)

Figure 1.1 : (a) Autogas demand by region, (b) Autogas consumption top 10 [25].

LPG (autogas) is the most popular alternative to gasoline and diesel for passenger cars and vans worldwide. Global autogas demand has increased since 2011 as shown in Figure 1.1(a). 2020 was a tumultuous year due to the Covid-19 pandemic that caused damage on the global economy and fuel industries. The collapse in demand for transportation fuels was evident. But the versatile use of LPG in different sectors contributed to its resilience during the crisis. As economies return to normality after the impact of the Covid crisis, the LPG industry is well placed to position itself as a vital transient fuel supplier in a world increasingly focused on decarbonization. LPG is still an economically viable option to achieve lower emissions from vehicles, and to provide access to cleaner cooking fuels in developing countries. Although autogas volumes decreased by 10% in 2020 compared to 2019, the number of autogas vehicles on the road increased by 5.9% and reached 29.2 million. Russia, Turkey, South Korea, Ukraine, and Poland accounted for under half of global autogas consumption in 2020 as shown in Figure 1.1(b). According to well to wheel analysis, autogas-fuelled vehicle produces 14% and 10% lower CO_2 emissions than petrol and diesel-run vehicles, respectively. In addition, LPG generates 96% less NO_x than diesel and 68% less NO_x than gasoline. Compared to their diesel-run counterparts, particulate matter (PM) emissions emitted by autogas vehicles are below reliably measurable level [26]. LPG also generates lower greenhouse gas emissions than petrol, diesel, and electricity, on an energy-equivalent basis.

LPG is a colorless and odorless gas in its vapor form and it is required in its natural odorless form in the aerosol industry. LPG is the most trusted and environmentally safe alternative since it does not contain any ozone depleting substances. As an ideal propellant, it has replaced the CFC gases which were earlier used by the aerosol industry. LPG aerosol propellant consists of a high purity mixture of propane, isobutane and n-butane and has been used in most aerosol products today [27].

Nowadays the process of hydrogen production is based on LPG to produce ultra clean fuel for on-board fuel cell applications and also to meet the coming legislations [28-30]. Large-scale hydrogen production is demanded because of the great interest in the application of fuel cells in domestic usage, transportation, and chemical industries. However, production and storage of high-purity hydrogen at the same place where it will be used is important criteria for fuel cell systems on large scale. Since hydrogen storage and distribution infrastructure is presently incomplete, on-board or in place

hydrogen production from fossil fuels with a distribution network is an attractive option [31]. Therefore, transition to a hydrogen-based economy via on-board generation of H_2 from LPG that already has a distribution network is a logical alternative.

There are some safety requirements to be considered for installation, storage, and usage of LPG. LPG can be stored in containers in liquid form after compressed under pressure. As LPG is gaseous at ambient conditions, pressurized storage tanks are needed both in the fueling stations and in vehicles, which is the major difference between conventional fuels and LPG. LPG tanks are a bit more costly, heavier and larger than gasoline or diesel tanks due to pressure-proof structure. Large volumes of LPG form flammable mixtures with air in concentrations range of 2-10% (v/v). Equipments using LPG must include suitable hydrocarbon detectors and ATEX precautions must be taken to avoid from explosive atmospheres [19, 20]. It is clear that any LPG handling has to be carried out by experts during the planning, installation, and maintenance stages of its life. Because of these safety rules and essential infrastructures, working with LPG is not very preferred by researchers in academia. It proves why academical studies on adsorptive desulfurization of LPG are so few. It shows that there is a gap in the literature and studies on this topic should be increased.

1.3 Desulfurization Methods

There are several methods used for desulfurization of fuels as shown in Figure 1.2. Today, refineries rely on catalytic HDS processes, operated at high pressures and elevated temperatures, to meet the regulations of close to zero sulfur, but these severe conditions would require high cost and cause fuel quality loss [32]. It has been reported that the classical HDS process that uses Co-Mo/Al_2O_3 or Ni-Mo/Al_2O_3 catalysts is highly efficient in removing thiols and sulfides but less effective for thiophene and derivatives [33]. Similarly, in gas oils, the removal of the alkyl-substituted thiophenes by HDS is more difficult than those of other sulfur-containing compounds. Desulfurization of fuels by HDS becomes increasingly difficult in the presence of some sulfur compounds with complex structures and high molecular weights [7]. Hence, because of both stringent sulfur regulations imposed on fuels and constraints of HDS process, deep desulfurization methods, such as adsorption, are required and heavily investigated.

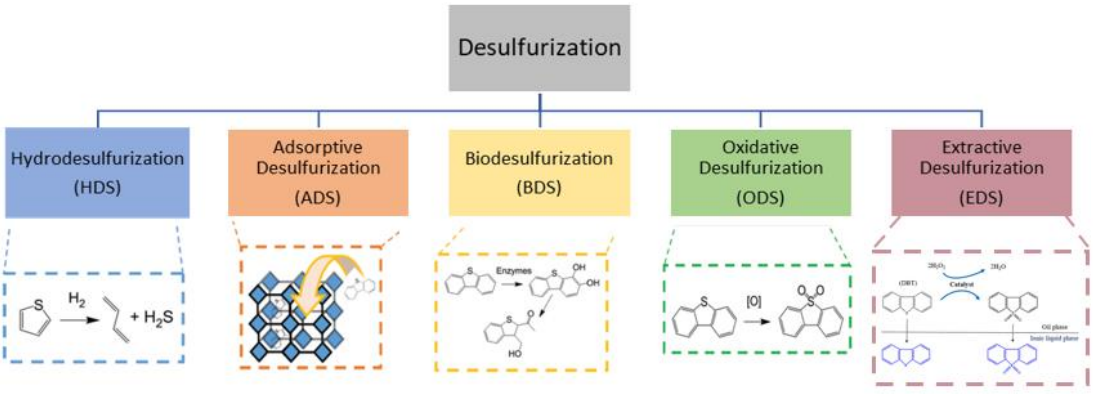

Figure 1.2 : Classification of desulfurization technologies [34].

Organic sulfur compounds can be selectively removed from fuels by biodesulfurization method in which microorganisms are used as catalyst. Various enzyme forms, modifications and supports have been investigated to improve the efficiency of the process. Transportation, storage, separation and cost of the microorganisms are critical points must be solved before applying this technology in the industrial scale. Therefore, a deep investigation on its efficiency and cost-effectiveness is desired [12, 35].

Oxidative desulfurization is a two-step process, which involves oxidation of sulfur compounds by an oxidant, which plays a key role, and then removed from the fuel by solvent extraction. The process is operated at mild conditions (<100 °C, environmental pressure), green alternative and does not affect carbon skeleton [10]. Although this process is technically proven, major obstacles such as low selectivity for sulfur compounds present in the real fuels, competitive removal of aromatic and olefinic compounds, waste management of the oxidized sulfur compounds, and recovery of oxidants hinder the commercialization [36].

Another method is extractive desulfurization which involves the removal of sulfur compounds from fuels by extractant solvents. EDS is promising due to its mild operating conditions, low octane loss and not requiring hydrogen or catalysts [14, 37]. However; high selectivity, low solubility, high thermal and chemical stabilities, and low cost are required properties for the suitable solvent. Currently, the most appealing extractants in the literature are ionic liquids (ILs) that prevent problems such as contamination and solvent loss. Although they are highly efficient for removing aromatic sulfur compounds, synthesis and regeneration of ionic liquids are complex

and expensive. Also, the mass transfer between solvent and sulfur compounds is limited due to the high viscosity of ionic liquids [36].

Adsorptive desulfurization method can be a good alternative to HDS, thanks to its relatively low cost, regeneration of adsorbents and environmentally friendly nature while operating at ambient conditions. As seen in Table 1.1, LPG can contain both aliphatic and aromatic sulfur compounds. Different desulfurization techniques can be used for removing of these sulfur compounds from LPG. While conventional desulfurization methods are effective in removing aliphatic sulfur compounds, it is very difficult to remove aromatic compounds by these techniques. Therefore, thiophene (T), benzothiophene (BT), dibenzothiophene (DBT) and their alkylated derivatives remain in the fuels. Compared to other desulfurization methods, the most important advantages of adsorption can be said as low temperature, low pressure, no need for hydrogenation and high-cost catalysts [16, 18]. In addition, the adsorbent used in the adsorptive desulfurization is selective for the sulfur compound to be removed. The selection and development of the ideal adsorbent material that is high-performance and selective for sulfur compounds is very important for desulfurization of LPG.

1.4 Theory and Background

1.4.1 Fundamentals of adsorption

Adsorption is a mass transfer phenomena that is the adhesion of gas or liquid molecules to the surface of a solid. The diversity of adsorption behaviors, including equilibrium separation based on guest-host interaction and non-equilibrium separations based on differentiated diffusion, is derived from the structural properties of adsorbents [38]. There are macropores outside and many nanoscale micropores inside the particles. Thus, the adsorption process can be divided into two parts: inter-particle mass transfer and intra-particle mass transfer. This process mainly includes external convection and diffusion, intra-particle diffusion, and intra-particle adsorption stages as shown in Figure 1.3.

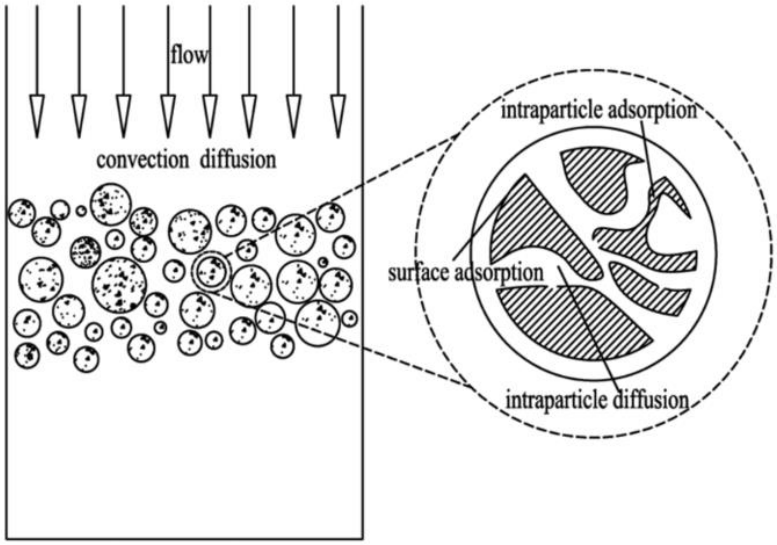

Figure 1.3 : Adsorption process of circular adsorbent particles [39].

Considering the forces acting on the adsorption process; the van der Waal's forces, chemical interaction and electrostatic attraction are responsible for adsorption of organic compounds in liquid fuels [40]. Adsorptive desulfurization is mainly based on physical adsorption (physisorption) and chemical adsorption (chemisorption) of organosulfur compounds according to the different adsorption forces (Figure 1.4). In physical adsorption, adherence to the surface occurs as a result of weak bonds and attraction forces. Physisorption is caused by the van der Waal's and electrostatic interactions, which is distinctive in zeolites. The process is reversible, and the adsorbed molecules can be easily removed from the surface by changing the process conditions. On the other hand, chemical adsorption specifies the phenomena of electron transfer, exchange or sharing between the adsorbate and adsorbent. Although this kind of adsorption is usually irreversible, there are some weak interactions denoted as reversible chemisorption, which can be utilized for separations with high selectivity. In addition, the ions can attach to the charged regions on the adsorbent surface by means of the electrostatic attraction forces. These adsorption processes are not isolated and can occur simultaneously at the surface [38, 40].

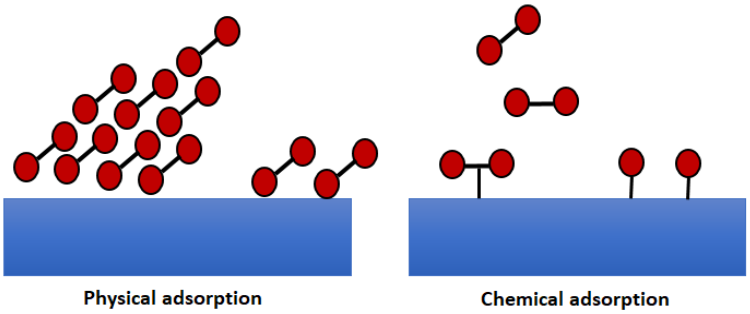

Figure 1.4 : Schematic illustration of physical and chemical adsorption.

The main performance criteria that define the viability of the adsorption process:

- **Equilibrium capacity** is the amount of adsorbate taken up by the adsorbent per unit mass (or volume) of the adsorbent at the equilibrium.
- **Breakthrough capacity** is defined as the amount of adsorbate removed by the adsorbent at break point concentration, which is also termed as the maximum acceptable amount of the adsorbates at the desired point.
- **Adsorption efficiency** is a percentage that represents the number of molecules of a compound removed by adsorbent.
- **Adsorption selectivity** of a mixture on a given material is the ability of the adsorbent to adsorb one component preferably to the other.

Since adsorption is a surface phenomena, the adsorption performance is an important function of surface properties of adsorbent. Among the surface properties of adsorbent, surface area is the most important parameter affecting the adsorption process and the adsorption capacity increases with increasing surface area. Therefore, porous materials or solids splitted into very small particles provide high adsorption capacity. Besides the surface properties of adsorbent, the amount of substance adsorbed by a solid material depends on the structure of the adsorbent and the adsorbate, bulk concentration of the adsorbate, process temperature and pressure.

Adsorption data is usually presented in the form of adsorption isotherm. It is known as the relationship between the amount of adsorbate taken up by the unit mass of adsorbent at constant temperature and the equilibrium solution concentration (or pressure).

1.4.2 Adsorptive desulfurization mechanisms

In view of various separation processes, understanding the separation mechanisms is necessary for determining suitable adsorbents. Adsorptive desulfurization can mainly follow different mechanisms including reactive adsorption, polar adsorption, selective adsorption, integrated adsorption, and π-complexation. Among these mechanisms, π-complexation and selective adsorption are commonly used for adsorptive desulfurization over zeolites [41].

In the π-complexation mechanism, the usual σ bonds can be formed with s orbitals of the cations, and their d orbitals can back-donate electron density to the antibonding π orbitals of the sulfur rings [42]. Bonds formed as a result of this interaction are stronger than physisorption and yet easily broken by changing the temperature or pressure which enhances the performance as well as the regenerability of adsorbents. On the other hand, selective adsorption requires designing effective adsorbents with active sites having high affinity for sulfur compounds in the presence of aromatics. The basis behind the selective adsorption technology is explained by the presence of site-specific interaction between sulfur and metal species [43]. Selective adsorption approach aims to selectively remove sulfur compounds from fuels by a direct sulfur-metal (S-M, σ) interaction, instead of π-complexation [44].

Besides π-complexation and S-M interaction, chemisorption can also occur by means of acid-base interaction. In this interaction, the lone pair electrons on the basic sulfur atoms interact directly with the Lewis acidic sites on the adsorbent [36]. Figure 1.5 shows the schematic representation of molecular adsorption modes of sulfur atom. Mechanistic behavior of zeolites can be changed by loading different metal ions onto zeolite structure. The main purpose of most studies on desulfurization adsorbents is to increase the adsorption selectivity by these proposed mechanisms [45]. Adsorption takes place mainly with the combination or any one of these mechanisms.

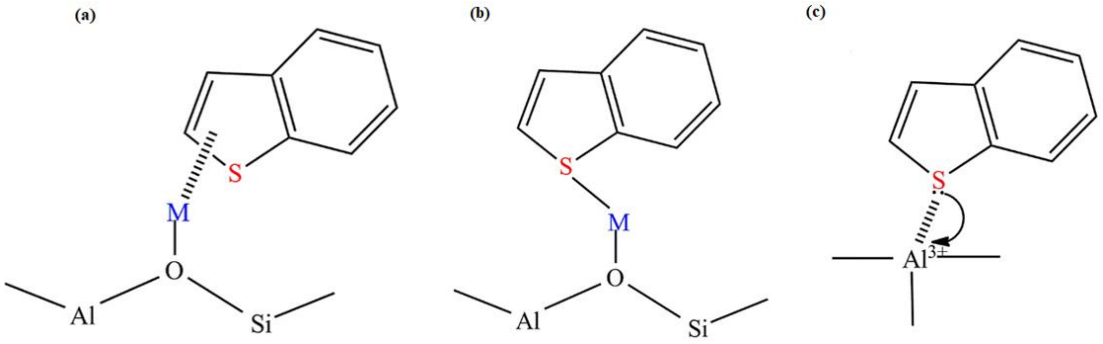

Figure 1.5 : Adsorption modes of BT via (a) π-complexation, (b) direct S-M interaction and (c) acid-base interaction [36].

1.5 Research Objectives and Organization of the Dissertation

The main objective of this thesis is to develop a high-performance adsorbent that is promising and can be potentially used for deep desulfurization of real LPG in industrial scale. The relationships between the structure and performance behavior of zeolite-based ion-exchanged adsorbent were investigated in order to estimate sulfur adsorption capacity, selectivity to aliphatic and aromatic sulfur compounds, and reusability of adsorbent. The effect of calcination temperature, concentration of metal ion solution, initial sulfur concentration and LPG flow rate were studied to optimize the adsorbent preparation and operational conditions. The effect of zeolite structure and the type of interaction between the sulfur compounds and adsorbent were aimed to be understood, as they are the factors that influence the adsorption mechanism and kinetics, which are important in the proper adsorbent material selection and design of the adsorption system. In particular,

- Chapter 1 gives background on general properties and industrial perspective of LPG, desulfurization methods, fundamentals of adsorption and adsorptive desulfurization mechanisms.
- In Chapter 2; activated carbon, zeolites and metal organic frameworks (MOFs) are discussed as desulfurization adsorbents.
- The desulfurization capacities of different commercial and ion-exchanged adsorbents are compared and the best performing one is chosen in Chapter 3. The adsorptive removal of dimethyl disulfide (DMDS) and thiophene (TP) that commonly exist in real LPG was studied. Cu^{2+}, Zn^{2+} and Cu^{2+}-Zn^{2+} loaded NaX and NaY zeolites were prepared through liquid phase ion-exchange (LPIE)

method. The effect of contact time on ion-exchange capacity of zeolites and the selectivity of zeolites towards the Cu^{2+} and Zn^{2+} ions in single and binary systems was determined. The adsorption behavior of original and prepared zeolites was investigated with both static and dynamic tests. Characterization analyzes of adsorbents were carried out to determine the crystal structure, textural properties, surface acidity, ion-exchange rate, and adsorption mechanism. Results are compared with original adsorbents to reveal the structure-performance relationships. In static tests, performances of original and modified zeolites were compared with commercial Cu-BTC adsorbent, a well-known MOF. The equilibrium isotherms and kinetics were also investigated for both DMDS and TP adsorbed onto the modified zeolites showing the best performance, which was studied for the first time in the literature. This work aims to develop ion-exchanged NaX and NaY zeolites and compare the structural and performance characteristics of zeolites in order to determine the best adsorbent which will be studied in detail.

- In Chapter 4, the detailed study on the adsorption of DMDS and TP from real LPG on Cu-modified Y zeolite, which exhibited the best desulfurization performance among all adsorbents tested in Chapter 3, was investigated. Cu-Y zeolite was prepared by LPIE method and the effects of different parameters on batch adsorption capacity of Cu-Y were systematically studied. It was necessary to study more deeply on Cu-Y zeolite to improve its performance. Different calcination temperatures and $Cu(NO_3)_2$ concentrations were studied to determine the optimum modification conditions. The effects of contact time and initial sulfur concentration on the desulfurization performance were also investigated by static adsorption method. Moreover, we focused on the auto-thermal reduction of copper species and its influence on performance, equilibrium isothermal adsorption and kinetics for both DMDS and TP compounds over newly developed Cu-Y zeolite in real LPG. Structural characterization was carried out to investigate the surface area, pore volume, pore diameter and surface morphology of zeolites in order to understand the effect of modification conditions on the structure-performance relationships of zeolites.

- In Chapter 5, the Cu-Y zeolite was tested in dynamic adsorption system which is practical and industrially applicable. It is necessary to develop new adsorbents with better performance, structural properties, and cost-benefits for adsorptive desulfurization. In order to improve the desulfurization efficiency, it is worth studying the optimization of adsorbent preparation and operational conditions. Therefore, the effects of calcination temperature, concentration of $Cu(NO_3)_2$ solution, initial sulfur concentration and LPG flow rate on dynamic desulfurization capacity were studied in this chapter. Also, the effect of competitive adsorption between DMDS and TP was investigated. To gain a better understanding on structure-performance relationships of Cu-Y zeolite, various characterizations have been conducted. Chemical composition, crystalline structure, textural properties, surface morphology, the type and relative amounts of surface acidic sites of the adsorbents, adsorption mechanism and established bonds between the sulfur compounds and adsorbent were determined. One of the main criteria in adsorbent selection for the industrial applications is reusability of adsorbent to make desulfurization process more economical. For this purpose, we also paid attention to thermal regeneration of Cu-Y to explore its full potential. The effects of the regeneration temperature and regeneration cycle on adsorption capacity were investigated.
- Finally, conclusions are given along with recommendations for future work in Chapter 6.

2. DESULFURIZATION ADSORBENTS

Different kind of adsorbents have been used for adsorptive desulfurization of fuels. The adsorbents used in desulfurization are expected to have some characteristics such as high selectivity against sulfur compounds and high sulfur adsorption capacity, appropriate physical and mechanical properties, suitable for working at ambient conditions, regenerable and economical [46].

The mostly preferred desulfurization adsorbents can be classified as: (1) oxygen-containing compounds like silica gel, activated alumina and zeolites, (2) carbon-based compounds like activated carbon and graphite, (3) polymer-based compounds like mixed-matrix pervaporation membranes and functionalized polymers, (4) organic frameworks like covalent organic frameworks (COFs) and metal organic frameworks (MOFs) and (5) new class of engineering adsorbents like ionic liquids (ILs) immobilized materials.

We discussed the current status of the most commonly used adsorbents; activated carbons, zeolites, and MOFs. Zeolites have both very high adsorption capacities and can be used many times while maintaining their capacity by showing superior regeneration properties. Activated carbons are generally preferred because they are efficient and cheaper than other adsorbents. As for MOFs they show superior desulfurization performance, but their costs are somewhat high for industrial applications.

2.1 Activated Carbons

Activated carbon (AC) is known as a versatile adsorbent that enables highly efficient adsorption of various types of gaseous and liquid compounds. AC has a high adsorptive capacity due to the high density of surface functional groups, large porosity, and high surface area. In addition, AC sources are over-abundant, and the production cost is relatively cheap. Commercial AC adsorbents have been used mainly for three

decades for removal of sulfur compounds from diesel, representative liquid hydrocarbon solutions and different fuel types.

The usage of AC for removal of sulfur compounds from naphtha has started in 1990's by the group of Salem [47, 48]. Percentage sulfur recoveries of AC from naphtha solutions were reported as 16 and 65% for solutions containing 50 and 800 ppm sulfur at 20 °C [47] and 35 and 56% for solution containing 60 and 300 ppm sulfur at 80 °C [48]. It was suggested that AC was less effective at low sulfur concentration compared to higher one at both temperatures. After these preliminary results, the use of AC in the investigation of desulfurization of fuels was accelerated in the beginning of 2000's.

In the light of all research carried out up to date, it was highlighted that adsorption capacity of AC for sulfur removal was affected by the specific surface area, pore structure, surface functional groups and operating conditions. Accordingly, specific surface area, pore volume and pore size of AC were accepted as the main factors that have direct influence on the desulfurization efficiency and adsorption capacity of AC. Additionally, several modification methods such as acid and alkaline modifications [49-62] and impregnation of metal, metal salts and metal oxides [63-76] have been investigated to improve the sulfur adsorption properties of AC.

2.1.1 Effect of surface chemistry

Altering the surface chemistry of AC by attaching functional groups which provide stronger interactions with acidic or alkaline gases results in improvement of the adsorption capacities and selectivity for these gases [77]. Mainly, alteration in the chemical environment of AC surface was targeted by attaching oxygen and nitrogen functional groups on the surface of carbon structure. Therefore, adsorption capacity of ACs can be increased by the alteration of chemistry via functional groups classified based on their acidity or basicity.

The surface acidity of AC is a function of the oxygen containing groups attached inherently to the surface of AC either by thermal treatment or through oxidation of carbon source [78]. Common oxygen-containing groups present on oxidized carbon surfaces are given in Figure 2.1(a). Oxygen containing groups such as ketone, chromene and pyrone radicals were reported to contribute to the basicity. However, the basicity provided by these groups is negligible compared to the dominant acidic nature of oxygen groups. On the other hand, surface basicity of adsorbent can be

improved by introducing the basic functional groups which enable the increase in selectivity for acidic gases [79]. Similarly, common basic nitrogen functional groups present on the surface of AC are given in Figure 2.1(b). In addition to these specific interactions originating from the functional groups of AC, among the mentioned sulfur adsorption mechanisms, adsorption affinity of AC was also described with different interactions such as hydrogen bonding and π-complexation between sulfur containing compounds and aromatic rings of AC. For instance, possible mechanisms for the adsorption of 4,6-Dimethyldibenzothiophene (4,6-DMDBT) from diesel fuel on three commercial nanoporous ACs from different origin and nature was examined by the FT-IR analysis in the study of Triantafyllidis and Deliyanni [80]. After the adsorption of 4,6-DMDBT, an increase in intensities of the bands at 1250 ($S=O_2$ in sulfoxides, sulfones or sulfonic acid) and 1730 cm^{-1} (–C=O vibration) were observed, which was attributed to the interactions of 4,6-DMDBT oxidation products with carboxylic groups by hydrogen bonding (Figure 2.1(c)) [80]. Additionally, shift was observed from the band at 1616 to 1590 cm^{-1} due to the interactions between the benzene rings of 4,6-DMDBT and aromatic ring of AC, revealing the π-complexation mechanism as given in Figure 2.1(c). Related studies were evidently revealed that functionalization with oxygen-containing groups is an effective as well as essential way to enhance the adsorption performance of AC. On the other hand, nitrogen functionalization, albeit being known as the most reliable method to improve adsorption efficiency of acid gases, its efficiency in the alteration of adsorption of sulfur compounds was also proved.

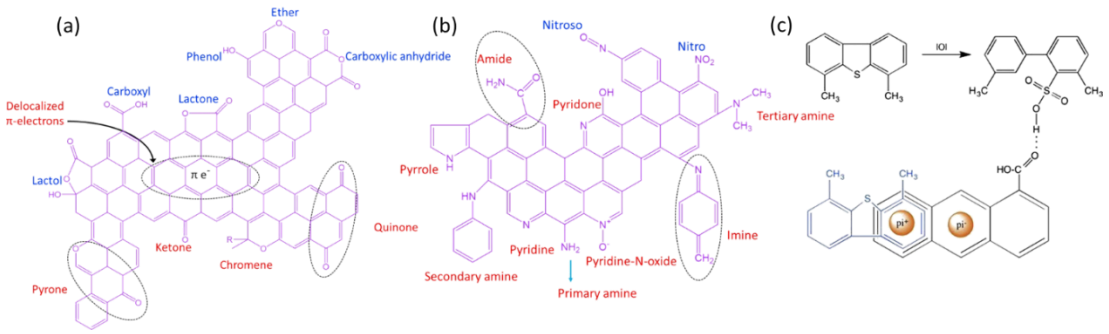

Figure 2.1 : Oxygen-(a) and nitrogen-(b) containing functional groups attached on AC [78]. (c) Possible other adsorption mechanisms with a specific example of 4,6-DMDBT adsorption on AC [80].

2.1.2 Effect of metal impregnation

Other strategies to enhance the adsorption properties of AC are the impregnation of either metals [63-67], metal salts [68-72], or metal oxides [73-76]. Mainly, surface modification of AC can be achieved by impregnation of metals such as Ag, Pd, Cu, Fe, and Pt in order to create a synergistic effect between existing properties of the AC and chemical agent introduced for the enhancement of sulfur removal. Within these metals, the significant increase in the sulfur adsorption capacity was observed for the mostly investigated Ag-impregnated ACs. For instance, Xiao et al. [63] compared the adsorption abilities of ACs impregnated by Ag, Cu, and Fe towards DBT either prepared with and without ultrasound assisted. Ag-impregnated ACs revealed the best DBT adsorption capacities in either case with the improvements of 44.3 and 32.9% after metal loading, respectively. This performance was attributed to the nature of compounds being as a soft acid of Ag and soft base of DBT to further improve the sulfur adsorption performance of ACs, loading of some metal species in the oxidized form on AC was studied and notable enhancement on the desulfurization capacity of AC was observed. Metal oxides are highly reactive towards the sulfur compounds and also the incorporation of metal oxides into the carbon structure could affect the textural properties.

Mechanism behind the efficient performance of metal oxide impregnated-ACs was identified by the study of Saleh et al. [75] where they investigated MgO/AC for desulfurization from model fuel including 150 ppm of TP, BT, and DBT in a mixture of hexane/toluene: 85/15 vol.%. They proposed several adsorption configurations that sulfur compounds formed with either MnO or AC, as given in Figure 2.2. They proposed that there are different interactions governing the sulfur adsorption as (i) an n-type donor (S-M interaction), (ii) a π-type donor (π-complexation), and (iii) Lewis acid, electronic, and van der Waals interactions. Collectively, compared with adsorption capacity of unmodified ACs, up to almost 130% increment was reported by the impregnation of metal particles. These developments in the desulfurization of model fuel provide us that ACs with specific modifications can be promising candidates, also taking into the consideration of being cheap, abundant and easy to be synthesized compared to other adsorbents.

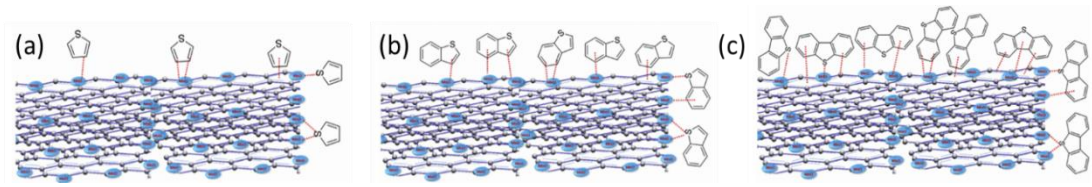

Figure 2.2 : Schematic illustration of possible adsorption mechanisms of (a) TP, (b) BT, and (c) DBT on MnO/AC [75].

2.1.3 Desulfurization of LPG over AC

In addition to safety issues related to the LPG desulfurization, high sulfur content, sulfur and hydrocarbon compound diversity, competition between sulfur and hydrocarbon compounds, and alteration in the hydrocarbon and sulfur composition within adsorption process are the main challenges that hinder the investigation of LPG desulfurization via adsorbents. We have only faced one study [81] in the literature that identified the performance of house made date pits AC for gaseous LPG desulfurization in fixed-bed adsorption columns. They studied the effects of flow rate and input sulfur concentration of LPG consisting of 100 ppm ethyl mercaptan (C_2H_6S, EM) and five different hydrocarbon compounds on adsorption performance of AC. Since the external diffusion resistance is low in the gaseous phase, the effect of flow rate on adsorption capacity was not significant, changing from 4.9 to 5.2 and 7.7 mg/g at LPG flow rates from 50 to 70 and 80 mL/min. However, the effect of initial sulfur concentration of LPG on adsorption capacity of AC was dominant where they investigated two different initial sulfur contents as 50 and 100 ppm EM. They attributed this difference to the increase in driving force of adsorption into the pores with the sulfur content, and hence the enhancement in diffusion.

2.2 Zeolites

Zeolites are alumina silicates which are formed by the formation of a network structure of tetrahedral AlO_4 and SiO_4 bonded to each other by oxygen atoms as shown in Figure 2.3 [82]. Zeolites are known to exhibit both acidic and basic sites on their surfaces. They are important alternatives of adsorbents to remove refractory sulfur compounds due to their pore structures and large surface areas. High selectivity, high capacity, reusability and reliable operating properties make these adsorbents efficient in removing sulfur compounds. In addition to their size-selective adsorption capacities, zeolites also have high thermal and mechanical stability. Transition metals are mostly

added to the zeolite structure in order to improve the adsorption performance and hence to obtain sulfur-free clean fuel.

Among the different kind of adsorption mechanisms proposed for the selective adsorption of different sulfur-containing compounds, π-complexation [83, 84], and direct S-M interaction between metal cations and sulfur compounds [85, 86] are mainly considered as responsible for the high desulfurization capacity of zeolites in the literature.

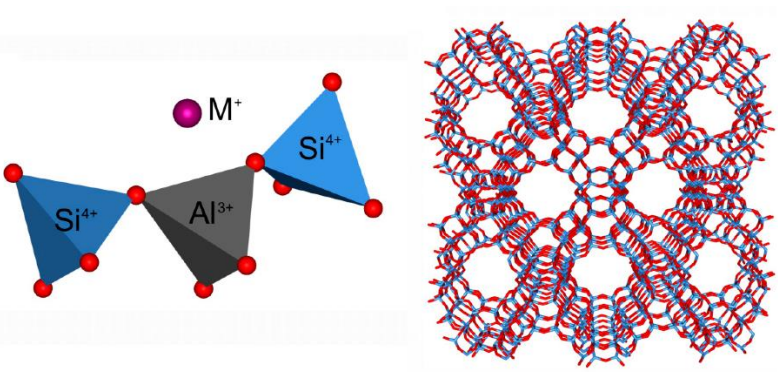

Figure 2.3 : The basics of the structural chemistry of zeolites [82].

Different types of zeolites (natural and synthetic) and modification methods are studied to improve the zeolite adsorption capacity [41, 87, 88]. Clinoptilolite [89, 90], bentonite [91, 92], phillipsite and chabazite [93] are known commercial natural zeolites used for desulfurization. On the other hand, FAU [94, 95], LTA [96], MFI (ZSM-5) [97-99] and Beta [100, 101] type zeolites are the synthetic zeolites used for desulfurization studies. Among the synthetic zeolites, FAU type X and Y zeolites are the two zeolites that have intensively investigated for adsorptive desulfurization due to their adjustable selectivity arising from their polar nature. Zeolites can be modified mostly with ion exchange method by incorporation of metal or metal oxide species and chemical treatment to enhance the desulfurization performance.

2.2.1 X type zeolites

The use of X type zeolites for desulfurization emerged in the beginning of twenty-first century. First attempt to remove sulfur compounds was done by Salem et al. [47, 48] using zeolites such as 5A and 13X. They compared sulfur adsorption capacity of zeolite 13X with AC and reported that adsorption capacity of zeolite 13X was 1.16 times than that of AC at 20 ºC, whereas it was 0.33 times than that of AC at 80 ºC. The adsorption selectivity of binary thiophene and toluene in model gasoline solution over

NaX zeolite was investigated by Boutet et al. [102]. Performing dynamic adsorption experiments, NaX exhibited very good thiophene/toluene selectivity for sulfur compound as 1.63 due to the cationic charges of zeolite which bring additional adsorption sites.

Ion exchange using single and binary cations were investigated for desulfurization of NaX zeolite. Tong et al. [103] proved the positive effect of binary metals on adsorption capacity of zeolites. They modified the 13X zeolite by ion-exchange with Cu^{2+} and La^{3+} (La^{3+}-Cu^{+}-13X) in order to measure single and binary adsorption capacities of Cu^{+}-13X and La^{3+}-Cu^{+}-13X for TP, 3-methylthiophene (3-MT), 2,5-dimethylthiophene (2,5-DMT), and BT dissolved in n-hexane fuels. According to characteristic and physicochemical properties of the studied adsorbents, they stated that the La^{3+} ion successfully penetrated into the pores of zeolite and stabilized the Cu^{2+} ion. They confirmed that Cu^{2+} has been successfully introduced into the zeolite channels and further loading of La^{3+} does not affect the crystallinity of zeolite framework as verified by stable peak intensity. High adsorption capacity was obtained by the synergistic effect of La^{3+} and Cu^{2+} ions into zeolites. In addition, with the ion-exchange with La^{3+}, the pore size was changed and more acidic centers accommodating larger sulfur compounds were created [103].

As distinct from aromatic sulfur compounds, Chen et al. [104] investigated the removal performance of linear sulfur compounds by NaX zeolites. They prepared Zn, Co and Ag modified NaX zeolites by ion-exchange method to improve the selective adsorption performances for hydrogen sulfide (H_2S) and carbonyl sulfide (COS) from Claus tail gas. Among all the zeolites, Ag-X showed the best adsorption performance, with the highest H_2S and COS breakthrough adsorption capacities up to 1.53 mmol/g and 10.5 μmol/g, respectively. This was attributed to the Ag-sulfide complex yielding in the strongest S-M interaction. Although mercaptans are another type of linear sulfur compounds can be found in petroleum derived fuels, any well accepted mechanism was not proposed for the adsorption of mercaptans. Yongping et al. [105] suggested that the rate of EM adsorption of 13X impregnated with Zn^{2+} from model fuel was likely to be diffusion controlled and the chemical adsorption was reported as an adsorption mechanism.

2.2.2 Y type zeolites

Among several adsorbents, Y type zeolites are promising and also the well-studied for the sulfur removal in the literature. Zeolites comprised of transition metals such as Ag, Cu, Ni, Zn, Ce and La possess a great performance for sulfur adsorption thanks to the enhanced selectivity [106-111]. The biggest portion of the desulfurization studies in which the adsorption mechanism was proposed as π-complexation belongs to the group of Yang [42, 83, 112-116]. Their most attractive paper was printed in Science, 2003, which was about the investigation of sulfur adsorption capacities of zeolites ion-exchanged with Cu^+ and Ag^+ from transportation fuels at ambient temperature and pressure. Their results showed the superior sulfur adsorption capacity of Cu-Y compared to previously known adsorbents such as ZSM-5, AC, and activated alumina (AA), for instance the sulfur content was reduced from 430 to <0.2 ppm [83].

Desulfurization can also be controlled with selective adsorption mechanism for both aliphatic and aromatic sulfur compounds by a direct sulfur-metal (S-M) interaction. The removal of thiophenic sulfur compounds from different fuels over Ce-exchanged Y zeolite was managed by the coordination between metal cation and sulfur compounds rather than π-complexation due to the high polarizability of Ce ions [85, 106, 117]. The adsorption mechanism of DMDS on Cu(I)-Y zeolite was also proposed as S-M interaction due to the increase in the adsorption bond energy of DMDS with zeolite. In addition, Lewis acid sites were contributed to the S-M interaction between metal cation and sulfur of DMDS [118].

One of the main factors that affect adsorption selectivity is competitive adsorption between organic sulfur compounds and aromatics existing in real fuels. Due to this reason, the binary ion exchange systems and the synergistic effect of different adsorption modes on the sulfur removal capacity were also studied in order to prevent competitive adsorption [24, 119-122]. The bimetal ion-exchanged Cu(I)-Ce(IV)-Y zeolite was prepared by different groups [24, 119, 120] and results confirmed that the Cu(I)-Ce(IV)-Y exhibited high performance for removal of organic sulfur compounds in the model fuels. They explained the increase in selectivity with the introduction of Ce ions which had influence on the locations of Cu^+ in zeolites and improve selectivity to sulfur compounds. Also, the aromatic sulfur compounds were removed via combination of π-complexation and S-M interaction, which improved the adsorption performance. On the other hand, Zhang et al. [122] tested NaY zeolites ion exchanged

with the combination of Cu^{2+}-Zn^{2+}, Zn^{2+}-Nd^{3+}, and Ni^{2+}-Nd^{3+} ions and Cu-Zn-Y was found to be a promising adsorbent through its desulfurization performance for aromatic sulfur compounds. The enhanced adsorption performance was explained with the synergistic effect between the Cu-Zn cations where the adsorption ability is dependent on the type of ions and the synergy between them.

2.2.3 Desulfurization of LPG over zeolites

Despite noteworthy research has been reported on desulfurization of diesel, gasoline and jet fuels over zeolites, there have been few studies carried out about the desulfurization of LPG [29, 81, 96, 121-123]. While most of the desulfurization studies for diesel and gasoline were performed with model fuels, the studies for LPG were mostly carried out with real LPG. This is very important to see the applicability of the desulfurization process on an industrial scale.

The actual performance of zeolites was targeted to be defined by testing them using real LPG by Wild et al. [29]. They aimed to remove the ethyl mercaptan (30 ppmw) exists in LPG by using adsorbents; Tokyo Gas zeolite TOSPIX94, 13X, and their own product NGDM1. Zeolite 13X within the studied different type of adsorbents showed the highest EM adsorption capacity with 7.3 g S/L. Xiang et al. [96] studied the desulfurization of real LPG using three commercial zeolites, namely 13X, NaY, and 5A. Results indicated that zeolite 13X and NaY with larger pore diameters had better access to adsorb sulfur components. Thus, zeolite 13X and NaY were reported to be applied for desulfurization from LPG. Jung et al. [121] prepared Ultra Stable Y (USY) based adsorbents impregnated with the rare-earth metals Ce (UC-10), La (UL-10) and Pr (UP-10). Modified adsorbents were tested to remove DMDS and dimethyl sulfide (DMS) from LPG using a fixed liquid flow reactor. UC-10 adsorbent showed the best DMDS and DMS removal performance, although the USY adsorbent had higher textural properties. [121].

A study on model LPG was reported by Lv et al. [122] for DMDS removal by using ion-exchanged NaY zeolites (Ag_2O/NaY, CuO/NaY, ZnO/NaY, CeO_2/NaY and NiO/NaY). Among all these adsorbents, 5 wt.% Ag_2O/NaY showed the highest breakthrough adsorption capacity owing to the direct S-Ag^+ interaction. Since Ag^+ shows weak acid character, it is more effective in the adsorption of DMDS which is a weak base character. They also used Ag_2O/NaY adsorbent for sulfur removal from real

LPG and reported that the performance of the adsorbent in real LPG was lower than that in model LPG [122].

In addition to FAU type zeolites, Meng and coworkers [123] used bentonite, which is attracting attention as a mesoporous adsorbent, to study the removal of sulfur compounds from LPG using a dynamic test system. They investigated the effect of the copper loading and the baking temperature. The bentonite loaded with 15 wt.% copper and calcined at 150 ℃ exhibited the optimum desulfurization. It was reported that the surface Lewis acidic sites improved the adsorption performance and the modified bentonite showed higher Lewis acidity than the raw adsorbent.

The above studies reveal that zeolite adsorbents and their modified forms can be used for desulfurization of model and real LPG fuels which is compatible with the results for desulfurization of diesel and gasoline fuels.

2.3 Metal Organic Frameworks (MOFs)

Well-studied classes of porous materials such as activated carbons and zeolites have been shown to adsorb sulfur compounds from liquid fuels until some level. Very recently, the MOFs have been investigated for the removal of sulfur compounds from model liquid fuels.

MOFs are a new type of porous inorganic-organic hybrid materials, which are formed from metal ions and organic linkers in a form of highly ordered framework (Figure 2.4). MOFs have superior properties such as large surface area, controllable pore size and diversity of chemical functionalities. They exhibit many outstanding advantages compared to other conventional porous materials. Thanks to their regular channels, great porosity and pore geometry, open coordinately unsaturated sites (CUS) and functionalized ligands; MOFs have shown unique adsorption performance for diverse sulfur compounds [124-127]. However, little has been understood for the high and rapid uptake of sulfur compounds.

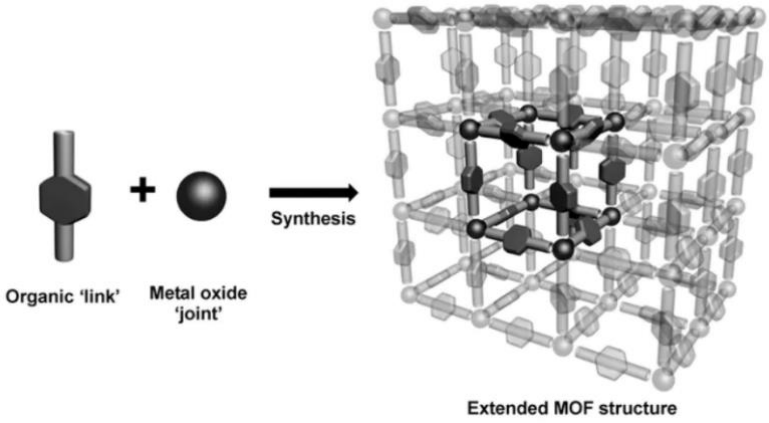

Figure 2.4 : Schematic illustration of structure of metal organic frameworks [128].

MOFs are hybrid crystalline porous materials that have uniform pore structures, tunable porosity, extensive varieties and flexibility in network topology, geometry, dimension, and chemical functionality. Due to this unique structural diversity, more than 20.000 different MOFs have been developed and characterized in the past decade [129]. It is very challenging to study all these MOFs in adsorption experiments due to the variety of the structural and chemical elements. Theoretical approaches have been employed toward the design and characterization of MOFs to predict the performance and new structure for ADS [130-134].

2.3.1 Desulfurization over virgin MOFs

Sulfur compounds present in LPG and other petroleum products differ in their molecular structure and these differences should be considered during separation processes. In LPG, sulfur compounds can be divided into aliphatic sulfur compounds and cyclic sulfur compounds (see Table 1.1). Aliphatic sulfur compounds such as thiols can be relatively easily removed by HDS due to lesser steric hindrance. On the other hand, cyclic sulfur compounds such as thiophenics are difficult to remove by conventional methods [135]. Therefore, more special, and high-performance materials like MOFs are required for the removal of cyclic sulfur compounds.

The combination of a variety of available metals and organic linkers can lead to a huge number of designed porous MOFs structures. They are also used in composite form with different materials in order to prepare efficient and cost-effective adsorbents. In addition, a number of simulation studies for MOFs are available in the literature, as well as experimental studies, due to their large variety and high cost. It can be a bit

complicated to classify MOF adsorbents according to the metal they contain, as there is a wide variety of MOF structures. Therefore, MOF adsorbents and their composites used in the removal of aliphatic and cyclic sulfur compounds have been researched with the simulation studies and modeling approaches over MOF adsorbents.

First study of the utilization of MOFs as adsorbents for the removal of cyclic sulfur compounds came across in 2008 by Cychosz et al. [136]. They examined the adsorption performances of UMCM-150, MOF-505, HKUST-1, MOF-5, and MOF-177 for desulfurization of BT, DBT, and DMDBT from iso-octane solutions, and found superior results compared to NaY adsorbent. After the high sulfur adsorption performance of Cu-based MOFs were revealed, the researchers highly focused on these adsorbents by many authors [137-141].

Studies on the adsorption of thiophene and its derivatives using MOFs are extensive, but there are very few studies on removal of chain sulfur compounds. Adsorption capacities of different MOF adsorbents for typical chain sulfur compounds such as hydrogen sulfide, thiols and dimethyl sulfide were investigated by researchers [142-144]. Wang et al. [143] investigated the performance of IRMOF-3 in DMS, EM and H_2S desulfurization. However, very limited breakthrough sulfur capacities were obtained. Li et al. [144] studied with MOF-199 (HKUST-1 or Cu-BTC) in order to remove H_2S, EM and DMS using a fixed bed reactor. The best breakthrough sulfur uptake capacities of MOF-199 for these sulfur compounds were approximately 5-15 times greater than IRMOF-3. The interaction between unsaturated copper sites in MOF-199 and sulfur compounds was shown as the main reason of this high adsorption.

Adsorption mechanisms have been explained with a number of interactions such as electrostatic interaction, acid-base interaction, H-bonding, π-π stacking, hydrophobic interactions, coordination and π-complexation. The interactions between sulfur compounds and specific metal ions in the MOF structure have a significant role in desulfurization [145-149].

2.3.2 Desulfurization over MOF composites

In order to improve the desulfurization performance of adsorbents, composite materials like the combination of MOFs with other materials were suggested to benefit from their synergetic effects [150-157]. Petit et al. [151] synthesized a composite adsorbent consisting of HKUST-1 and graphite oxide (GO) and tested for H_2S removal

at ambient conditions. The highest H_2S breakthrough capacity of MOF/GO composite was found as 199 mg/g whereas HKUST-1 showed an adsorption capacity of 92 mg/g. This improvement was explained with the strong dispersive forces in the new pore space created at the interface between HKUST-1 and GO, and reactive adsorption of H_2S on MOF/GO composites. Similarly, for cyclic sulfur compounds, the composite materials were studied to further enhance the desulfurization performance of adsorbents. Qin et al. [156] synthesized the HKUST-1@γ-Al_2O_3 composite for desulfurization of BT, 3-MT, DBT and 4, 6-DMDBT from model oil. The composite material exhibited an excellent adsorptive desulfurization capacity which was greater than the bare HKUST-1 and γ-Al_2O_3. The superior adsorptive desulfurization performance of HKUST-1@γ-Al_2O_3 was explained with the shorter diffusion channels, larger surface area, and more active sites resulting in larger positive entropy change in the nanosize HKUST-1@γ-Al_2O_3 [156]. Adsorption capacity of MOFs can be enhanced by making well-defined composites of them with different materials to increase of pore size, mechanical strength, and chemical stability.

In addition to the studies given above, the effect of incorporation of metal ions into the MOF structure on the adsorption performance was also investigated [45, 158-160]. Khan et al. prepared Cu^+/MIL-100-Fe adsorbent by loading MIL-100-Fe framework with Cu^+ species, which were obtained from one-step synthesis of Cu_2O particles at low temperature. The Cu^+-loaded MOFs were used for the liquid-phase adsorption of BT in n-octane. Results indicated that Cu^+/MIL-100-Fe showed higher BT adsorption capacity than parent MIL-100-Fe due to the π-complexation between the BT and Cu^+ species [159] Later, they investigated the effect of Cu_2O and CeO_2 loading on MIL-101 on the selective adsorption of BT from model fuels [45]. The sulfur adsorption capacity for MIL-101 loaded with Cu_2O and CeO_2 showed 188% increase. This increase was related to the synergistic effects on the removal of various thiophenic compounds by means of dual interactions (π-complexation and S-M bond formation).

2.3.3 Desulfurization of LPG over MOFs

Although MOF adsorbents are very successful in desulfurization from hydrocarbon fuels, there is no study with MOFs conducted for LPG in the literature. MOFs are the adsorbents that show the highest performance in removing aromatic sulfur compounds thanks to their chemical functionality and relatively high surface area. In addition, the

desulfurization capacity of MOFs can be increased by the use of various metal ions or combining with different materials such as AC, Gr, GO and γ-Al_2O_3 to develop both high performance and more economical adsorbents. Theoretical approaches can be used to design and synthesis of different MOF adsorbents. Simulation studies will encourage the researchers to develop new porous MOF materials for desulfurization applications. In literature, there have been most studies with MOFs on adsorption using model diesel and gasoline to mimic real fuels. LPG, like other hydrocarbon fuels, can contain aromatics and olefins that compete with sulfur compounds to occupy adsorption sites. Thus, MOFs can be tested in real LPG to determine the desulfurization performance of adsorbents to get a perspective for industrial systems.

2.4 New Generation Adsorbents for Deep Desulfurization

Different kind of potential materials that can be used for sulfur removal from hydrocarbon fuels by adsorptive desulfurization were explained so far. Adsorbent materials can be modified via various methods to enhance the desulfurization performance. However, more effective ways are required to develop high performance adsorbents for deep desulfurization. Recently, the environmentally friendly solvents, ionic liquids (IL) have become popular for sulfur removal applications in accordance with green chemistry concept. ILs are salts usually composed of an organic cation with an anion which can be organic or inorganic [37]. The ILs can be used in combination with solid materials like AC [161, 162], zeolite [163-165] and especially MOFs [166-170] to improve chemical functionality of adsorbents.

There have been few studies on preparing IL immobilized in AC and zeolites for desulfurization applications. Valdes et al. [161] prepared a composite with immobilization of 1-Butyl-3-methylimidazolium tetrafluoroborate [Bmim][BF4] on oxidized AC to evaluate the adsorption capacity of TP, BT, diphenyl sulphide (DPS) and DBT from model fuel. The sulfur removal percentages of TP, BT, DPS and DBT were reported as 52, 65, 45 and 70% for pure IL and 82, 71, 53 and 82% for IL@AC composite, respectively. Results indicated that the structure and geometry of the S-compounds determine the extension of the interaction with the imidazolium ring of the ionic liquid. Shirani et al. [163] synthesized NaY zeolite immobilized with [Bmim]Cl and tetrachloroferrate ($FeCl_3$) IL. The sulfur removal of 97.9% was obtained due to the double π-π interaction of DBT with zeolite and IL.

To explore the effects of ILs toward the sulfur removal performance, they were more dominantly incorporated into MOFs. Khan et al. [166] developed the MIL-101 doped with different amount of [Bmim]Cl ILs. The improved adsorption capacities were attributed to the acid-base interactions between the acidic ILs and basic BT [166]. To further investigate the performance of these composites, they incorporated [Bmim]Br IL and a heteropoly acid into highly porous MOFs, ZIF-8, and MIL-100(Fe) (Figure 2.5) [168]. They evaluated the efficiency of the tri-component adsorbents for the removal of BT and DBT from liquid fuel. The BT or DBT removal capacity of the composite MOFs was reported as 1.3-1.6 and 2.0-2.5 times to that of the original MOFs based on the unit weight and unit surface area of the adsorbents, respectively. They attributed the increased capacity to the synergistic affinity of IL and HPA toward thiophenics. Qi et al. [170] developed [mim$(CH_2)_3$COO]$FeCl_4$@UiO-66 composite based on the post-synthetic ligand exchange between MOFs and monocarboxylic functional IL by for DBT removal. The DBT removal efficiency reached up to 99.1% at optimal conditions and preserved 95% after 6 recycle runs. The synergistic effect between adsorptive and oxidative desulfurization was responsible for high DBT removal efficiency, where [mim$(CH_2)_3$COO]$FeCl_4$@UiO-66 can be accepted as both an adsorbent and a catalyst [170]. Collectively, ILs was mainly used to prepare composite materials in order to obtain adsorbents with high desulfurization capacity. Development of new adsorbents with higher performance and lower cost is now becoming of interest in the academic research. The new generation ILs may be developed by combining ILs with another chemical group to create synergistic effect and provide high performance, biodegradability, reusability, and low-cost properties. Nowadays, deep eutectic solvents (DESs), a substitute to ILs, have been gradually applied to desulfurization of fuels. DESs are composed of a hydrogen bond donor (such as urea, glycerol, metal salt etc.) and a hydrogen bond acceptor (such as quaternary ammonium, sulfonium, or phosphonium salts) [171]. DESs are generally applied in ODS and EDS processes with advantages such as adjustable structure, thermal and chemical stability, no need of purification. However, due to the inconvenient transportation and separation, DESs have less application in fuel desulfurization [172]. Further research are needed to combine the extractive desulfurization method using ILs and DESs with ADS for deep desulfurization of real fuels.

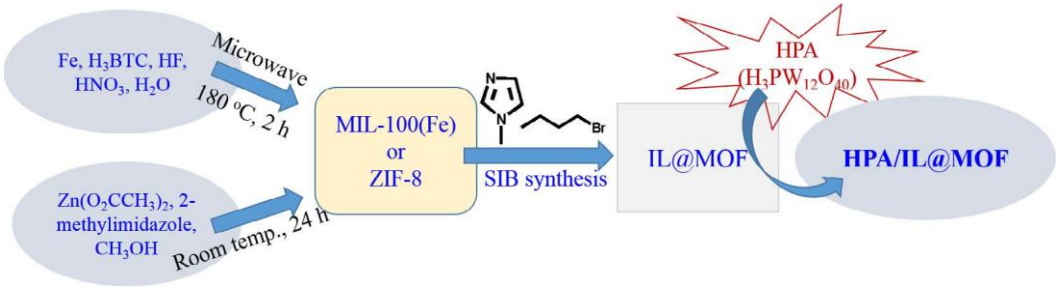

Figure 2.5 : A schematic diagram of the preparation of HPA/IL@MOF [168].

2.5 Regeneration of Adsorbents

Regenerability is one of the main factors that is important for adsorbent development and making adsorption process cost-effective. Although adsorption can be highly efficient, the reusability is one of the key steps where the adsorbents are often treated by solvent washing or calcination. Activated carbon [52, 68, 173] and zeolites [95, 106, 108, 118, 174] with high thermal and chemical stabilities can be regenerated easily by thermal and solvent regeneration. On the other hand, MOF-type adsorbents [157, 175, 176], which have comparatively low thermal and chemical stabilities can usually be regenerated using a solvent or under gas flow at low temperatures [142]. In the case of solvent regeneration ethanol, methanol, toluene and benzene are mostly preferred solvents for this purpose [52, 68, 95, 175]. Thermal regeneration of adsorbents is performed under gas flows including air, N_2, H_2, O_2, and He [52, 69, 102, 157, 173-176]. Regeneration may also be performed by combining solvent and thermal processes [52, 95, 177].

Regeneration and reusability of AC and zeolites were highly investigated due to the considerable sulfur separation performance of adsorbents. A couple of solvent and thermal regeneration for AC modified with boric acid was carried out by Ganiyu et al. [52]. For regeneration, adsorbent was treated in an ethanol at 60 °C for 60 min under continuous stirring, then the solvent was dried completely at 105 °C for 10 h. After solvent treatment, the sample was calcined at 600 °C in N_2 flowing at 30 mL/min for 150 min. And the regenerated adsorbent was reused for five adsorption cycle in batch processes, where it performed a remarkable regeneration performance with an only 7% loss in adsorption capacity. Yi et al. [118] regenerated the Cu(I)-Y zeolite by adding nitrogen or air to the reactor at 50 mL/min flow rate, while the temperature was

increased from room temperature to 450 °C and maintained for 4 h. The effect of different atmosphere and regeneration times on DMDS desulfurization rate of adsorbents after regeneration is shown in Figure 2.6. They reported that the desulfurization performance of the adsorbent regenerated in air and then in N_2 at 450 °C can still be recovered to 66.7% after three times of regeneration.

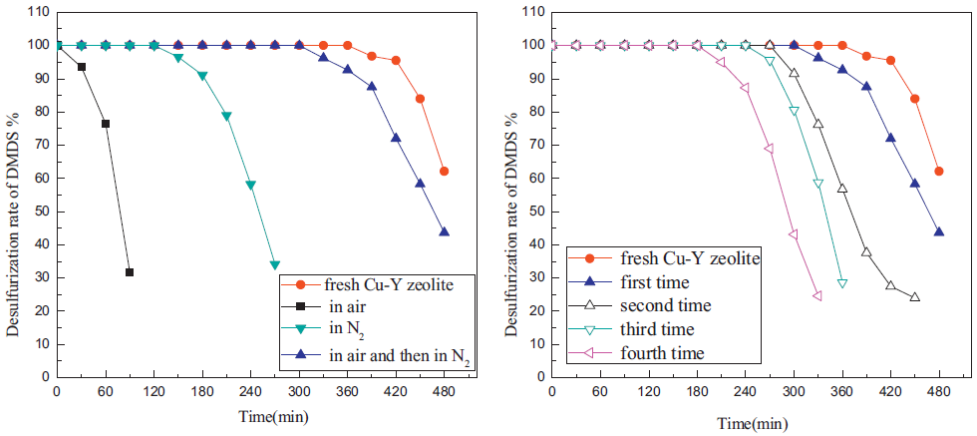

Figure 2.6 : Breakthrough curves for DMDS adsorption after regeneration in different atmosphere and regeneration time [118].

Development of effective regeneration methods is under research for MOFs to make the adsorption process economically feasible. Tan et al. [157] synthesized and tried the magnetically responsive HKUST-1/Fe_3O_4 composites for deep desulfurization of hydrocarbon fuels. After getting high TP and BT adsorption capacities, they also investigated the regeneration performance of adsorbents. The used adsorbents were recycled from liquid phases by using a magnet and washed with the 50% methanol and 50% toluene mixture under sonication for several times. After degassed in vacuum at 150 °C for 2 h, the adsorbents were tested again. Adsorption performance of regenerated adsorbents was comparable to that of the fresh one indicating the reusability of adsorbents for the purification of hydrocarbon fuels. Aslam et al. [175] developed 10, 20 and 30 wt.% of Ni loaded MIL-101 (labelled as 10Ni-MIL-101, 20Ni-MIL-101 and 30Ni-MIL-101, respectively) to investigate TP removal. After three times regeneration with air for 2 h at 300 °C, 20Ni-MIL-101 (best composite adsorbent) was found to have TP adsorption capacity of 23.5 mg/g compared fresh one with 25 mg/g, which was suggested as a suitable adsorbent for industrial applications.

In the light of these studies, it can be concluded that it is important to develop an adsorbent with high regenerability as well as high selectivity, adsorption capacity,

mechanical and thermal stability for practical applications. MOFs typically perform high adsorption performance on their first use but their regenerability was limited due to the low thermal stability. Further investigation is needed to focus on providing ideal regeneration conditions to develop stable adsorbent structures for high desulfurization performance.

3. ADSORPTIVE REMOVAL OF DIMETHYL DISULFIDE AND THIOPHENE FROM LIQUEFIED PETROLEUM GAS BY ZEOLITE-BASED ADSORBENTS[1]

3.1 Introduction

Sulfur oxides (SOx), which originate from combustion of sulfur-rich fuels, have become one of the most serious environmental problems in the world as they cause significant pollution in the atmosphere, global warming, and acid rain. Desulfurization processes have become a research focus in pursuit to minimize the negative health and environmental effects of sulfur in liquid and gas fuels. Since a significant portion of air pollution is produced by transportation, most of the technologies studied are related to desulfurization of the transportation fuels.

Among petroleum-derived transportation fuels, liquefied petroleum gas (LPG) is cleaner and more environmentally friendly than others because it causes less emissions. However, it still contains some sulfur compounds, depending on its source and production method. Minimization of the environmental impact of commercial fuels and emissions from refineries are among the main objectives of current environmental regulations. The sulfur limit value for LPG (autogas) has been reduced to 30 ppmw according to EN 589:2018 standard [6] and expected to decrease further in the upcoming years. In addition to its use as transportation fuel, LPG is widely used today as an environmentally safe aerosol propellant replacing the chlorofluorocarbon (CFC) gases in an effort to reduce damage to the ozone layer [178]. Moreoever, on-board generation of hydrogen from ultra clean LPG that already has a distribution network is a logical alternative to fully implement a hydrogen-based economy [179]. Therefore, the sulfur limit requirements for these applications are even more stringent.

[1] Adsorptive removal of dimethyl disulfide and thiophene from liquefied petroleum gas by zeolite-based adsorbents, *Microporous and Mesoporous Materials* 337 (2022) 111924.

Several techniques including hydrodesulfurization [8, 9], oxidative desulfurization [10, 11], bio-desulfurization [13, 180], extractive desulfurization [14, 15] and adsorptive desulfurization [16-18] have been used for the removal of sulfur compounds from fuels. Among these technologies, adsorption is considered as an effective and reliable method due to its favorable properties such as low energy consumption, operation at ambient conditions, and regenerability. In addition, the removal of aromatic sulfur compounds like thiophene (TP) and its derivatives is difficult by conventional methods such as hydrodesulfurization and amine scrubbing. Therefore, adsorptive desulfurization technology is regarded as one of the most appropriate and promising methods to meet low sulfur emission limits provided that highly selective adsorbents capable of reducing the LPG sulfur content to the desired level in an efficient and cost-effective manner are developed.

Several studies have been carried out in the past few decades to develop a novel and adequate adsorbent which has high adsorptive capacity and high selectivity for liquid fuel desulfurization. Many porous materials such as zeolites, activated carbon (AC), mesoporous silicas, and metal organic frameworks (MOFs) can be used for this purpose. Among the adsorbents investigated for desulfurization, MOFs are superior due to their high and tailorable porosity, large surface area, various pore architectures, and open metal sites [87]. However, their high cost, complex synthesis process, poor chemical and thermal stability hinders their use in industrial scale applications. On the other hand, microporous zeolites are promising for adsorption of sulfur compounds due to their ion-exchange capability, high selectivity, high adsorption capacity, and thermal and mechanical stability. In addition, different metals can be added to the structure of zeolites by a modification process to increase the number of active sites for adsorption, thereby improving their capacity. Modified zeolites with increased adsorption capacity are strong alternatives to MOFs and preferred in large scale applications thanks to their cost-benefit advantage. There are numerous studies on desulfurization of liquid hydrocarbon fuels over zeolites. So far, it has been shown that sulfur compounds in diesel and gasoline fuels can be effectively removed by adsorption over ion-exchanged zeolites. Yang and co-workers [42, 83, 112-116] studied desulfurization of gasoline and diesel fuels using π-complexation adsorbents. They demonstrated that Faujasite type zeolites ion-exchanged with transition metals can selectively adsorb thiophenic sulfur compounds with high adsorption capacities.

On the other hand, Velu et al. prepared ion-exchanged Y zeolites for selective adsorption of sulfur compounds in the jet fuel. Their results revealed that adsorption capacity of Ce-exchanged Y zeolite was managed by the direct sulfur-metal (S-M) interaction between metal cation and sulfur compounds rather than π-complexation [85].

In addition to ion-exchange using single cation, zeolites ion-exchanged with binary cations were also investigated for desulfurization. Song et al. [119] prepared modified Y zeolites ion-exchanged with Cu^{+}, Ce^{4+} and combined Cu^{+}-Ce^{4+} metal ions. They confirmed that the bimetal ion-exchanged Cu-Ce-Y zeolite exhibited higher sulfur adsorption capacity and high adsorption selectivity to organic sulfur compounds in the model gasoline. The increase in sulfur adsorption selectivity was attributed to the fact that the introduction of Ce^{4+} ions affected the locations of Cu^{+} ions in zeolites and changed the electronic properties of Cu^{+}. Zhang et al. [108] tested NaY zeolites ion-exchanged with the combined Cu^{2+}-Zn^{2+}, Zn^{2+}-Nd^{3+}, and Ni^{2+}-Nd^{3+} ions for removal of organosulfur compounds including dibenzothiophene (DBT) and 4,6 dimethyl dibenzothiophene (4,6-DMDBT) in model systems. According to their results Cu-Zn-Y was found to be a promising adsorbent in terms of the desulfurization performance.

Although considerable research has been carried out on desulfurization of diesel and gasoline fuels over zeolites, only a few studies have been reported on desulfurization of LPG [29, 96, 121, 122]. Wild et al. [29] aimed to eliminate the odorant EM presents in LPG by using Tokyo Gas zeolite TOSPIX94, 13X, and their own proprietary NGDM1 adsorbents at low temperature. The capacity results indicated that TOSPIX94 displayed higher EM adsorption performance compared to other tested adsorbents. Xiang et al. [96] investigated the removal of sulfur and butanes (i-butane and n-butane) from real LPG using three commercial zeolites, namely 13X, NaY, and 5A. Results of adsorptive desulfurization revealed that zeolite 13X and NaY had better desulfurization performance than zeolite 5A due to their larger pore diameters. On the other hand, Jung et al. [121] prepared Ultra Stable Y (USY) based adsorbents promoted with the rare-earth metals Ce (UC-10), La (UL-10) and Pr (UP-10) by an impregnation method. They used modified adsorbents to remove DMDS and DMS from real LPG using a fixed liquid flow reactor. Their results indicated that UC-10 adsorbent had the best DMDS and DMS adsorption capacities among the adsorbents examined. A study on model LPG was reported by Lv et al. [122] for DMDS removal

by using ion-exchanged NaY zeolites (Ag_2O/NaY, CuO/NaY, ZnO/NaY, CeO_2/NaY and NiO/NaY). Among all these adsorbents, 5 wt.% Ag_2O/NaY showed the highest breakthrough adsorption capacity owing to the direct S-Ag^+ interaction [122].

There is a need to develop new adsorbents with better performance, physical properties, and cost-benefits for adsorptive desulfurization of LPG. However, there are only a limited number of studies on adsorptive removal of aliphatic sulfur compounds from LPG while the removal of thiophene from LPG by zeolites has not been reported yet. To the best of our knowledge, there is also no systematic study of the adsorption mechanisms, adsorption isotherms and kinetics for adsorption of both sulfur compounds in LPG on zeolites. With this motivation, we studied the adsorptive removal of DMDS and TP from real LPG. Cu^{2+}, Zn^{2+} and Cu^{2+}-Zn^{2+} loaded NaX and NaY zeolites were prepared through liquid phase ion-exchange (LPIE) method and investigated their adsorption behavior under both static and dynamic experimental conditions. We carried out structural characterization of the best performing modified zeolites and compared the results with original adsorbents to understand the structure-performance relationships. In static experiments, adsorption performances of original and modified zeolites were compared with commercial Cu-BTC adsorbent (BASF, Basolite C 300), a well-known MOF. We also investigated the equilibrium isotherms and kinetics for DMDS and TP adsorption onto the best performing modified zeolites.

3.2 Experimental

3.2.1 Materials

NaX (Si/Al: 1.32) and NaY (Si/Al: 3.86) zeolites were used as starting materials for preparing ion-exchanged zeolites. NaX, NaY zeolites and Cu-BTC were obtained from Zeochem, Zeolyst and Sigma-Aldrich, respectively. Copper nitrate ($Cu(NO_3)_2 \cdot 3H_2O$) and Zinc nitrate ($Zn(NO_3)_2 \cdot 6H_2O$), both with a purity of 98%, were supplied by Merck and used without further purification. Pyridine (analytical grade, ≥ 99.5%) was supplied by Merck. Analytical reagent grade DMDS (≥ 99.0%) and TP (≥ 99.0%) were selected as the target aliphatic and aromatic sulfur compounds that commonly exist in real LPG and procured from Sigma-Aldrich. The sulfur rich fuel was prepared with 196 mg S /L in real LPG (< 0.28 mg S /L, density: 0.56 kg/L) supplied from Aygaz Company in Istanbul, Turkey.

3.2.2 Adsorbent preparation

The ion-exchanged zeolites used in this study were prepared by liquid phase ion-exchange method. NaX and NaY zeolites in powder form were treated with 0.5 M $Cu(NO_3)_2$ aqueous solution for 12 h at room temperature. After ion-exchange, the zeolites were filtered, washed with plenty of deionized water, and dried in an oven at 105 ºC overnight. Then, the samples were calcined at 350 ºC for 3 h under N_2 atmosphere and Cu-X and Cu-Y adsorbents were obtained. Zn-X and Zn-Y zeolites were prepared by a similar procedure. CuZn-X and CuZn-Y zeolites were prepared by co-ion exchanging of NaX and NaY zeolites with equimolar mixed solutions of $Cu(NO_3)_2$ and $Zn(NO_3)_2$ at room temperature for 12 h. The ion-exchanged zeolites were then filtered, washed with deionized water, dried at 105 ºC overnight, and calcined at 350 ºC in N_2 atmosphere for 3 h. The non-modified zeolites were also characterized for comparison after activation at 350 ºC under N_2 gas flow for 3 h.

3.2.3 Static adsorption experiments

The adsorption performance of the original and modified zeolites and Cu-BTC for DMDS and TP removal from LPG were assessed through adsorption tests in a batch system. A specified amount of the adsorbent was placed in a closed tube of 4.2 cm inner diameter and 35.4 cm height and contacted with LPG containing 196 mg/L total S concentration. Adsorbents and LPG were mechanically mixed throughout the experiments which were conducted for 48 h to ensure that equilibrium had been reached. The sulfur content of the fuel before and after adsorption experiments was determined with elemental sulfur analyzer (Analytik Jena Multi EA 5000). The sulfur adsorption capacity (q) of adsorbents was calculated by the following formula:

$$q = \frac{(C_o - C_e) \times V}{1000 \times m} \tag{3.1}$$

where C_o was the initial sulfur concentration in LPG (mg S/L), C_e was the adsorption equilibrium sulfur concentration in LPG (mg S/L), V was the volume of LPG (mL), and m was the weight of the adsorbent (g).

3.2.4 Dynamic adsorption experiments

Dynamic adsorption experiments were carried out at room temperature and atmospheric pressure in a laboratory scale fixed-bed adsorption system shown in Figure 3.1. It consists of an adsorption column, a LPG feeding tank, a LPG pump, and a desulfurized LPG storage tank. The adsorption column had an inner diameter of 2.3 cm and a height of 25.5 cm. In all dynamic adsorption experiments, the system was pressurized up to 5 bar to ensure that LPG is in liquid phase. The LPG stream containing 196 mg/L S was pumped from the feed tank and passed through a mass flow controller where the LPG flow rate was adjusted. Then LPG was introduced to the adsorption column at 0.5 L/h flow rate. Temperature and pressure at the entrance and exit of the column were continuously measured. Sulfur content of the effluent sampled at regular intervals was determined by elemental sulfur analyzer. The desulfurized LPG was stored in the product tank during operation.

In the dynamic adsorption experiments, 2.8 mg/L S concentration in the effluent was taken as the breakthrough point and the sulfur adsorpion capacities of the adsorbents were determined based on the breakthrough point. The desulfurization efficiency (R) and sulfur capacity (q) of adsorbents at any breakthrough point were calculated by equation (3.2) and equation (3.3), respectively:

$$R = \frac{\text{S in feedstock} - \text{S in effluent}}{\text{S in feedstock}} \times 100 \qquad (3.2)$$

$$q = \frac{\left(C_o - C_e\right) \times V_p}{1000} \qquad (3.3)$$

where C_o was the initial sulfur concentration in LPG (mg S/L), C_e was the sulfur concentration in the effluent (mg S/L), and V_p was the volume of purified LPG per gram adsorbent at the breakthrough point (mL/g).

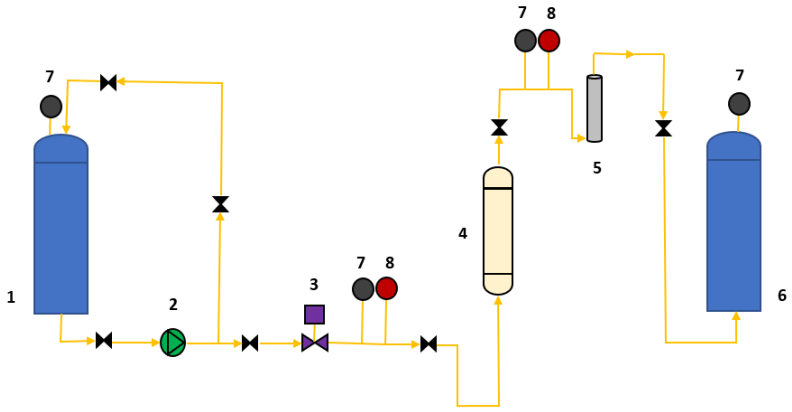

Figure 3.1 : Laboratory scale dynamic adsorption system. 1-LPG feed tank; 2-LPG pump; 3-Mass flow controller; 4-Adsorption column; 5-Sample tube; 6-Product tank; 7-Pressure reader; 8-Temperature reader.

3.2.5 Characterization of adsorbents

Chemical compositions of the original and modified zeolite adsorbents were determined by inductively coupled plasma (ICP) analysis (Thermo Scientific XSERIES 2) after microwave assisted acid digestion. Effect of contact time on ion-exchange rate, ion-exchange ratio of zeolites, competitive adsorption between Cu^{2+} and Zn^{2+} ions, affinity of zeolites to each metal ion were also investigated through ICP analysis.

The crystalline structures of the original and Cu-exchanged zeolites were analyzed by X-ray diffraction (XRD) (Mini Flex Rikagu) with Cu Kα radiation in the 2θ range of 10-50°.

The Fourier transform infrared (FT-IR) spectra of the samples were recorded at room temperature on a Perkin-Elmer FT-IR spectrometer to determine the adsorption mechanism between the sulfur compounds and adsorbent. The type and relative amounts of surface acidic sites of the adsorbents, NaX, NaY, Cu-X and Cu-Y, were also measured via FT-IR spectroscopy using pyridine as the probe molecule. 10 mg adsorbent samples were pressed into self-supporting wafers (diameter: 13 mm) and then were exposed to pyridine adsorption. IR spectra of samples were recorded after desorption at 200 °C and 400 °C for 30 min.

Surface area and pore volume of the adsorbents were determined by using a Micromeritics ASAP 2020 analyzer and the data were analyzed based on the Brunaeur, Emmert and Teller (BET) method. Pore size distribution was analyzed by using the Horvath-Kawazoe method.

3.3 Results and Discussion

3.3.1 Chemical composition of the adsorbents

The chemical composition of the original and the ion-exchanged zeolites are presented in Table 3.1. As expected, the amount of Cu and Zn ions in the zeolite increases while the amount of Na ions decreases after ion-exchange. No noticeable change, however, was observed in the amount of Si and Al ions after ion-exchange.

The amount of metal ions incorporated into the zeolite by ion-exchange per available ion-exchangeable site is indicated by the molar ratio of M^{m+}/Al^{3+}, where M^{m+} is the amount of metal ions incorporated by ion-exchange [109]. The Cu/Al molar ratios of Cu-X and Cu-Y are 0.447 and 0.431, respectively. Considering that one Cu^{2+} ion compensates for two aluminum tetrahedral, then the $M^{m+}/Al^{3+} = 2Cu^{2+}/Al^{3+}$ which is 0.89 for Cu-X and 0.86 for Cu-Y. This indicates that Cu^{2+} ion-exchange degree of 89% and 86% were attained for NaX and NaY, respectively. Similarly, the extent of the Zn^{2+} ion-exchange was found to be 75% for NaX and 72% for NaY. The Cu and Zn ion-exchange ratios were 71% and 25% for CuZn-X and 68% and 23% for CuZn-Y, respectively. The exchange ratios of the individual metal ions in binary ion-exchange remained lower compared to those in single ion-exchange due to the competitive nature of the binary system. The $n(2Cu^{2+}+ 2Zn^{2+}+ Na^{+})/n(Al)$ ratios calculated for Cu-X, CuZn-X and Zn-X changed in the range of 1.02-1.14 which were close to Na/Al ratio (1.018) of the original NaX zeolite. A similar trend was observed for Cu-Y, CuZn-Y and Zn-Y; their $n(2Cu^{2+}+ 2Zn^{2+}+ Na^{+})/n(Al)$ ratios varied between 1.04-1.16 and were comparable to that of the original NaY zeolite (1.024). These results indicate that ion-exchange process proceeds almost stoichiometrically for both zeolites.

Table 3.1 : Chemical composition of the original and ion-exchanged zeolites.

Zeolite	Chemical composition (mmol/g)					Molar ratio			
	Si	Al	Na	Cu	Zn	Si/Al	Na/Al	Cu/Al	Zn/Al
NaX	6.834	5.162	5.255			1.324	1.018		
Cu-X	6.830	5.151	0.670	2.302		1.326	1.130	0.447	
CuZn-X	6.827	5.141	0.931	1.825	0.648	1.328	1.181	0.355	0.126
Zn-X	6.825	5.128	1.410		1.913	1.331	0.275		0.373
NaY	13.289	3.441	3.524			3.862	1.024		
Cu-Y	13.163	3.404	0.609	1.467		3.867	0.179	0.431	
CuZn-Y	13.095	3.381	0.849	1.153	0.389	3.873	0.251	0.341	0.115
Zn-Y	13.026	3.359	1.078		1.216	3.878	0.321		0.362

3.3.2 Ion-exchange capacity of zeolites in single and binary ion systems

Contact time is a significant factor that affects the ion-exchange extent on zeolites. The single and binary ion-exchange of NaX and NaY zeolites were conducted in a time range of 0-18 h with 0.5 M initial Cu^{2+} and Zn^{2+} ion concentrations. The extent of ion-exchange as a function of contact time in single ion system is shown in Figure 3.2(a).

NaX zeolite displayed a superior ion-exchange capacity in comparison to NaY irrespective of ion type. Higher ion-exchange capacity has been observed for zeolites with lower Si/Al ratio (NaX lower than NaY) [181, 182]. Also, both zeolites displayed higher exchange capacity for copper than zinc. The ion-exchange for both zeolites proceeded rapidly in the early stages of the process, then the ion-exchange rate gradually decreased with time and finally attained equilibrium state for both cations. The maximum Cu^{2+} and Zn^{2+} exchange amount reached up to 146 and 125 mg per gram of adsorbent, respectively. The time to reach maximum ion-exchange amount was found as 12 h for all zeolites.

The slight decrease after equilibrium was attained for all cases can be attributed to impregnation of metal ions on surface pores of the zeolite via physical adsorption. In summary, the amount of metal ions that can be incorporated on the zeolite structure had a maximum value and there was an optimum contact time for maximum ion-exchange.

We investigated the influence of the presence of competing cations on the individual adsorption of Cu^{2+} and Zn^{2+} on NaX and NaY zeolites. The affinity of zeolites to metal ions and the effect of the competitive adsorption on their ion-exchange capacity are illustrated in Figure 3.2(b). Comparison of Figures 3.2(a) and (b) revealed that ion-exchange conducted with binary ion solutions resulted in lower ion-exchange capacity than that in single ion-exchange irrespective of zeolite and cation type. The drops in the ion-exchange capacities of the zeolites were higher for zinc than copper. The Cu^{2+} and Zn^{2+} ion-exchange capacities of zeolites attained in binary ion-exchange were 20-21% and 66-68% lower than that in the single ion-exchange, respectively. This indicates that both zeolites have a higher affinity to Cu^{2+} than Zn^{2+} in the binary ion-exchange process. The affinity of the zeolites may be quantified based on the maximum ion-exchange capacities measured.

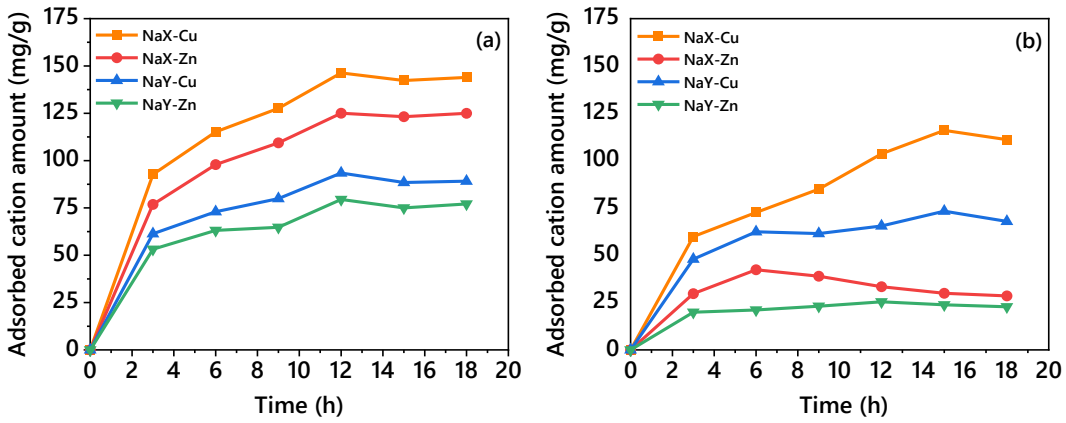

Figure 3.2 : Variation of copper and zinc ion-exchange capacity of NaX and NaY zeolites with time in (a) single ion-exchange and (b) binary ion-exchange systems.

Table 3.2 : Physical characteristics of the cations studied [183].

Cation	RBS	PE	IR	IP	HR
Cu^{2+}	2.66	1.90	0.73	7.73	4.19
Zn^{2+}	2.20	1.65	0.74	9.39	4.30

RBS: relative binding strengths, PE: Pauling electronegativity, IR: ionic radius, IP: ionization potential, HR: hydrated radius.

The selectivity of zeolites towards the metal ions may be influenced by the characteristic properties of ions [183]. Physical characteristics of Cu^{2+} and Zn^{2+} are presented in Table 3.2. The higher competitive Cu^{2+} capacities of zeolites result from its higher electronegativity and lower ionization potential. In addition, the presence of Cu^{2+} suppressed the adsorption of Zn^{2+} thanks to its higher relative binding strength, which enhanced ability of the binding interaction between the metal ion and zeolite [184]. The difference in the adsorption capacity of the zeolites for the metal ions in binary systems can also be due to hydration radii of the cations. Copper with its smaller hydration radii can diffuse through the micropores and channels of zeolites faster than zinc despite their similar ionic radii. Therefore, the incorporation of copper ions into the zeolite structure is faster and in higher amounts. This is partially responsible for higher copper selectivity of zeolites over zinc.

3.3.3 Adsorbent characterization

The XRD patterns of original and copper-exchanged zeolites after calcination at 350 °C are shown in Figure 3.3. The diffraction patterns of the Cu-X and Cu-Y zeolites with characteristic peaks positioned nearly at $2\theta = 10.20^{o}$, 15.85^{o}, 20.50^{o}, 23.80^{o} and

30.95º were similar to the patterns of the original NaX and NaY zeolites, which are in good agreement with typical diffraction patterns of FAU type zeolites [185]. The similar XRD patterns of the copper-modified and original adsorbents imply that the zeolite structure is retained after ion-exchange. Any diffraction peaks assigned to Cu related compounds or metal Cu can not be observed in ion-exchanged zeolites, suggesting that the Cu^{2+} species have entered the channels of zeolites or are highly dispersed on the surface of zeolites. These results indicate that the ion-exchange and calcination processes did not affect the structure of zeolites. However, the ion-exchanged Cu might overlay some structures in zeolites resulting in decreased crystallinity, confirmed by the decreased peak intensity in the modified zeolite structures.

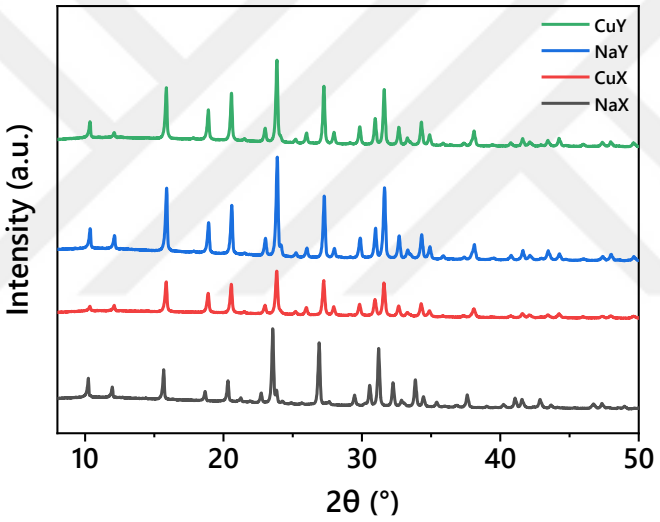

Figure 3.3 : XRD patterns of original and modified zeolites.

The textural characteristics of original and Cu-exchanged zeolites are summarized in Table 3.3. NaY zeolite has the highest BET surface area, pore volume and pore diameter. The textural properties of both zeolites decreased when Na^{+} was ion-exchanged by Cu^{2+}. Incorporating the Cu^{2+} ion into NaY zeolite reduced the surface area, pore volume and pore size by 9.2%, 8.3% and 4.0%, respectively. On the other hand, the surface area of NaX zeolite was reduced by 14.7% while reduction in pore volume and pore size was 12.5% and 4.4% after ion-exchange, respectively. These reductions were probably caused by the dispersion of ions in the channels of the zeolite structure and partial pore blockage due to the presence of copper ion.

Table 3.3 : Surface area, pore volume and pore diameter of adsorbents.

Adsorbent	BET surface area (m^2/g)	Pore volume (cm^3/g)	Pore diameter (nm)
NaX	477	0.32	0.91
NaY	665	0.36	0.99
Cu-X	407	0.28	0.87
Cu-Y	604	0.33	0.95

3.3.4 Acidity investigation

The type and amount of surface acidic sites of the adsorbents were investigated in order to explore the relationship between adsorption performance and acidic properties of the zeolites. The acidity of NaX, NaY, Cu-X and Cu-Y zeolites were determined by pyridine-FT-IR analysis method. The results of the analysis of Lewis and Brønsted acid sites after desorption at 200 °C and 400 °C are presented in Figure 3.4. The FT-IR patterns display the spectrum of bands which are attributed to the interaction of pyridine with Lewis and Brønsted acid sites on the zeolites. The characteristic bands observed at 1450 cm^{-1} and 1540 cm^{-1} are resulting from the vibrations of adsorbed pyridine in the Lewis acid and the Brønsted acid sites, respectively. The band seen at 1490 cm^{-1} is due to the overlapping signals resulting from the contributions of both Lewis and Brønsted acid sites to pyridine adsorption [186].

The FT-IR patterns of total acid sites recorded at 200 ℃ in Figure 3.4(a), revealed a considerable increase in the intensity of bands at 1450 cm^{-1} for both zeolites after Cu ion-exchange. The band intensity at 1540 cm^{-1} increased for Cu-Y zeolite while Cu-X zeolite showed little decrease in the intensity of this band compared to NaX. This indicates that some of the Brønsted acid sites has turned into Lewis acid sites. As seen in Table 3.1 and Table 3.4, NaX with higher Al^{3+} content has higher Brønsted acid site density than NaY. These results are in line with the findings of previous studies indicating that the density of Brønsted acid sites increases with the Al^{3+} content [187]. Table 3.4 also indicates that the Cu-exchanged zeolites are superior to the original ones with respect to total acidity. Figure 3.4(b) shows the IR spectra of strong acid sites of zeolites which were obtained after desorption at 400 ℃. The intensity of the bands

drastically decreased with increasing the temperature from 200 ℃ to 400 ℃ due to the weak bonding of pyridine at these sites [118].

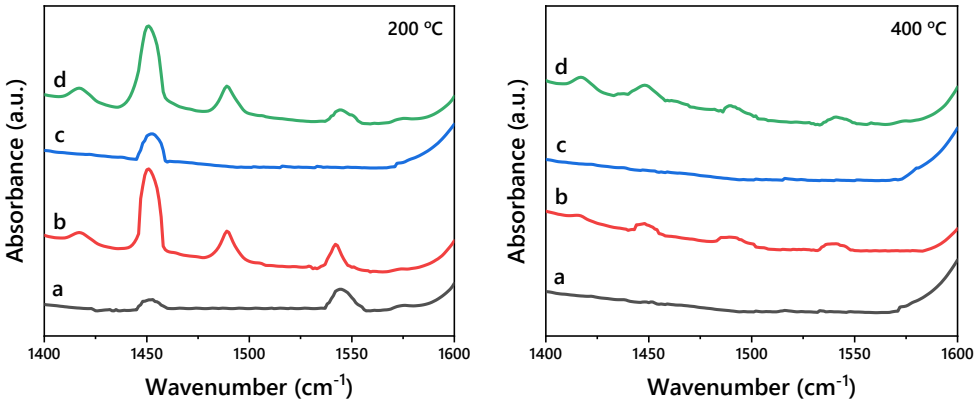

Figure 3.4 : Pyridine-FT-IR spectra of zeolites at 200 °C and 400 °C: (a) NaX, (b) Cu-X, (c) NaY and (d) Cu-Y.

Table 3.4 : Type and amount of surface acidic sites of adsorbents* (μmol/g).

Adsorbent	Total acidity	Total Brønsted	Total Lewis	Strong Brønsted	Strong Lewis	Weak Brønsted	Weak Lewis
NaX	104.45	92.14	12.31	0	0	92.14	12.31
Cu-X	541.22	81.43	459.79	32.57	34.06	48.86	425.73
NaY	78.17	0	78.17	0	0	0	78.17
Cu-Y	512.46	38.93	473.54	15.09	24.50	23.83	449.04

*Acidity values were calculated based on the methods reported by Emeis [188].

Table 3.4 shows that the highest amount of the Lewis acid sites was observed for Cu-Y zeolite, whereas the increase in the amount of the Lewis acid sites was higher for Cu-X. Results also revealed that the Cu ions, which are electron acceptors, improve mainly the Lewis acid centers. Thus, it enhances the adsorption of sulfur which is an electron donor element [100]. These findings also suggest that the acidity of NaX and NaY can be enhanced by liquid-phase ion-exchange.

3.3.5 Performance analysis

3.3.5.1 Removal of DMDS and TP by static adsorption experiments

In static adsorption experiments, sulfur removal capacities of original and modified NaX and NaY zeolites were investigated and compared to that of a commercial MOF, Cu-BTC, a new type of porous inorganic-organic hybrid material known for its high surface area, controllable pore size and diversity of chemical functionalities [135]. LPG with 196 mg/L sulfur concentration was used for static adsorption experiments.

The DMDS and TP removal performances of NaX, modified zeolites and Cu-BTC after 48 h of contact time are shown in Table 3.5 and Figure 3.5.

Table 3.5 : Sulfur removal performance of adsorbents in static adsorption experiments (C_0: 196 mg/L S).

Adsorbent	Sulfur in effluent (mg/L)		Sulfur removal efficiency (%)		Sulfur adsorption capacity (mg S/g)	
	DMDS	TP	DMDS	TP	DMDS	TP
NaX	77.3	138.3	61	29	23.8	11.6
Cu-X	43.1	126.6	78	35	30.7	13.9
CuZn-X	57.1	131.6	71	33	27.9	12.9
Zn-X	66.1	135.5	66	31	26.1	12.1
NaY	53.2	127.1	73	35	28.7	13.8
Cu-Y	7.3	110.9	96	43	37.9	17.1
CuZn-Y	20.7	118.2	89	40	35.2	15.6
Zn-Y	33.0	122.6	83	38	32.8	14.8
Cu-BTC	1.1	101.9	99	48	39.1	18.9

Type Y adsorbents attained higher sulfur adsorption capacity and sulfur removal efficiency than type X adsorbents for both sulfur compounds because of their higher surface area and pore volume (Table 3.3). All adsorbents displayed a 2.1-2.3 times higher adsorption capacity for DMDS than that for TP. All modified zeolites displayed a better adsorption performance than the original zeolites. Among the modified zeolites, the copper-loaded adsorbents had the highest adsorption capacity. Cu-X adsorbent had a desulfurization capacity of 30.7 mg S/g and 13.9 mg S/g while Cu-Y adsorbent had 37.9 mg S/g and 17.1 mg S/g capacity for DMDS and TP, respectively. The adsorption performances of the modified NaX and NaY zeolites for DMDS and TP removal were in the following order: Cu > CuZn > Zn. These results are in good agreement with the results of the ion-exchange experiments which showed that both zeolites have higher exchange capacity for Cu^{2+} ion. Cu-BTC displayed the highest desulfurization performance for both sulfur compounds in comparison to other examined adsorbents. The adsorption capacity of Cu-BTC for DMDS and TP was 39.1 mg S/g and 18.9 mg S/g, respectively. In spite of its high desulfurization capacity, the commercial use of Cu-BTC, like most MOFs, is limited due to its high cost. On the other hand, copper-exchanged Y zeolite can be a good alternative for desulfurization of LPG with its advantages of high capacity, close to Cu-BTC, and relatively low cost.

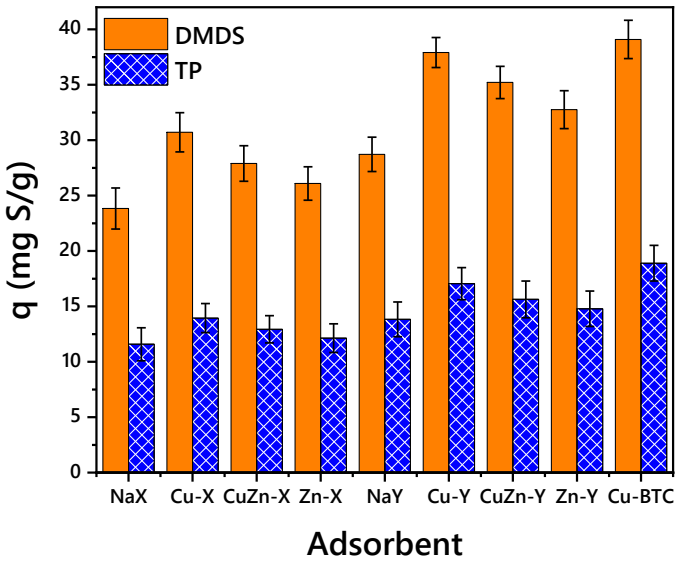

Figure 3.5 : Sulfur adsorption capacities of adsorbents.

3.3.5.2 Removal of DMDS and TP by dynamic adsorption experiments

The breakthrough curves of adsorbents for removal of DMDS from LPG in dynamic experiments are shown in Figure 3.6 in which the amount of sulfur in the effluent is plotted as a function of the cumulative volume of the purified LPG. Figure 3.6 shows that all modified zeolites adsorbed more sulfur than their original forms. Figure 3.6(a) displays that Cu-X had the highest adsorption capacity leading to complete removal of DMDS up to 100 mL LPG was purified per gram adsorbent. The cumulative LPG volume at the breakthrough point for Cu-X was 187 mL per gram adsorbent. The breakthrough DMDS adsorption capacity of zeolites was in the order of Cu-X > CuZn-X > Zn-X > NaX. Modified zeolites showed 14-37% increase in capacity compared to the original NaX zeolite. Figure 3.6(b) shows that Cu-Y zeolite displayed the highest DMDS removal performance with 100% desulfurization efficiency achieved up to 200 mL LPG was purified per gram adsorbent whereas 260 mL purified LPG passed through the adsorber at the breakthrough point. Modified zeolites showed 16-45% increase in capacity compared to the original NaY zeolite in the order of Cu-Y > CuZn-Y > Zn-Y > NaY.

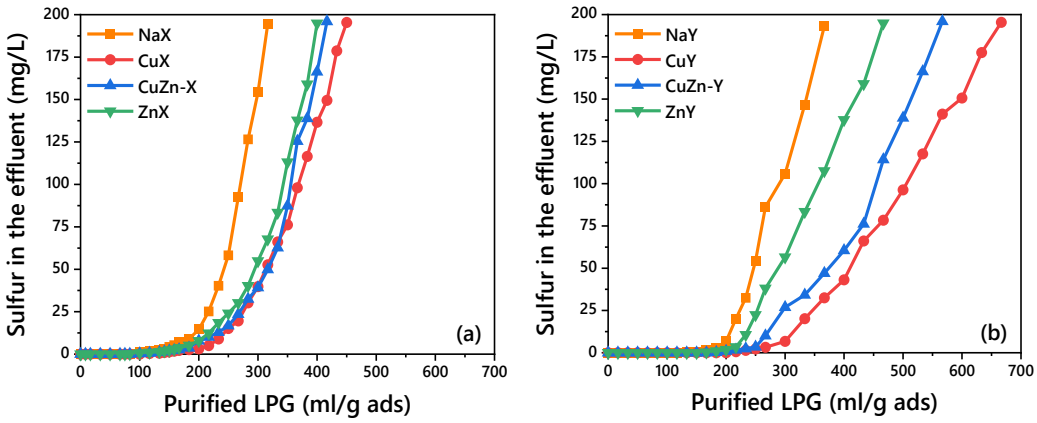

Figure 3.6 : Breakthrough curves of adsorbents for removal of DMDS from LPG (a) NaX-based adsorbents and (b) NaY-based adsorbents.

The inclusion of copper and zinc ions considerably improved the adsorptive desulfurization ability of the zeolites for DMDS. Loading metal ions into the zeolite structure increased the number of active sites, which directly affected the adsorption performance of zeolites. Among all adsorbents investigated in this this study, Cu-Y emerged with the best DMDS removal performance. This improvement can be explained in terms of the hard and soft acids and bases (HSAB) principle, which states that soft acids react faster and form stronger bonds with soft bases, whereas hard acids react faster and form stronger bonds with hard bases [189]. Since Cu^{2+} is a softer acid than Na^{+} with a high polarization of valence electrons, it tends to interact with DMDS which is a soft base to form a direct S-M interaction. This is mainly due to the strong interaction strength between DMDS and Cu^{2+}. Similar findings have been reported by Lv et al. [122], who carried out a study for the removal of DMDS by different ion-exchanged NaY zeolites from model LPG containing 1000 ppmw S. Among all adsorbents, Ag_2O/NaY exhibited the best desulfurization performance, followed by CuO/NaY. They also used Ag_2O/NaY adsorbent in real LPG conditions and reported that Ag_2O/NaY zeolite showed 64.13 mg S/g breakthrough desulfurization capacity in real LPG which was lower than that in model LPG. Our results for Cu-Y zeolite are compatible with these findings. On the other hand, Jung and co-workers prepared modified zeolites impregnated with rare-earth metals (Ce, La or Pr) for the adsorption of DMDS from real LPG. Their results showed that UC-10 adsorbent (USY impregnated with Ce) had a DMDS adsorption capacity of 11.5 mg S/g [121] which was higher than the other adsorbents they examined but lower than the performance of Cu-Y adsorbent in our study.

The breakthrough curves of adsorbents for removal of TP from LPG are shown in Figure 3.7. The adsorptive desulfurization ability of all modified adsorbents was better than that of original zeolites. As shown in Figure 3.7(a), 80 mL of desulfurized LPG volume at the breakthrough point was achieved per gram adsorbent for Cu-X. The breakthrough TP adsorption capacity of zeolites was in the order of Cu-X > CuZn-X > Zn-X > NaX. Modified zeolites showed 9-22% increase in capacity compared to the original NaX zeolite. On the other hand, Cu-Y zeolite displayed a TP removal performance providing up to 100 mL purified LPG per gram adsorbent at the breakthrough point (Figure 3.7(b)). Modified zeolites showed 10-25% increase in adsorption capacity compared to the original NaY zeolite in the order of Cu-Y > CuZn-Y > Zn-Y> NaY. The breakthrough desulfurization capacities increased with increasing sulfur uptake of the adsorbents, as expected.

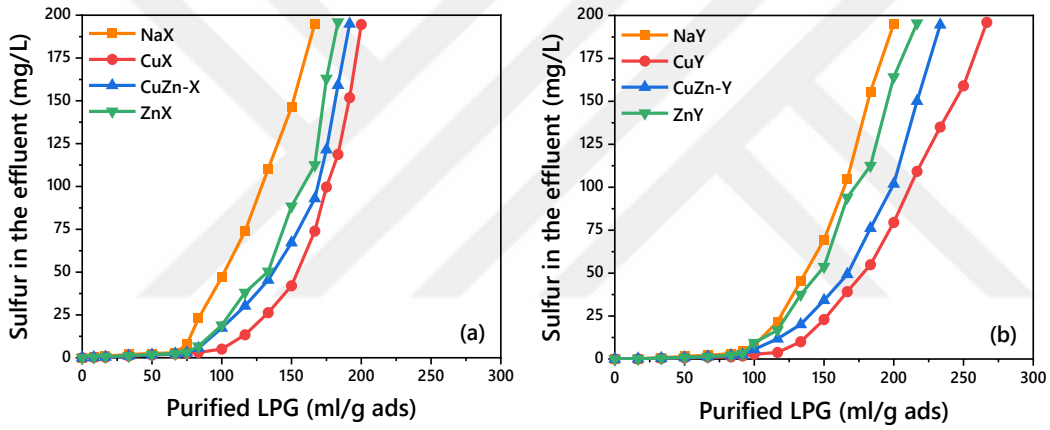

Figure 3.7 : Breakthrough curves of adsorbents for removal of TP from LPG (a) NaX-based adsorbents and (b) NaY-based adsorbents.

Cu-Y adsorbent showed the best TP removal performance. The observed trend between the desulfurization performance and acidity of the adsorbents suggests that Lewis acid sites may promote the interaction between the metal cation and sulfur. Our results are consistent with that of Song et al. [119] who attributed the similar outcomes to the enhanced adsorption ability which originates from the improved Lewis acid centers of zeolites due to the inclusion of metal ions. According to the HSAB principle, thiophene which is the soft Lewis base, could be adsorbed on Lewis acid sites more easily.

Moreover, the results of acidity measurement showed that weak Lewis acid sites are mainly responsible for the adsorption of sulfur. There is no study in the literature on the removal of thiophene from LPG. However, our results are compatible with that of

Yang's group (Table 3.6) who prepared Cu-Y based adsorbents to remove thiophenic sulfur compounds from different fuels.

There are different parameters that affect the performance of adsorbent materials. The structural properties of the adsorbent, type of sulfur compounds used, initial sulfur concentration, and flow rate are effective parameters on desulfurization capacity making a direct comparison difficult. Nevertheless, Table 3.6 shows that Cu-Y adsorbent we developed displayed higher breakthrough adsorption capacity than the adsorbents prepared by group of Yang, although our system was operated at higher flow rate.

Table 3.7 summarizes the breakthrough adsorption capacities of the original and modified adsorbents calculated based on the breakthrough point of 2.8 mg/L sulfur concentration in the effluent. The breakthrough adsorption capacities of the modified zeolites for DMDS and TP removal were in the order of Cu > CuZn > Zn. Among all adsorbents tested, Cu-Y had the highest breakthrough adsorption capacity of 50.3 mg S/g and 19.4 mg S/g for DMDS and TP, respectively. These findings are in line with the results of static desulfurization experiments.

All adsorbents also showed higher desulfurization performance for DMDS than TP. Thiophene, being an aromatic sulfur compound, is more difficult to remove due to its chemical structure [190]. In addition, the results of static and dynamic adsorption tests revealed that better interaction between adsorbent and sulfur is achieved when they come into contact in dynamic conditions. Sulfur compounds can interact with the surface and active sites of the adsorbent more effectively when LPG is flowing through the adsorbent in column. Desulfurization process is more effective in dynamic nature.

Table 3.6 : Comparison of our study with the adsorbents prepared by the group of Yang.

Adsorbent	Fuel	Sulfur compounds	Adsorption parameters	Adsorption capacity	Breakthrough point	Ref.
Cu-Y	Real LPG	TP	196 mg/L S (350 ppmw S) 0.5 L/h FR† (8.3 cm^3/min)	19.4 mg S/g (100 cm^3 clean LPG/g)	~ 2.8 mg/L S (~5 ppmw)	This study
Cu-Y	Benzene/Octane	TP	190 ppmw S 0.5 cm^3/min FR†	0.22 mmol S/g (7.04 mg S/g)	~ 4 ppmw	[112]
Cu-Y	Commercial Gasoline	TP	335 ppmw S 0.5 cm^3/min FR†	0.14 mmol S/g (4.48 mg S/g)	~ 0.28 ppmw	[113]
Cu-Y	Commercial Diesel	Mixture of TP, BT, DBT	297 ppmw S	0.167 mmol S/g (5.34 mg S/g)	~ 1 ppmw	[114] [42]
AC/Cu-Y	Commercial Diesel	Mixture of BT, DBT	430 ppmw S 0.5 cm^3/min FR†	34 cm^3 clean diesel /g	~ 3 ppmw	[83]

† The abbreviation FR stands for flow rate.

Table 3.7 : Breakthrough adsorption capacities of original and modified adsorbents (C_0: 196 mg/L S).

Adsorbent	Breakthrough capacity (mg S/g)	
	DMDS	TP
NaX	26.4	12.7
Cu-X	36.2	15.5
CuZn-X	33.1	14.6
Zn-X	30.2	13.8
NaY	34.8	15.5
Cu-Y	50.3	19.4
CuZn-Y	45.8	18.1
Zn-Y	40.5	17.0

3.3.6 Adsorption isotherms

Langmuir and Freundlich isotherms were used to understand the interaction between the adsorbate and adsorbent. In this study, adsorption of DMDS and TP onto Cu-X and Cu-Y adsorbents was investigated by fitting static adsorption equilibrium data with initial sulfur concentration in the range of 28-196 mg/L S. The parameters of the adsorption isotherm were calculated by non-linear curve fitting to the experimental data.

The Langmuir model assumes that adsorption occurs on the homogeneous adsorbent surface composed of specific active sites with the same sorption energies and capable of binding the adsorbate. It is also assumed that no interaction takes place between the adsorbed molecules [109]. The Langmuir equation is represented as:

$$q_e = \frac{q_m K_L C_e}{1 + K_L C_e} \qquad \textbf{(3.4)}$$

where q_e (mg/g) is the equilibrium capacity, C_e (mg/L) is the equilibrium sulfur concentration in solution, q_m (mg/g) is the maximum monolayer capacity and K_L (L/mg) is the Langmuir adsorption equilibrium constant. Experimental data are plotted in Figure 3.8(a) and (c) and the results and corresponding regression coefficients (R^2) are shown in Table 3.8.

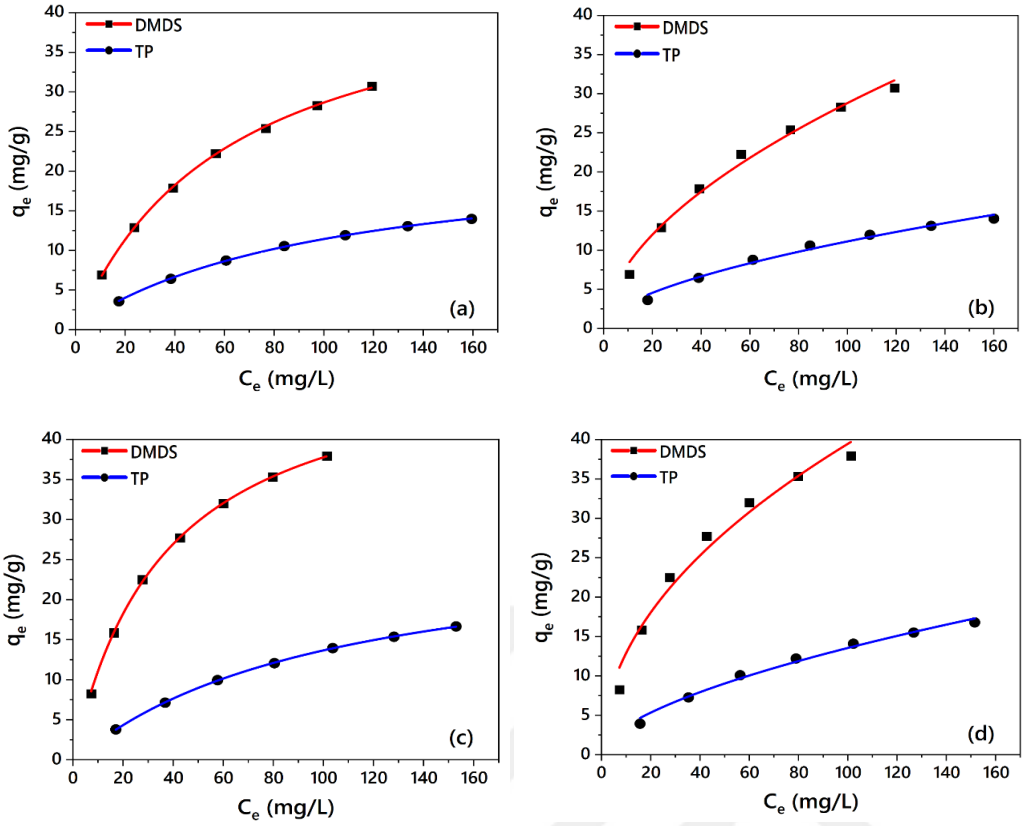

Figure 3.8 : Equilibrium isotherms of adsorption of DMDS and TP on Cu-X (a) Langmuir and (b) Freundlich; Cu-Y (c) Langmuir and (d) Freundlich.

Table 3.8 : Langmuir and Freundlich parameters determined by non-linear fitting for equilibrium DMDS and TP adsorption on Cu-X and Cu-Y.

Adsorbent /Adsorbate	Langmuir parameters				Freundlich parameters			
	q_m	K_L	R^2	R_L	K_F	1/n	n	R^2
Cu-X/DMDS	46.3	0.016	0.999	0.238	2.342	0.545	1.835	0.988
Cu-X/TP	22.9	0.010	0.999	0.342	0.770	0.577	1.734	0.986
Cu-Y/DMDS	51.6	0.028	0.999	0.158	4.211	0.486	2.058	0.976
Cu-Y/TP	28.3	0.010	0.999	0.342	0.917	0.587	1.705	0.990

The R^2 values indicate that the experimental data fit the Langmuir model very well. The maximum DMDS adsorption capacity, q_m, was determined to be 46.3 mg/g and 51.6 mg/g for Cu-X and Cu-Y, respectively. Their TP adsorption capacities, however, are much lower, 22.9 mg/g for the former and 28.3 mg/g for the latter. The maximum adsorption capacities of adsorbents correlated with their surface areas and pore volumes. Adsorption affinity has been quantified by separation factor (R_L) expressed by equation 3.5. Langmuir isotherm can be categorized to irreversible ($R_L = 0$), linear ($R_L = 1$), unfavorable ($R_L > 1$), or favorable ($0 < R_L < 1$) [191]:

$$R_L = \frac{1}{1 + K_L C_o} \tag{3.5}$$

where C_o is the highest initial concentration of the adsorbate (mg/L), and K_L (L/mg) is the Langmuir constant. The data presented in Table 3.8 shows that R_L of Cu-X and Cu-Y adsorbents change between 0 and 1 which indicate that the adsorption of DMDS and TP on these adsorbents is a favorable process.

The Freundlich isotherm is represented by an empirical model that describes heterogeneous adsorption and assumes that the adsorption energy decreases exponentially with surface coverage. This isotherm is given in the following formula:

$$q_e = K_F C_e^{1/n} \tag{3.6}$$

where K_F and n are the Freundlich constants related to the adsorption capacity and intensity, respectively; K_F (mg/g) is the adsorption capacity of the adsorbent and 1/n (g/L) gives an indication of how favorable the adsorption process is. The plots of the experimental data are presented in Figure 3.8(b) and (d) and the results of the Freundlich fit are shown in Table 3.8. The regression coefficients (R^2) obtained for the Freundlich fit are lower than that obtained for the Langmuir fit indicating that the adsorption isotherms fitted better with the Langmuir model for both zeolite adsorbents. The numerical value of $1/n < 1$ indicates that adsorption capacity is only slightly suppressed at lower equilibrium concentration [109].

Figure 3.9 shows the effect of initial sulfur concentration (C_o) on the equilibrium adsorption of DMDS and TP on adsorbents. It is evident that adsorption of these compounds may be considerably enhanced by increasing their initial concentration in LPG. For Cu-Y, the equilibrium DMDS and TP adsorption increased from 8.3 mg/g to 37.9 mg/g and from 4.2 mg/g to 17.1 mg/g, respectively, as the initial sulfur concentration was increased from 28 mg/L to 196 mg/L. A similar trend was observed for both adsorbents. This may result from the fact that mass transfer driving force increases due to the higher concentration gradient developed between the bulk solution and surface of the adsorbent as the initial sulfur concentration in LPG increases [192]. Again, TP adsorption was significantly lower in comparison to that of DMDS. Cu-Y displayed a stronger adsorption ability than Cu-X in the range of initial LPG sulfur concentrations studied. This is consistent with results of the other performance

analysis. The higher surface area and pore volume of Cu-Y adsorbent may provide more void spaces for the adsorption of sulfur compounds.

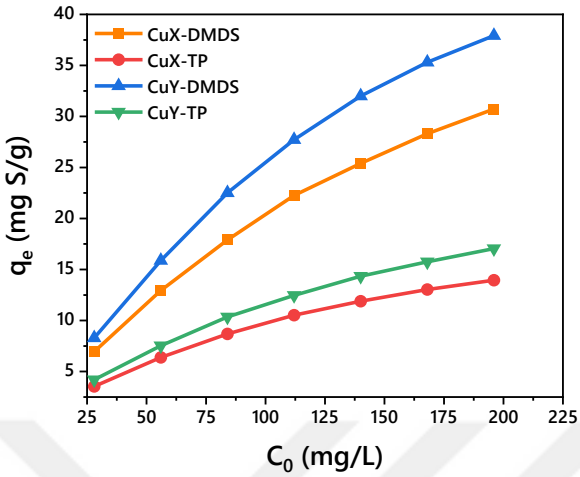

Figure 3.9 : Effect of initial concentration of DMDS and TP in LPG on sulfur uptake of Cu-X and Cu-Y.

3.3.7 Adsorption kinetics

Different kinetic models can be used to gain a better understanding of the adsorption process. For this purpose, pseudo-first-order kinetics (Lagergren model; equation 3.7) which describe the initial stage of the adsorption process, and pseudo-second-order kinetics (equation 3.8) which is based on the adsorption capacity and usually gives good description of the whole adsorption process can be used [193]:

$$q_t = q_e\left(1-e^{-k_1 t}\right) \tag{3.7}$$

$$q_t = \frac{k_2 q_e^2 t}{1+k_2 q_e t} \tag{3.8}$$

where q_e (mg/g), q_t (mg/g), k_1 (min^{-1}), and k_2 (g/mg·min) represent the quantity of sulfur adsorbed at equilibrium, quantity of sulfur adsorbed at time t (min), rate constants for pseudo-first- and second-order kinetics, respectively. The non-linear fitting of the q_t versus t plots are shown in Figures 3.10 and 3.11. The calculated rate constants, the equilibrium adsorption capacities, and the correlation coefficients are given in Table 3.9.

High correlation coefficient (R^2) indicates that the adsorption obeys a pseudo-second-order model which is based on the assumption that the rate limiting step may be

chemisorption involving valence forces through sharing or exchange of electrons between adsorbent and adsorbate [76].

The adsorption kinetic data were also applied to the Weber–Morris equation [191, 192] to gain an insight into the mechanisms and rate controlling steps affecting the adsorption kinetics.

$$q_t = k_i \times t^{1/2} + C \tag{3.9}$$

where C is the intercept (mg/g) which is related to the boundary layer thickness and k_i is the intraparticle diffusion rate constant (mg/g.min$^{1/2}$). The value of C and k_i can be evaluated from the non-linear fitting of q_t versus t in Figures 3.10(c) and 3.11(c). The regions fit with the experimental data on the plots indicate that intraparticle diffusion controls the adsorption process. However, the poorer fitting of intraparticle diffusion model with the experimental data and deviation of the plots indicates that the intraparticle diffusion is not the only rate controlling step [191, 192]. The overall kinetic analysis suggests that the pseudo-second-order adsorption mechanism is predominant and the rate of DMDS and TP adsorption process is controlled by more than one step.

Table 3.9 : Kinetic parameters obtained by non-linear fitting for adsorption of DMDS and TP on Cu-X and Cu-Y.

Adsorbent	Adsorbate	q_e, exp (mg/g)	Pseudo-First Order			Pseudo-Second Order			Intraparticle Diffusion		
			k_1 (min^{-1})	q_e, cal (mg/g)	R^2	k_2 (10^4) (g/mg·min)	q_e, cal (mg/g)	R^2	k_i (mg/g·$min^{1/2}$)	C	R^2
Cu-X	DMDS	30.7	0.0123	28.8	0.879	5.03	33.0	0.975	0.806	12.56	0.971
	TP	13.9	0.0121	13.1	0.914	10.8	15.1	0.988	0.368	5.630	0.955
Cu-Y	DMDS	37.9	0.0140	36.1	0.919	4.94	40.7	0.995	0.899	18.16	0.927
	TP	17.1	0.0141	16.2	0.865	11.3	18.2	0.970	0.401	8.209	0.942

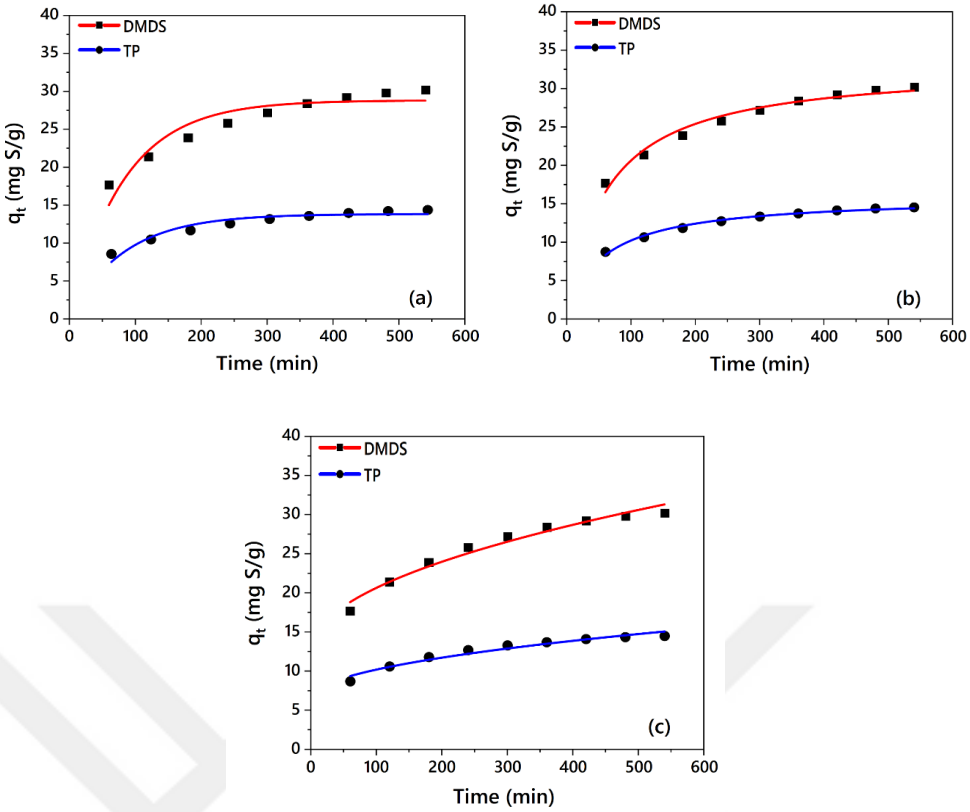

Figure 3.10 : Kinetic plots for adsorption of DMDS and TP over Cu-X: (a) Pseudo-first-order (b) Pseudo-second-order (c) Intraparticle diffusion.

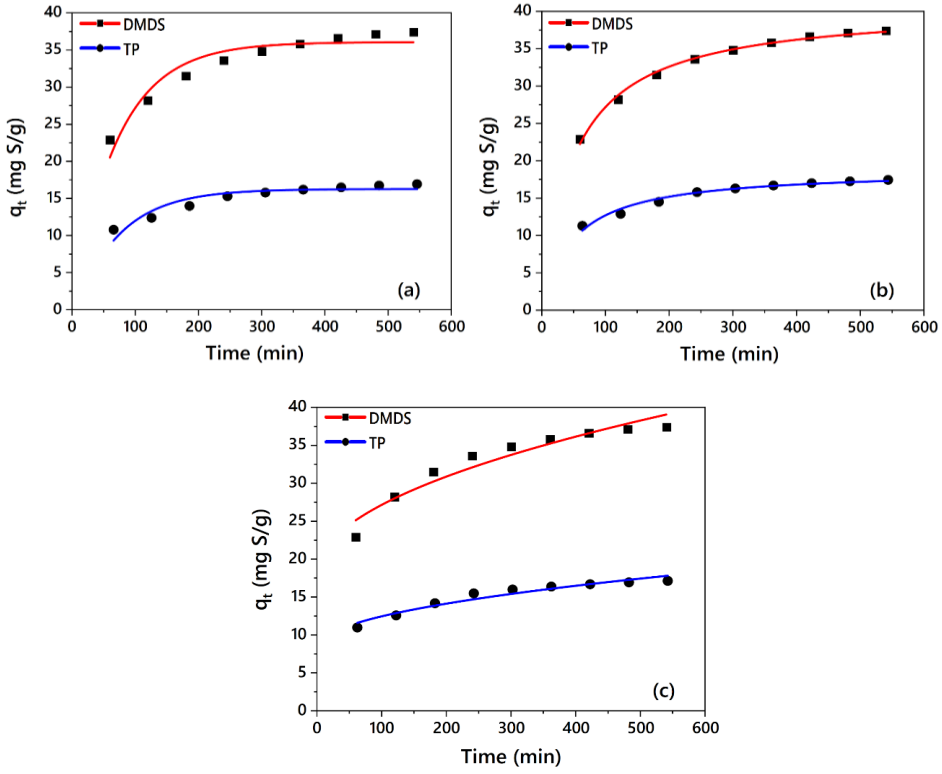

Figure 3.11 : Kinetic plots for adsorption of DMDS and TP over Cu-Y (a) Pseudo-first-order (b) Pseudo-second-order (c) Intraparticle diffusion.

3.3.8 Analysis of the adsorption mechanism

In order to develop a selective adsorbent for desulfurization, it is necessary to understand the nature of interaction between the sulfur compounds and adsorbents. Adsorptive desulfurization can be carried out mainly by selective adsorption and π-complexation mechanisms. DMDS, an aliphatic sulfur compound, can be removed from fuels by selective adsorption based on direct sulfur-metal interaction. As for TP, two different adsorption mechanisms may occur in desulfurization. Thiophene has two pairs of electrons on S atom. One pair is in the six-electron π system and the other lies in the plane of the ring. Consequently, thiophene can act as either an n-type donor by donating the lone pair of electrons of the sulfur atom to the metal (direct S-M bond) or as a π-type donor by utilizing the delocalized electrons of the aromatic ring to form a π-complex with the metal or metal ion [7, 85]. This indicates that thiophenic sulfur compounds can be removed from the transportation fuels either by the formation of direct S-M interaction or by π-complexation.

FT-IR analysis can provide insight information on the interaction between the sulfur molecules and adsorbent. IR spectra showing the shift of bands as compared with free sulfur compounds could give information on whether the sulfur molecule stands end-on (direct S-M bonds) or side-on (π-complexation interaction) on the surface of the adsorbent [16]. The FT-IR analysis of the modified Cu-X and Cu-Y zeolites before and after DMDS adsorption are presented in Figure 3.12. Bands at 1431 and 1416 cm^{-1} can be observed when DMDS is introduced into zeolite structure. The site-specific interaction between sulfur and metal is responsible for this adsorption [122].

Figure 3.12 also shows the IR spectra of Cu-X and Cu-Y zeolites before and after TP adsorption. Peaks can be seen at 1396 cm^{-1} and 1452 cm^{-1} after adsorption of TP. The band at 1396 cm^{-1} is assigned to the perturbed symmetrical C=C stretching vibration of the adsorbed thiophene, which is shifted about 13 cm^{-1} to lower wavenumbers compared to fundamental thiophene ring at 1409 cm^{-1} [107]. The shift to lower wavenumbers caused by a decrease in the electron density of the entire thiophene ring implies that the ring of the adsorbed thiophene molecule is parallel to the surface of the adsorbent [194] which can occur when TP ring is adsorbed on Cu-X and Cu-Y zeolites by π electronic interaction. In addition, the new band at 1452 cm^{-1} is ascribed to the shifting of symmetrical C=C vibrations to higher frequency. This shift is caused by the increased electron density within the C=C–C=C fragment when thiophene is

coordinated via an S atom. It can be concluded that some of the thiophene compound can be removed with an interaction between metal ions of Cu-X and Cu-Y adsorbents and S atoms of thiophene in addition to π-complexation.

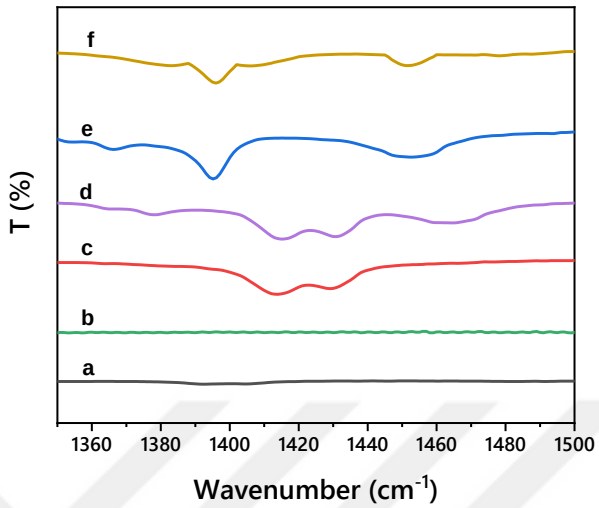

Figure 3.12 : IR spectra of zeolites before and after DMDS and TP adsorption (a) Cu-Y, (b) Cu-X (c) Cu-Y, DMDS, (d) Cu-X, DMDS, (e) Cu-Y, TP, (f) Cu-X, TP.

3.4 Summary

In this work, the adsorptive removal of dimethyl disulfide (DMDS) and thiophene (TP) from real LPG was investigated. These two compounds are among the most common sulfur species that exist in LPG. NaX and NaY type zeolites and new adsorbents prepared by loading Cu^{2+}, Zn^{2+} and Cu^{2+}-Zn^{2+} ions using liquid phase ion-exchange (LPIE) method, were employed for desulfurization. Six adsorbents were prepared and designated as Cu-X, Zn-X, CuZn-X, Cu-Y, Zn-Y and CuZn-Y. The adsorbents were characterized, and their desulfurization performance were tested under both static and dynamic adsorption conditions.

Both zeolites had higher affinity towards Cu^{2+} than Zn^{2+}. The ion-exchange capacity of the zeolites, however, decreased in the ion-exchange conducted with binary Cu^{2+}-Zn^{2+} solution due to the competitive adsorption of ions. Zeolites maintained their original structure after ion-exchange which pointed that ions were successfully dispersed in the zeolites. The experimental findings indicated that ion-exchange could improve Lewis acid sites of the zeolites which enhances the adsorption of sulfur.

Inclusion of copper and zinc ions enhanced the LPG desulfurization performance of the zeolites and followed the order of Cu > CuZn > Zn for DMDS and TP under both static and dynamic desulfurization conditions. Cu-Y displayed the highest sulfur uptake capacity in both the static and dynamic desulfurization tests. The breakthrough adsorption capacity of Cu-Y for DMDS (50.3 mg S/g adsorbent) and TP (19.4 mg S/g adsorbent), measured under dynamic conditions was 45% and 25% higher than that of the original NaY zeolite, respectively. The adsorption of both DMDS and TP on the adsorbents appeared to fit Langmuir adsorption and the pseudo-second-order kinetic models. A mechanistic investigation indicated that Cu-X and Cu-Y adsorbents bind DMDS compound by direct sulfur-metal interaction while both direct sulfur-metal interaction and π-complexation play a role in the TP adsorption onto zeolites. The Cu-Y zeolite is a promising adsorbent and can be potentially used in industrial LPG desulfurization applications.

4. MODIFICATION OF ZEOLITE Y FOR ADSORPTIVE DESULFURIZATION OF LIQUEFIED PETROLEUM GAS

4.1 Introduction

In recent years, the economic and social development of countries depends on the availability, affordability and use of energy. In addition, the discovery of new oil reserves increases the interest in the use of fossil fuels, especially in the transportation sector. However, the increasing demand for fossil fuels is fast becoming a global concern due to the fatal emissions given into the atmosphere [24]. Considerable amounts of organic sulfur compounds may be existed in petroleum-derived transportation fuels. The higher demand for cleaner fuels would also bring stricter regulations to reduce the sulfur content [36].

Liquefied petroleum gas (LPG), a low-carbon fuel, is cleaner and more economic alternative among the fossil-based transportation fuels. Also, the use of LPG is important at the transition point to the 2030 targets specified in Paris climate aggrement. Due to its environmentally friendly nature, LPG causes less carbon emissions, but it still includes some sulfur compounds depending on the production method and source.

To achieve low sulfur (<10 ppm) or zero content in transportation fuels, various factors such as desulfurization methods, cost, type and source of fuel should be considered. Desulfurization of fuels is done by different technologies to lower the sulfur levels to an acceptable limit to meet regulatory standards. Therefore, most of the techniques would still be studied either to replace the hydrodesulfurization (HDS) or to serve as complementary techniques to achieve low sulfur and a greener environment.

Adsorptive desulfurization (ADS) technique has become highly popular among researchers due to its cost advantage and relative ease of operation and adaptability to different fuels. The textural properties of the adsorbent are highly effective on the desulfurization performance. High surface area and pore volume, surface-active sites,

good structural strength and stability are required characteristics for adsorption [18]. To date, different adsorbents have been studied, and the process technology has been modified to achieve ultra-low desulfurization. Various adsorbents such as metal oxide, zeolite, metal framework (MOF), activated carbon were examined for desulfurization [36].

Adsorptive desulfurization is usually accomplished by using solid adsorbents with different porosity and functionalities to reach maximum capacity. Zeolites are widely studied materials for ADS process because of their stable structure and cation-exchange ability. The sulfur adsorption performance of cation-exchanged zeolites are found to be very high thanks to the formation of active sites on the surface. Also, zeolites are known to have high adsorption capacities and potentials for aromatic and aliphatic sulfur compounds. Among the different zeolites, modified Y types such as Ag/Y, Cu/Y, Ce/Y, Na/Y, Ni/Y, La/Y have been reported to significantly improve the adsorption efficiency, selectivity and regeneration due to their adjustable porosity, high ion-exchange capacity and good thermal stability [18].

Wang and co-workers [195] studied the adsorptive desulfurization of model gasoline containing thiophene over Ce(IV)Y zeolite. Ce(IV)Y performed 4.90 mg S/g breakthrough (below 1 μg/g) adsorption capacity. They also investigated the adsorptive desulfurization mechanism via FT-IR characterizations. Results showed that two types of thiophene adsorption onto Ce(IV)Y can exist. Thiophene can be adsorbed onto Ce(IV)Y zeolite by π-interaction and thiophene can interact directly with Ce(IV)Y via sulfur-metal (S-M) interaction. Velu et al. [196] investigated the adsorptive removal of organic sulfur compounds from model jet fuel over Ni loaded Y zeolites. They synthesized Ni-Y zeolites with different Ni loadings by incipient wetness impregnation and liquid-phase ion-exchange methods using NH_4Y and KY zeolites. The prepared Ni-Y zeolites were tested as adsorbents for removing organic sulfur compounds under ambient conditions either without reduction or after reduction around 600 °C. They observed the better sulfur adsorption performance with the Ni-Y zeolite synthesized by ion exchange and reduced before sulfur adsorption. It was reported that the sulfur compounds were adsorbed over the reduced sample by a direct S-M interaction, while their adsorption on the unreduced samples may involve π-complexation.

Modified Y zeolites were developed by Yi et al. [118] and used for the removal of DMDS from model liquid fuels containing 2000 ppm sulfur. Cu(I)-Y zeolite was prepared by ion-exchanging of Na-Y zeolite followed by reduction of Cu^{2+} to Cu^{+} at 450 °C in the inert atmosphere. Results revealed that DMDS is adsorbed on modified Y zeolites via multilayer intermolecular forces and S-M interaction which increase adsorption bond energy of DMDS on the adsorbents. Run-dong et al. [33] prepared Cu-NaY zeolites with different Cu loadings by LPIE method. The adsorptive desulfurization performance of zeolites were evaluated with a model oil containing thiophene by the dynamic adsorption method. All the Cu-NaY samples were treated at 773 K in a flowing nitrogen stream for reduction to enhance the Cu^{+}/Cu^{2+} ratio. The results indicated that the π-complexation of Cu^{+} with thiophene plays a dominant role during the adsorption of thiophene on the Cu(I)NaY zeolite.

In literature, just a few papers have focused on the adsorption of sulfur compounds from LPG onto zeolites [29, 81, 96, 121-123, 197] while significant research has been carried out on desulfurization of diesel, gasoline and jet fuel. In our previous study, we investigated the adsorption of DMDS and TP from real LPG over Cu^{2+}, Zn^{2+} and Cu^{2+}-Zn^{2+}-exchanged NaX and NaY zeolites [197]. Among tested adsorbents, Cu-Y exhibited the best desulfurization performance. But still, it is necessary to study more deeply on Cu-Y zeolite to improve its performance, that is why we need to carry out our current study. To the best of our knowledge, there is not any paper including the detailed research on modification, performance-structure relations, and adsorption mechanisms for desulfurization of LPG. From this point, we prepared modified Cu-Y zeolite in order to improve the desulfurization capacity to purify real LPG in this study. The effects of calcination temperature, metal concentration and initial sulfur concentration on the desulfurization were investigated by static adsorption method. Moreover, we systematically focused on the auto-thermal reduction of copper species, adsorption mechanisms, equilibrium isothermal adsorption and kinetics for both DMDS and TP compounds over Cu-Y zeolite in real LPG. We also examined the structural characterization of prepared zeolites to reveal their relationships with performance.

4.2 Experimental

4.2.1 Materials

NaY (Si/Al: 3.82) zeolite obtained from Zeolyst was used as starting material for preparing ion-exchanged zeolites. Copper nitrate ($Cu(NO_3)_2 \cdot 3H_2O$) with a purity of 98%, was supplied by Merck and used without further purification. Analytical reagent grade DMDS (≥ 99.0%) and TP (≥ 99.0%) were selected as the target aliphatic and aromatic sulfur compounds that commonly exist in real LPG and procured from Sigma-Aldrich. The sulfur rich fuel was prepared with different amounts of S (from 28 to 308 mg/L) in real LPG (<0.28 mg/L S, density: 0.56 kg/L) supplied from Aygaz Company in Istanbul, Turkey.

4.2.2 Adsorbent preparation

The ion-exchanged zeolites used in this study were prepared by liquid phase ion-exchange (LPIE) method. NaY zeolite in powder form was treated with $Cu(NO_3)_2$ aqueous solution at different concentrations (from 0.1 M to 0.5 M) for 12 h at room temperature. After ion-exchange, the zeolite was filtered, washed with plenty of deionized water, and dried in an oven at 105 ºC overnight. Then, the sample was calcined at a designated temperature (from 350 ºC to 750 ºC) for 3 h under N_2 atmosphere and Cu-Y adsorbent was obtained. The adsorbent prepared is labeled as Cu-Y(T-C), where T and C in the parenthesis mean the calcination temperature in ℃ and Cu content loaded on zeolite in wt.%, respectively.

4.2.3 Static adsorption experiments

The adsorption performance of the original and modified zeolites for DMDS and TP removal from LPG were carried out using a batch system described in our previous study [197] and contacted with LPG containing different amounts of sulfur. Adsorbents and LPG were mechanically mixed and conducted for 24 h to be sure that equilibrium had been reached. Elemental sulfur analyzer (Analytik Jena Multi EA 5000) was used to determine total elemental sulfur before and after adsorption experiments. The desulfurization efficiency (R) and sulfur adsorption capacity of adsorbents (q) calculated by equation (4.1) and equation (4.2), respectively:

$$R = \frac{\text{S in feedstock} - \text{S in effluent}}{\text{S in feedstock}} \times 100 \quad (4.1)$$

$$\frac{(C_o - C_e) \times V}{1000 \times m} \quad (4.2)$$

where C_o was the initial sulfur concentration in LPG (mg S/L); C_e was the adsorption equilibrium sulfur concentration in LPG (mg S/L), V was the volume of LPG (mL), and m was the weight of the adsorbent (g).

4.2.4 Auto-thermal reduction of metal ions

The transition metal ions can be reduced in an inert atmosphere at high temperature without the use of a reducing gas. This phenomenon has indeed been proven and is called as auto-reduction or self-reduction [198]. According to the literature, a thermal treatment under inert gas could result in the auto-reduction of the Cu^{2+} species into Cu^{+} ones [199].

The auto-reduction mechanism of cupric ions to cuprous ones in synthetic zeolites has been studied and discussed by various groups. [200-205]. The thermal reduction of Cu^{2+} ions has been assumed to proceed the following mechanism [200-202]:

$$2[Cu^{2+}OH^{-}]^{+} \leftrightarrow [CuOCu]^{2+} + H_2O \quad (4.3)$$

$$[CuOCu]^{2+} \leftrightarrow 2Cu^{+} + 1/2O_2 \quad (4.4)$$

The Cu^{2+} species in the form of $[Cu(H_2O)_4]^{2+}$ may be converted to $Cu^{2+}(OH^{-})$ and H^{+}, after the water molecules are removed [33]. Then, $Cu^{2+}(OH^{-})$ species are condensed by dehydration followed by the formation of Cu^{2+}–O^{2-}–Cu^{2+} dimer or oligomer species and the bridging extra-lattice oxygen atoms are desorbed as oxygen molecules accompanied by reduction of Cu^{2+} ions to Cu^{+} ions [200-202, 206] The self-reduction of the Cu^{2+} species in N_2 atmosphere, which $Cu(OH)^{+}$ species could be converted to Cu^{+}, is illustrated in Figure 4.1.

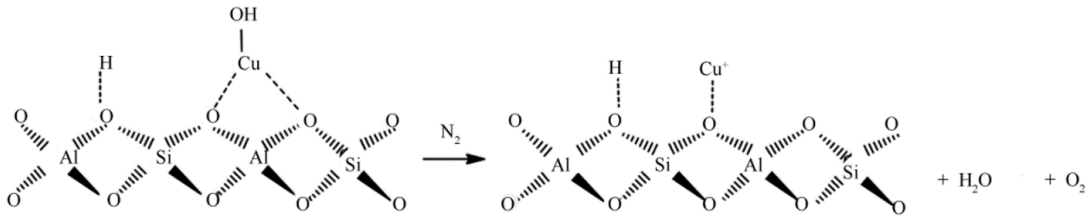

Figure 4.1 : Self-reduction of copper species in modified Y zeolite under N_2 atmosphere [33].

We investigated the auto-thermal reduction of Cu^{2+} ions into Cu^{+} on the Cu-Y zeolite calcinated at 350 ℃ and 550 ℃ in order to understand the effect of temperature.

4.2.5 Characterization of adsorbents

The elemental composition of adsorbents was determined by X-ray fluorescence (XRF) spectrometry (Thermo Fisher Scientific Niton XL3t-980 GOLDD XRF Analyzer). The quantitative results of samples were used to analyze elemental content and their molar ratio.

X-Ray Photoelectron Spectroscopy (XPS) spectra was obtained to determine the chemical state of copper ion on the adsorbent surface. XPS spectra of the samples were taken by a Thermo Scientific K-alpha spectrometer using an aluminum anode (Al Kα= 1468.3 eV) at an electron take-off angle of 90º (between the sample surface and the axis of the analyzer lens). The spectra were recorded using an Avantage 5.9 data system. The binding energy scale was calibrated by assigning the C1 s signal at 284.5 eV.

Surface area, pore volume and pore size of the adsorbents were determined by using a Micromeritics ASAP 2020 analyzer and the data were analyzed based on the Brunaeur, Emmert and Teller (BET) method. Pore size distribution was analyzed by using the Horvath-Kawazoe method.

The surface morphological details were studied with Jeol JSM-6390 LV model Scanning Electron Microscopy (SEM) device which were obtained at a magnification of 5000 times.

4.3 Results and Discussion

4.3.1 Chemical composition of the adsorbents

NaY and Cu-Y zeolites ion-exchanged with 0.1-0.5 M $Cu(NO_3)_2$ solution were characterized by XRF analysis to determine the elemental content. Table 4.1 shows that the amount of Cu ions in the zeolite increases after ion-exchange while the amount of Na ions decreases, as expected. However, the amount of Si and Al ions is almost the same after ion-exchange.

Table 4.1 : Elemental composition of NaY and ion-exchanged Cu-Y zeolites.

Zeolite*	Chemical composition (mmol/g)				Molar ratio		
	Si	Al	Na	Cu	Si/Al	Na/Al	Cu/Al
NaY	12.986	3.396	3.461		3.82	1.02	
Cu-Y(0.1)	13.009	3.387	2.527	0.464	3.84	0.75	0.14
Cu-Y(0.2)	12.970	3.374	1.788	0.830	3.84	0.53	0.25
Cu-Y(0.3)	12.936	3.361	1.106	1.163	3.85	0.33	0.35
Cu-Y(0.4)	12.915	3.351	0.868	1.280	3.85	0.26	0.38
Cu-Y(0.5)	12.905	3.345	0.599	1.415	3.86	0.18	0.42

* () : the concentration of $Cu(NO_3)_2$ solution used in the ion-exchanging.

The Cu/Al molar ratios of Cu-Y zeolites were increased in the range of 0.275-0.421 with increasing $Cu(NO_3)_2$ concentration from 0.1 to 0.5 M. Considering that one Cu^{2+} ion compensates for two aluminum tetrahedral, then the amount of metal ions introduced into the zeolite per available ion-exchangeable site ($2Cu^{2+}/Al^{3+}$) is calculated and changed between 0.28 and 0.84 [109]. This indicates that Cu^{2+} ion-exchange degree attained from 28% to 84% for Cu-Y(0.1)-Cu-Y(0.5) zeolites.

As shown in Table 4.1, the $(2Cu^{2+}+ Na^{+})/(Al)$ ratios calculated for Cu-Y(0.1)-Cu-Y(0.5) varied between 1.020-1.025 which were close to Na/Al ratio (1.019) of the original NaY zeolite. These results indicate that the charge balance between the cations in the zeolite structure maintained and ion-exchange proceeds nearly stoichiometrically.

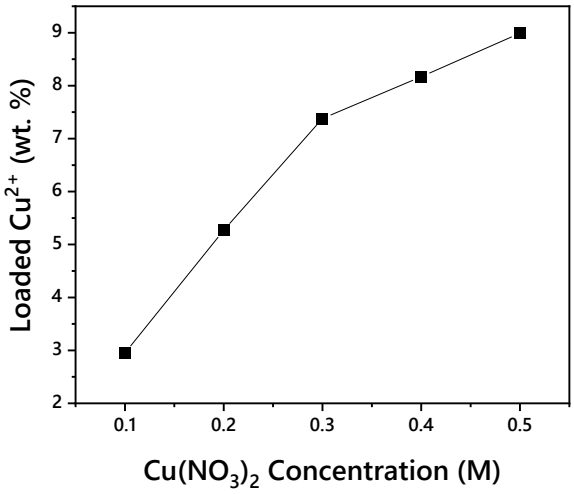

Figure 4.2 : Effect of $Cu(NO_3)_2$ concentration on Cu^{2+} content of zeolite.

The relation between the effect of $Cu(NO_3)_2$ concentration and the amount of Cu^{2+} loaded to zeolite structure is shown in Figure 4.2. It can be seen from Figure 4.2 that the Cu^{2+} content in Cu-Y increases in the range of 3-9 wt.% with $Cu(NO_3)_2$ concentration changes between 0.1-0.5 M. The loading rate of Cu^{2+} is high up to 0.3 M, then it decreases slightly which indicating that Cu^{2+} will be reached equilibrium and does not change significantly above higher concentrations.

4.3.2 Effect of calcination temperature

NaY zeolite was ion-exchanged with 9 wt.% Cu^{2+} and then calcined at different temperatures in the range of 350-750 ºC with intervals of 100 ºC in order to investigate the effect of calcination temperature on the adsorption capacity. The prepared adsorbents were labeled as Cu-Y(T-9), where T is the calcination temperature. Static adsorption experiments were carried out using LPG with 196 mg/L sulfur concentration. The DMDS and TP adsorption performances of NaY and modified zeolites after 24 h of contact time are shown in Figure 4.3.

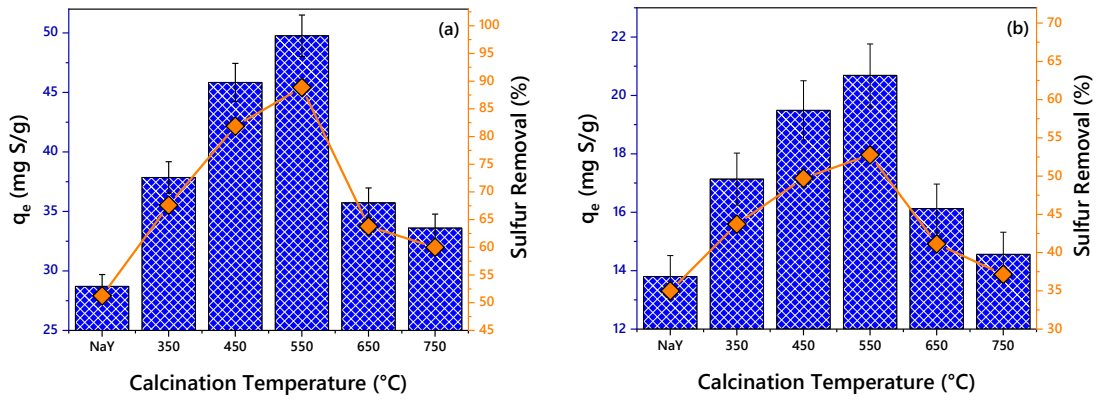

Figure 4.3 : Equilibrium adsorption capacity of Cu-Y zeolites calcined at different temperatures (a) DMDS removal and (b) TP removal.

Figure 4.3 shows that all modified zeolites removed more sulfur than original NaY which performed adsorption capacity of 28.7 and 13.8 mg S/g for DMDS and TP, respectively. The best adsorption performance for both sulfur compounds was obtained for the Cu-Y zeolite calcined at 550 ℃. Figure 4.3(a) displays that Cu-Y(550-9) had the best DMDS removal performance with 49.8 mg S/g adsorption capacity and 89% sulfur removal efficiency. Zeolites modified at different calcination temperatures showed 17-73% increase in DMDS removal capacity compared to the original NaY zeolite. On the other hand, Cu-Y(550-9) displayed the highest TP removal performance with 20.7 mg S/g adsorption capacity and 53% sulfur removal efficiency as shown in Figure 4.3(b). Compared to the the original NaY zeolite, modified zeolites showed 6-50% increase in TP adsorption capacity.

The equilibrium adsorption results revealed that desulfurization performance of zeolites improved with increasing calcination temperature up to 550 ℃. This can be explained with the fact that Cu^{2+} ions reduced into Cu^{+} ones under inert atmosphere at high temperature. As the calcination temperature increases, the auto-reduction of Cu^{2+} species also increases (see Figure 4.4). Since Cu^{+} is a softer acid than Cu^{2+}, it reacts faster and shows higher adsorption performance for the soft bases DMDS and TP [122]. In addition, Cu^{+} ion exhibits the ability to adsorb sulfur via π-complexation which is believed to be responsible for the high thiophene removal capacity [33, 119]. Hence, the interest to the sulfur compounds and adsorption capacity of the zeolites increased with increasing calcination temperature.

Table 4.2 : Equilibrium sulfur adsorption capacity of Cu-Y under different conditions.

Calcination Temperature (°C)	Equilibrium Capacity (mg S/g) [a]		Ion Concentration (wt.%)	Equilibrium Capacity (mg S/g) [b]		Initial Sulfur Concentration (mg/L)	Equilibrium Capacity (mg S/g) [c]	
	DMDS	TP		DMDS	TP		DMDS	TP
350	37.9	17.1	3	35.4	15.8	28	8.1	5.5
450	45.8	19.5	5	44.8	17.1	84	23.7	12.1
550	49.8	20.7	7	54.8	22.4	140	39.4	18.3
650	35.7	16.1	8	52.6	21.7	196	54.8	22.4
750	33.6	14.6	9	49.8	20.7	252	67.0	24.8
						308	74.7	26.1

[a] Ion concentration: 9 wt.%, Initial sulfur concentration: 196 mg/L.
[b] Calcination temperature: 550 °C, Initial sulfur concentration: 196 mg/L.
[c] Calcination temperature: 550 °C, Ion concentration: 7 wt.%.

However, performance results showed that desulfurization capacity decreased obviously at the calcination temperatures higher than 550 ℃. That may be originated from the collapses of crystal structure and decrease in relative crystallinity of the zeolite at high temperatures.

Table 4.2 summarizes the equilibrium adsorption capacities of the modified adsorbents under different conditions. The DMDS and TP adsorption capacities of zeolites calcined at different temperatures were in the order of Cu-Y(550-9) > Cu-Y(450-9) > Cu-Y(350-9) > Cu-Y(650-9) > Cu-Y(750-9). It can be concluded that the calcination temperature has a strong influence on desulfurization capacity of the modified Y zeolites. According to the performance analysis results, optimum calcination temperature was determined as 550 ℃.

4.3.3 Auto-thermal reduction of Cu^{2+} to Cu^{+}

The XPS analysis was carried out to demonstrate the change of Cu^{2+} ions into Cu^{+} ones on the Cu-Y(350-7) and Cu-Y(550-7), and the results are shown in Figure 4.4. Cu^{2+} can be confirmed by the Cu $2p_{3/2}$ binding energy in the range of 933-936 eV and the shake-up satellite contribution. Cu^{+} can be attributed to the binding energy of the XPS band ranging from 932 to 933 eV without any shake-up satellite contribution [119]. As shown in Figure 4.4, the XPS spectra of copper in the Cu-Y(350-7) existed at peaks 932.2 eV, 933.8 and 935.3 eV binding energy were assigned to Cu^{+}, tetrahedral and octahedral Cu^{2+} species, respectively. The characteristic peak of the Cu $2p_{3/2}$ appearing at 932.2 eV can be noticed remarkably in the XPS pattern of Cu-Y(550-7). This is because the increasing of the temperature favors the auto-reduction of Cu^{2+} species to Cu^{+} [199]. Although the auto-reduction of cupric ions to cuprous ions had occurred in an inert atmosphere at high temperatures, the presence of Cu^{2+} had also been observed on the surface of the adsorbents. As a reason of this, it can be said that the Cu^{2+} can not absolutely change into Cu^{+} under the inert atmosphere at 550 ℃. The peak at 944.8 eV in the XPS spectra of the adsorbents indicated the Cu $2p_{3/2}$ shake-up satellite contribution and the intensity decreased as the calcination temperature increased [118].

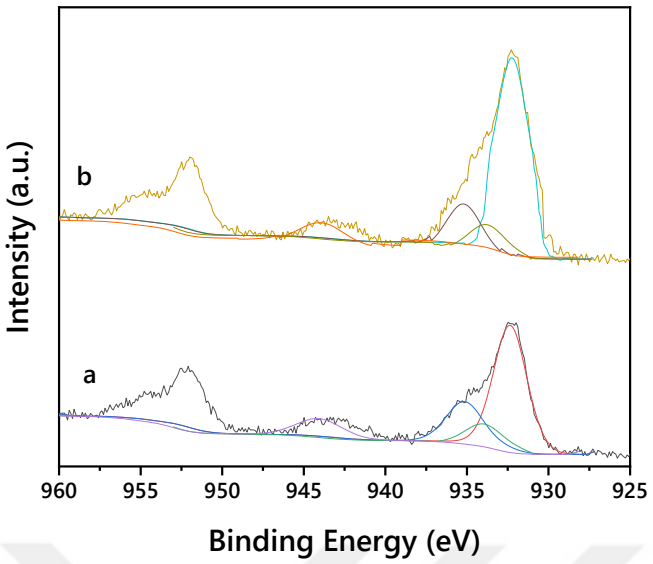

Figure 4.4 : XPS analysis results: (a) Cu-Y(350-7) and (b) Cu-Y(550-7).

Thus, it seems that the Cu-Y material exhibiting highly dispersed copper species allows the reduction of most of the Cu^{2+} species into Cu^{+} ones at 550 °C under N_2 flow. Cu^{+} ions being softer acid with higher interaction to soft basic sulfur compounds had better desulfurization performance. Cu^{+} is a key cation that can form the usual S-M bond and π-complexation with sulfur atoms. As illustrated in Figure 4.3, Cu-Y calcined at 550 °C exhibits the best desulfurization performance, showing that Cu^{+} plays a dominant role and can promote the adsorption of sulfur compounds [199].

4.3.4 Effect of metal concentration

Zeolites loaded with different Cu^{2+} concentration ranging from 3 to 9 wt.% were prepared by liquid phase ion exchange and then calcined at 550 °C. The resulting adsorbents, with different ion concentrations, were labeled as Cu-Y(550-C), where C indicates the weight percentage of Cu^{2+} in the adsorbents. The equilibrium adsorption results of modified zeolites for removal of DMDS and TP are shown in Figure 4.5.

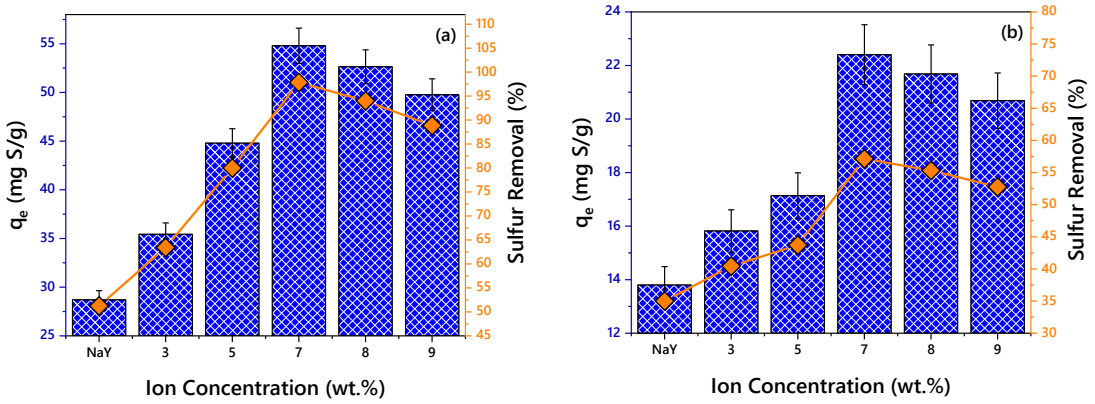

Figure 4.5 : Equilibrium adsorption capacity of Cu-Y zeolites loaded with different Cu^{2+} concentrations (a) DMDS removal and (b) TP removal.

As shown in Figure 4.5, Cu-Y zeolite loaded with 7 wt.% performed the highest adsorption capacity for both sulfur compounds. It can be seen from Figure 4.5(a) that the Cu-Y(550-7) had the best DMDS removal performance with 54.8 mg S/g adsorption capacity and 98% sulfur removal efficiency. Ion-exchanged zeolites showed 24-91% increase in DMDS adsorption capacity compared to the original NaY zeolite. On the other hand, Cu-Y(550-7) zeolite exhibited a TP removal performance with 22.4 mg S/g adsorption capacity and 57% sulfur removal efficiency as shown in Figure 4.5(b). The TP adsorption capacity of modified zeolites was 16-62% higher than the original NaY zeolite.

Table 4.2 shows that the equilibrium DMDS and TP adsorption capacities of ion-exchanged zeolites were in the order of Cu-Y(550-7) > Cu-Y(550-8) > Cu-Y(550-9) > Cu-Y(550-5) > Cu-Y(550-3). Apparently, copper ions loaded into the zeolite structure increased the adsorption performance of zeolites by improving the number of active sites. The desulfurization performance of zeolites increased with $Cu(NO_3)_2$ solution concentration increasing from 0.1 to 0.5 M (Cu ion loaded in the range of 3-9 wt.%). For the Cu-Y zeolite with an over high Cu loading, however, the adsorption capacity is decreased. Presumably, the redundant ions may decrease the active surface area by blocking the active sites of zeolite and adsorption towards sulfur compounds is hindered [33].

BET analysis was performed to investigate the surface area, pore volume and pore diameter of NaY and Cu-Y(550-C) samples ion-exchanged at different concentrations. BET analysis results are presented in Table 4.3. Results show that the textural properties of original NaY zeolite decreased after modification process whereas the

number of active sites is increased. The surface area, pore volume and pore size of NaY zeolite decreased by 4.1-9.4%, 2.8-11.1% and 1.0-4.0%, respectively with incorporating the copper ions in the range of 3-9 wt.%. Table 4.3 also indicates that the textural properties of zeolites decreased as the metal concentration increased. One should keep in mind that not only textural properties but also the number of active sites is important to determine the adsorption capacity of zeolites. This is further supported by the performance results shown in Figure 4.5. Thereof, Cu-Y(550-7) zeolite with high ion-exchange rate and surface area exhibits the best desulfurization performance.

Table 4.3 : Surface area, pore volume and pore diameter of zeolites.

Zeolite	Surface Area (m^2/g)	Pore Volume (cm^3/g)	Pore Diameter (nm)
NaY	659	0.36	0.99
Cu-Y(550-3)	632	0.35	0.98
Cu-Y(550-5)	624	0.35	0.97
Cu-Y(550-7)	615	0.34	0.96
Cu-Y(550-8)	607	0.33	0.96
Cu-Y(550-9)	597	0.32	0.95

SEM analysis was performed to determine the surface morphology of the NaY, Cu-Y(550-7) and Cu-Y(550-9) zeolites. Figure 4.6 shows the SEM patterns obtained with 5.000X magnification. It can be seen from Figure 4.6 that the shape and the homogeneity of the particles in NaY and Cu-Y zeolites are almost the same, which proves the well dispersion of copper ions. Nevertheless, there is slight increase in the number of large particles for Cu-Y(550-9) zeolite. This is also consistent with the performance and textural analysis results.

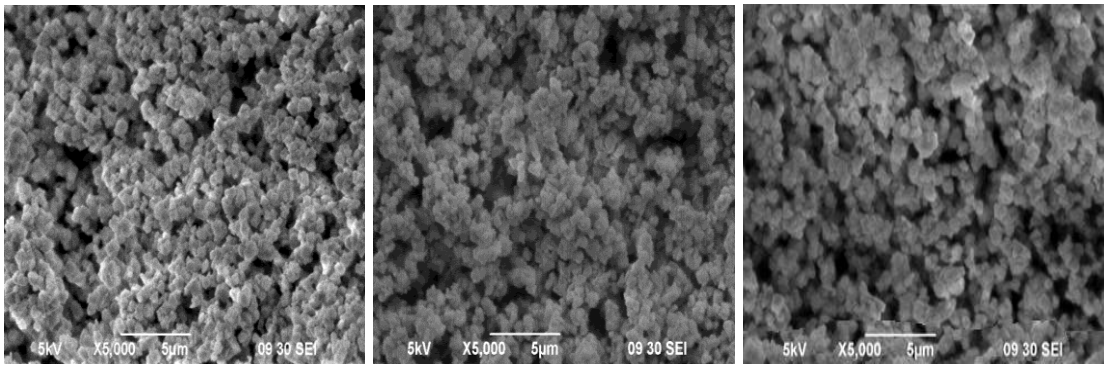

Figure 4.6 : SEM images of (a) NaY, (b) Cu-Y (550-7) and (c) Cu-Y(550-9).

Performance results showed that the optimum modification conditions for Cu-Y zeolite, which has the highest equilibrium sulfur adsorption capacity, was determined as 550 ℃ calcination temperature and 7 wt.% Cu^{2+} loading.

4.3.5 Effect of initial sulfur concentration

The effect of the initial sulfur concentration on the equilibrium adsorption over Cu-Y(550-7) is shown in Figure 4.7. It is observed that the adsorptive removal of DMDS and TP varied with their initial concentration. As shown in Figure 4.7, the sulfur removal efficiency decreases with increasing initial sulfur concentration. However, the equilibrium DMDS and TP adsorption capacities of Cu-Y(550-7) increased from 8.1 mg/g to 74.7 mg/g and from 5.5 mg/g to 26.1 mg/g, respectively, as the initial sulfur content was changed from 28 mg/L to 308 mg/L. This is because as the initial sulfur concentration in LPG increases, the mass transfer driving force between the bulk solution and the adsorbent surface also increases. Besides, Figure 4.7 reveals that the adsorption capacity becomes flat at higher initial S concentrations. This shows that the capacity will reach a constant value over a certain concentration. Cu-Y(550-7) adsorbent performs 100-85% sulfur removal efficiency for DMDS in the range of 28-308 mg/L S concentration whereas TP adsorption efficiency dropped from 98 to 42%. In all experimental conditions, Cu-Y showed higher adsorption performance for DMDS than TP, which is more difficult to remove due to its chemical structure [190].

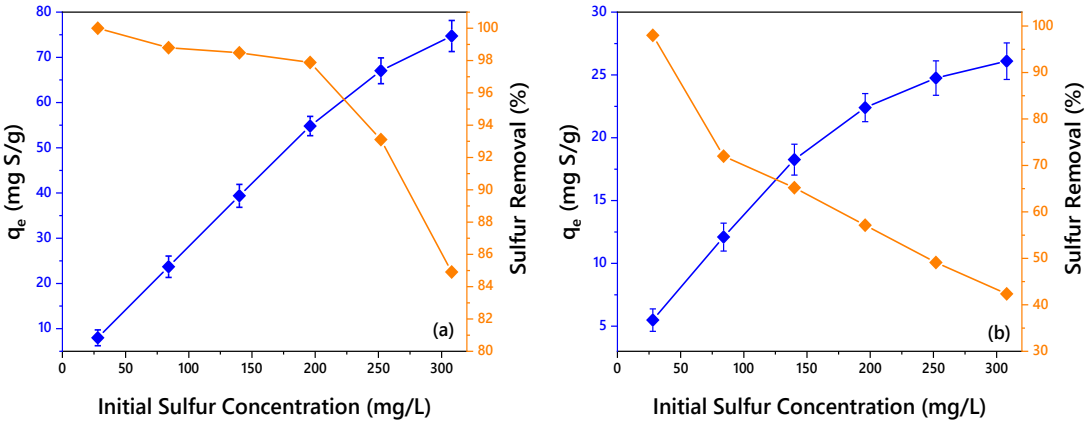

Figure 4.7 : Effect of initial sulfur concentration on equilibrium adsorption capacity of Cu-Y(550-7) (a) DMDS removal and (b) TP removal.

4.3.6 Effect of contact time

The effect of contact time on the sulfur adsorption of Cu-Y(550-7) is shown in Figure 4.8, using LPG with an initial sulfur concentration of 196 mg/L. Figure 4.8 illustrates that the adsorption amount of DMDS and TP increases rapidly at the beginning of the process and then increases slightly for contact time longer than 300 min. The adsorption equilibrium for Cu-Y(550-7) zeolite was achieved after 660 min, and the removal of DMDS and TP reaches 98% and 57%, respectively. As can be seen from Figure 4.8, adsorption of sulfur occurs rapidly at the initial times and then increases gradually with increasing contact time and tends to reach an equilibrium. The initial adsorption rate is faster because of the higher sulfur concentration at the beginning. This also clarified that an increase in the initial sulfur concentration leads to an increase in the adsorption capacity of zeolite, as shown in Figure 4.7.

Figure 4.8 shows that both compounds can be removed in large amount in the first 60 min, and the sulfur adsorption capacity reaches 32.9 mg S/g and 11.4 mg S/g for DMDS and TP, respectively. The residual sulfur concentration is further decreased after 300 min adsorption and keeps almost unchanged with extended period of adsorption. Then, the adsorption of DMDS and TP can readily reach the equilibrium point of 54.8 mg/g and 22.4 mg/g over the Cu-Y(550-7) adsorbent for DMDS and TP, respectively.

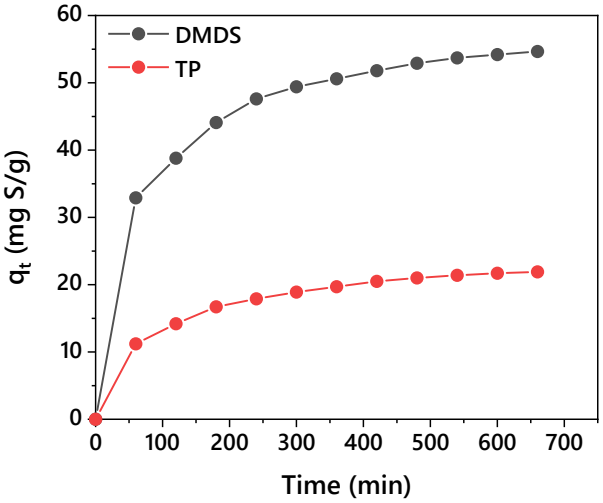

Figure 4.8 : Effect of contact time on the sulfur adsorption of Cu-Y(550-7).

4.3.7 Adsorption isotherms

The equilibrium isothermal adsorption of DMDS and TP on Cu-Y(550-7) was conducted by using LPG with initial sulfur concentration in the range of 28-308 mg/L sulfur. Langmuir and Freundlich isotherm models were used to describe the interaction between the adsorbate and adsorbent.

The Langmuir model is probably the most widely applied adsorption isotherm assuming that there is no lateral interaction between adjacent adsorbed molecules. According to this model, adsorbent surface is homogeneous and each molecule occupies a single surface site [207]. The Langmuir equation is represented in the linear form as:

$$\frac{C_e}{q_e} = \frac{1}{K_L q_m} + \frac{C_e}{q_m} \tag{4.5}$$

where q_e (mg/g) is the equilibrium capacity, C_e (mg/L) is the equilibrium sulfur concentration in solution, q_m (mg/g) is the maximum monolayer capacity and K_L (L/mg) is the Langmuir adsorption equilibrium constant. The slope and intercept of the linear plots of C_e/q_e versus C_e yield the values of $1/q_m$ and $1/K_L q_m$, respectively. Experimental data are plotted in Figure 4.9 and the results and corresponding regression coefficients (R^2) are shown in Table 4.4.

The Freundlich isotherm is represented by an empirical model that describes the surface heterogeneity of adsorbents and gives an exponential distribution of active sites and their energies [90]. This isotherm is given in the following linearized form:

$$\ln q_e = \ln K_F + \frac{1}{n} \ln C_e \tag{4.6}$$

where K_F and n are the Freundlich constants related to the adsorption capacity and intensity, respectively. K_F (mg/g) is the adsorption capacity of the adsorbent and 1/n (g/L) gives an indication of how favorable the adsorption process is. The plots of ln (q_e) against ln (C_e) may be used to determine the constants K_F and n (Figure 4.9). The results of the Freundlich fit of the experimental data and corresponding regression coefficients (R^2) are shown in Table 4.4.

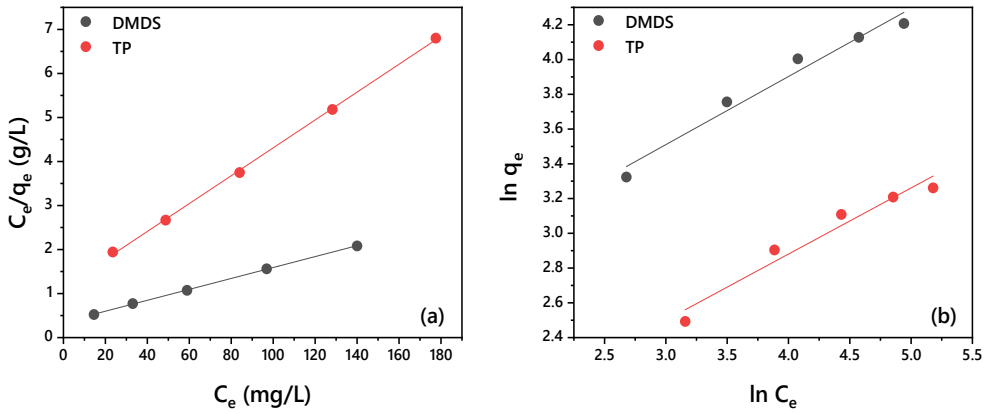

Figure 4.9 : Equilibrium isotherms of adsorption of DMDS and TP on Cu-Y(550-7): (a) Langmuir and (b) Freundlich.

Table 4.4 : Langmuir and Freundlich parameters for equilibrium DMDS and TP adsorption on Cu-Y(550-7).

Adsorbate	Langmuir Parameters				Freundlich Parameters			
	q_m	K_L	R^2	R_L	K_F	1/n	n	R^2
DMDS	80.7	0.035	0.999	0.084	10.33	0.392	2.552	0.960
TP	31.7	0.028	0.999	0.105	3.891	0.381	2.628	0.939

The higher R^2 values verify that the Langmuir model can be used to describe the adsorption isotherm. The maximum DMDS adsorption capacity, q_m, was determined as 80.7 mg/g. Its TP adsorption capacity, however, is much lower, 31.7 mg/g. The maximum adsorption capacity of adsorbent is related to its surface area and pore volume. Adsorption affinity has been quantified by separation factor (R_L) expressed by equation 4.7. Langmuir isotherm can be categorized to irreversible ($R_L = 0$), linear ($R_L = 1$), unfavorable ($R_L > 1$), or favorable ($0 < R_L < 1$) [191]:

$$R_L = \frac{1}{1 + K_L C_o} \tag{4.7}$$

where C_o is the highest initial concentration of the adsorbate (mg/L), and K_L (L/mg) is the Langmuir constant. R_L values range from 0 to 1 as shown in Table 4.4 reveals that the adsorption process of DMDS and TP on the Cu-Y(550-7) is favorable. The regression coefficients (R^2) obtained for the Freundlich model are lower than that obtained for the Langmuir model pointing out that the experimental data meet the Langmuir adsorptive isothermal equation better for Cu-Y(550-7) zeolite. The

numerical value of 1/n < 1 indicates that adsorption capacity is only slightly suppressed at lower equilibrium concentration [109].

The relationship between the equilibrium concentration of DMDS and TP in the solution (C_e) and the experimental and calculated Langmuir and Freundlich equilibrium adsorption capacities of adsorbent (q_e) are shown in Figure 4.10(a) and (b). As seen from Figure 4.10, both C_e and q_e increase with increasing initial sulfur concentration. Initially, q_e increases sharply with the increase of C_e, then changes slightly for higher C_e values. This indicates that sulfur removal efficiency of Cu-Y(550-7) zeolite is higher at lower initial sulfur concentrations whereas adsorption capacity is enhanced with increasing concentration. However, on a sufficiently high concentration, the adsorption capacity of Cu-Y(550-7) tends to the maximum adsorption (q_m). Compared to Langmuir and Freundlich data with experimental one, it is clear that Langmuir model is more in line with the experimental data.

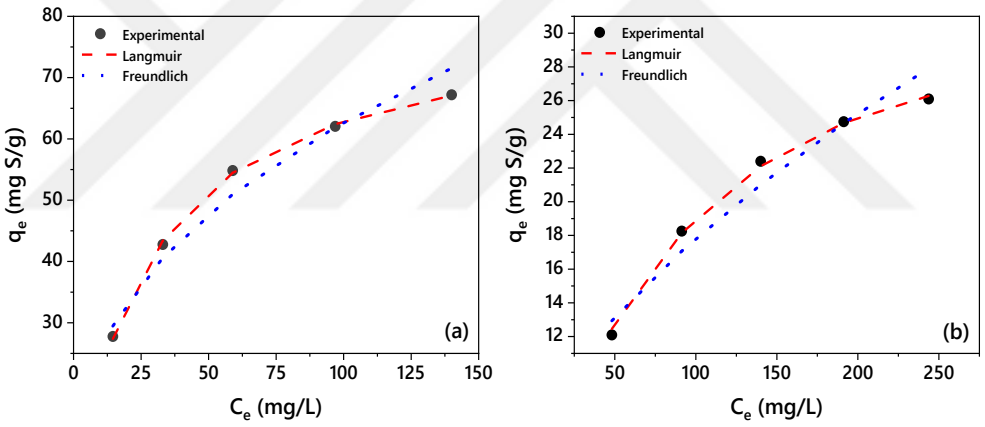

Figure 4.10 : Plot of Experimental, Langmuir and Freundlich models for adsorption of (a) DMDS (b) TP on Cu-Y(550-7).

4.3.8 Adsorption kinetics

The transfer of adsorbate from the solution into the pores of the adsorbent is a complex process and the analysis of adsorption kinetics is important in the design of the adsorption system. Therefore, different kinetic models are used to test the experimental data to gain a better understanding of the adsorption process. For this purpose, the commonly used kinetic models, namely, pseudo-first-order and pseudo-second-order models can be used to investigate the adsorption of sulfur compounds over Cu-Y(550-7). The pseudo-first-order and pseudo-second-order kinetics are given by equations 7 and 8 [193]:

$$\ln(q_e - q_t) = \ln(q_e) - k_1 t \tag{4.8}$$

$$\frac{t}{q_t} = \frac{1}{k_2 \times q_e^2} + \frac{t}{q_e} \tag{4.9}$$

where q_e (mg/g), q_t (mg/g), k_1 (min^{-1}), and k_2 (g/mg.min) represent the equilibrium quantity, the amount of sulfur adsorbed at time t (min), rate constants for pseudo-first- and second-order kinetics, respectively. The k_1 and q_e were calculated from the slope and intercept of the ln (q_e-q_t) versus t plots, respectively, whereas k_2 and q_e were calculated from the slope and intercept of the t/q_t versus t plots, respectively.

In the adsorption process, adsorption behavior may also be represented by the intraparticle diffusion model to gain an insight into the mechanisms [191, 192]. The intraparticle diffusion model is written as:

$$q_t = k_i \times t^{1/2} + C \tag{4.10}$$

where C is the intercept (mg/g) which is related to the boundary layer thickness and k_i is the slope which represents the intraparticle diffusion rate constant (mg/g.$min^{1/2}$). The value of k_i can be evaluated from the slope of the linear plot of q_t versus $t^{1/2}$.

The adsorption kinetic models including pseudo-first-order model, pseudo-second-order model, and intraparticle diffusion model were evaluated to fit the adsorption kinetics of DMDS and TP onto Cu-Y(550-7). Experimental data are plotted, and the results are shown in Figures 4.11. The values of the rate constants, the equilibrium adsorption capacities, and the correlation coefficients are given in Table 4.5. As shown in Table 4.5, the values of q_e calculated from the pseudo-second-order model (59.2 mg/g and 24.6 mg/g) are closer to the experimental q_e values (54.8 mg/g and 22.4 mg/g). High correlation coefficients R^2 (0.999) indicate that the pseudo-second-order model is fit to describe the adsorption kinetics, and the rate limiting step may be chemisorption which defines the sharing or exchange of electrons between adsorbent and adsorbate [76]. As for Figure 4.11(c), the curved and linear parts may be suggested that adsorption proceed via a complex mechanism. The linear portion of plots is the result of intraparticle diffusion effect whereas the deviation of the plots from linearity implies the surface adsorption [120, 208]. The overall kinetic analysis shows that the pseudo-second order adsorption model is suitable for kinetics of adsorptive desulfurization and more than one mechanism is involved in DMDS and TP adsorption process [192, 193].

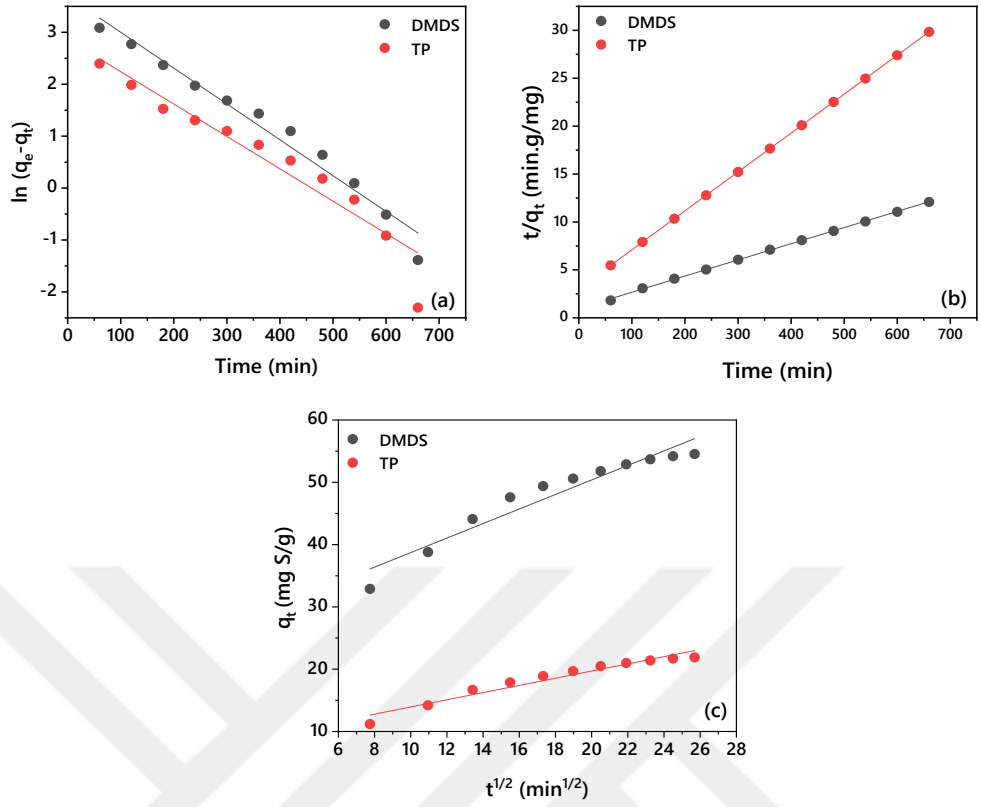

Figure 4.11 : Kinetic plots for adsorption of DMDS and TP over Cu-Y(550-7): (a) Pseudo-first-order (b) Pseudo-second-order (c) Intraparticle diffusion.

Table 4.5 : Kinetic parameters for adsorption of DMDS and TP on Cu-Y(550-7).

Adsorbate	q_e, exp (mg/g)	Pseudo-First-Order			Pseudo-Second-Order			Intraparticle Diffusion		
		k_1 (min^{-1})	q_e, cal (mg/g)	R^2	k_2 (10^4) (g/mg·min)	q_e, cal (mg/g)	R^2	k_i (mg/g·$min^{1/2}$)	C	R^2
DMDS	54.8	0.0069	40.1	0.968	2.90	59.2	0.999	1.166	27.06	0.920
TP	22.4	0.0063	18.9	0.913	5.42	24.6	0.999	0.551	9.123	0.909

Figure 4.12 shows the variation of q_t determined from the experimental data and presented kinetic models with respect to the time for Cu-Y(550-7) adsorbent. It is obvious that the shape of the pseudo-second-order model plot is found in good agreement with the experimental data. Based on the correlation coefficient (R^2), it reveals that the kinetic of DMDS and TP adsorption on Cu-Y(550-7) zeolite can be described with pseudo-second-order model very well.

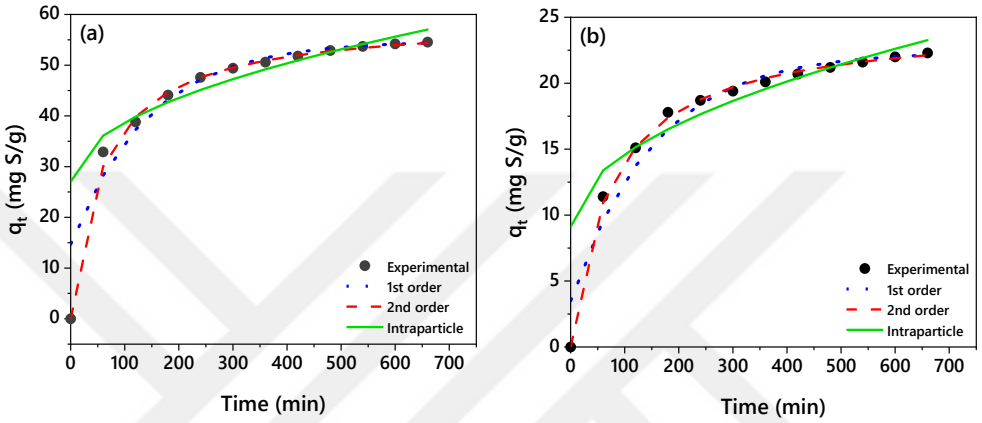

Figure 4.12 : Plot of Experimantal, Pseudo-first-order, Pseudo-second-order and Intraparticle diffusion models for adsorption of (a) DMDS (b) TP on Cu-Y(550-7).

4.4 Summary

In this study, the adsorptive removal of DMDS and TP from the real LPG on ion-exchanged NaY zeolite was investigated. Cu-Y zeolite was prepared by liquid phase ion-exchange and the effect of different parameters on batch adsorption capacity was systematically studied.

Cu-Y zeolite ion-exchanged with 7 wt.% Cu^{2+} ion and calcined at 550 °C exhibited the highest equilibrium sulfur adsorption capacity. Compared to original NaY zeolite, Cu-Y(550-7) exhibited 91% and 62% higher equilibrium DMDS (54.8 mg S/g) and TP (22.4 mg S/g) removal capacities, respectively. The results of the performance analysis revealed that the calcination temperature has great influence on adsorption capacity.

XPS characterizations confirmed the formation of active Cu^{+} species after the thermal treatment under N_2 flow. Results revealed that calcination at 550 °C leads to the auto-reduction of Cu^{2+} ions into Cu^{+} ones in higher amount than calcination at 350 °C, which noticeable increases the adsorbent efficiency. This shows the relation between

the active sites and adsorption desulfurization performance of Cu-Y zeolite towards sulfur compounds. These results also verified the formation of Cu^{+} species which may be ascribed to the π-complexation adsorption as well as S-M interaction.

BET analysis revealed that the modification process decreased the surface area, pore volume and pore size of zeolite. It is clearly seen that the decline in textural properties increases with increasing metal ion concentration. SEM images showed that copper ions were successfully dispersed in the zeolite structure after modification. However, the metal loading over a certain amount caused agglomeration in some regions on zeolite structure and increased the number of large particles, which supported the BET analysis and performance results.

Langmuir isotherm model was best fitted to understand the interaction between the Cu-Y and sulfur compounds. Kinetic studies revealed that the adsorption process followed pseudo-second-order model, exhibiting more accordance with the experimental data.

It is proved that the equilibrium adsorption performance of Cu-Y zeolite can be improved by changing the modification and desulfurization test conditions. Based on these results, the Cu-Y adsorbent can be reported to be efficiently used for adsorptive desulfurization of LPG.

5. DEEP ADSORPTIVE DESULFURIZATION OF LIQUEFIED PETROLEUM GAS OVER Cu ION-EXCHANGED Y ZEOLITE

5.1 Introduction

Sulfur removal from hydrocarbon fuels has recently attracted significant research interest mainly due to the regulations for environmental protection. The emissions originated from commercial fuels are among the main targets of current environmental regulations. European Union (EU) has introduced different emission limits for diesel, gasoline and liquefied petroleum gas (LPG) powered vehicles. The maximum sulfur content was set to be around 10 ppmw for diesel and gasoline fuels in 2009 (European Directive 2009/30/EC). As for LPG (autogas), the sulfur limit value is reduced to 30 ppmw according to EN 589:2018 standard. These limits are expected to become even lower in the coming years.

In order to align with the Paris climate agreement, major world economies have made commitments to reach the ambitious goal of net-zero carbon emission by 2050. EU has recently adopted policies fit for reducing emissions up to 55% by 2030 as compared to 1990 levels [23]. In this regard, the use of low-carbon fuels like LPG may be considered as an important key to achieve the 2030 targets. Among petroleum-derived transportation fuels, LPG with lesser emissions, is more environmentally friendly than others. LPG is also a promising alternative hydrogen source and aerosol propellant because of its environmentally friendly nature, presence of distribution network and cost benefit advantage [178, 179]. However, the commercial LPG may contain certain sulfur compounds depending on its source. Thus, the sulfur content of LPG needs to be reduced to meet ultra-low-sulfur limit requirements (<1 ppm) such as fuel cell applications [43].

Adsorptive desulfurization (ADS) technology has received attention due to its advantages of low energy consumption, variety of applications, and operation at ambient conditions. Moreover, it also enables removal of refractory aromatic sulfur

compounds such as thiophene (TP) and its derivatives, which can be hardly removed by conventional techniques. Development of high-performance, low-cost, and regenerable adsorbents have been the major challenges of the adsorptive desulfurization process. Among the various adsorbents investigated for desulfurization, zeolites are found to be promising due to their high adsorption capacity and affinity toward both aromatic and aliphatic sulfur compounds. Furthermore, the adsorption efficiency and selectivity of zeolites can be improved by introducing metal ions into their structure [18]. There are numerous studies on desulfurization of diesel, gasoline and jet fuel by zeolites and ion-exchanged zeolites. Yang et al. [42, 83, 112-115] reported that sulfur compounds can be selectively removed from diesel and gasoline fuels by π-complexation over Y type zeolites ion-exchanged with transition metals. Velu et al. [85] in their study on desulfurization of jet fuels concluded that the Ce-exchanged Y zeolite can be effectively used for selective adsorption of sulfur compounds by direct sulfur-metal (S-M) interaction. Lee et al. [24] prepared bimetal-exchanged zeolite by ion-exchanging Y zeolite with Cu and Ce to remove organic sulfur compounds in a model fuel. Cu-Ce-Y zeolite displayed high capacity, thanks to the synergistic interaction between the two metal cations which lead to stronger interaction with sulfur compound via π-complexation and σ-bonding.

Although remarkable investigation has been devoted to desulfurization of diesel, gasoline and jet fuel over zeolites, only limited studies have been reported on desulfurization of LPG [29, 96, 121, 122, 197]. Jung et al. [121] prepared Ultra Stable Y (USY) based adsorbents via impregnation method using the rare-earth metals (Ce, La and Pr). Their results indicated that, among the adsorbents examined (Ce (UC-10), La (UL-10) and Pr (UP-10)), Ce-impregnated USY attained the highest dimethyl disulfide (DMDS) and dimethyl sulfide (DMS) adsorption capacities from real LPG. A study on model LPG was reported by Lv et al. [122] for DMDS removal by using ion-exchanged NaY zeolites (Ag_2O/NaY, CuO/NaY, ZnO/NaY, CeO_2/NaY and NiO/NaY). 5 wt.% Ag_2O/NaY adsorbent was found to have the highest breakthrough adsorption capacity thanks to the direct S-Ag^+ interaction. They also used Ag_2O/NaY adsorbent for sulfur removal from real LPG and reported that the performance of the adsorbent in real LPG was lower than that in model LPG.

To the best of our knowledge, our group was the first in the literature to use modified zeolites in removal of both DMDS and TP [197]. We studied adsorptive removal of DMDS and TP from real LPG by Cu^{2+}, Zn^{2+} and Cu^{2+}-Zn^{2+} ion exchanged NaX and NaY zeolites. The desulfurization performance of the zeolites tested followed the order of Cu > CuZn > Zn. The Cu -ion exchanged NaY (Cu-Y) exhibited the highest sulfur adsorption capacity for DMDS (50.3 mg S/g adsorbent) and TP (19.4 mg S/g adsorbent) under dynamic desulfurization conditions [197].

It is evident that new adsorbents with better performance, physical properties, and economical advantage should be developed for ADS. However, there is a lack of systematic and detailed studies on various aspects of adsorptive desulfurization of LPG by zeolites including the adsorption mechanisms, performance-structure relationships, regeneration, adsorption isotherms and kinetics for DMDS and TP. In this work, we further improved the Cu-Y zeolite adsorbent in our previous work to remove DMDS and TP from real LPG. In order to enhance the desulfurization efficiency, we optimized the preparation and operation conditions of the adsorbent by tuning the parameters such as calcination temperature, concentration of $Cu(NO_3)_2$ solution, initial sulfur concentration and LPG flow rate. We paid attention specifically to performance optimization, material characterization, and regeneration in order to explore its full potential.

5.2 Experimental

5.2.1 Materials

NaY (Si/Al: 3.86) zeolite obtained from Zeolyst was used as the starting material for adsorbent preparation. Copper nitrate ($Cu(NO_3)_2 \cdot 3H_2O$) with a purity of 98%, was supplied by Merck and used without further purification. Pyridine (analytical grade, ≥ 99.5%) was supplied by Merck. Analytical reagent grade DMDS (≥ 99.0%) and TP (≥ 99.0%) were selected as the target aliphatic and aromatic sulfur compounds that commonly exist in real LPG and procured from Sigma-Aldrich. The sulfur rich fuel was prepared with varied amounts of S (from 28 to 308 mg/L) in real LPG (<0.28 mg/L S, density: 0.56 kg/L) supplied from Aygaz Company in Istanbul, Turkey.

5.2.2 Adsorbent preparation

The ion-exchanged zeolites used in this study were prepared by liquid phase ion-exchange (LPIE) method. NaY zeolite in powder form was treated with $Cu(NO_3)_2$ aqueous solution of different concentrations (0.1-0.5 M) for 12 h at room temperature. After ion-exchange, the zeolite was filtered, washed with plenty of deionized water, and dried in an oven at 105 ºC overnight. Then, the sample was calcined at a designated temperature (between 350-750 ºC) for 3 h under N_2 atmosphere to obtain the adsorbent (Cu-Y). The adsorbent prepared is labeled as Cu-Y(T-C), where T and C in the parenthesis mean the calcination temperature in ℃ and Cu content loaded on zeolite in wt.%, respectively.

5.2.3 Dynamic adsorption experiments

Dynamic adsorption experiments were assessed through a laboratory scale fixed-bed adsorption system described in our previous study [197]. The LPG stream containing 28-308 mg/L S was pumped from the feed tank and passed through a mass flow controller where the LPG flow rate was adjusted. Then LPG was introduced to the adsorption column at different flow rates varied from 0.5 to 1.5 L/h which correspond to liquid hourly space velocity (LHSV) changing in the range of 5-15 h^{-1}. Temperature and pressure at the entrance and exit of the column were continuously measured. Sulfur content of the effluent sampled at regular intervals was quantified by elemental sulfur analyzer (Analytik Jena Multi EA 5000) whereas the type of sulfur compounds in the fuel was determined by gas chromatography (GC) analysis (Agilent 7890 B, using flame ionization detector (SCD-355).

In the dynamic adsorption experiments, a sulfur concentration of 0.28 mg S/L (5 ppmw) in the effluent was taken as the breakthrough point and the breakthrough sulfur adsorption capacities of the adsorbents were determined based on this concentration. This concentration was chosen to test our adsorbent for more stringent limitations than the current which is 30 ppmw. The sulfur capacity of adsorbents at any time or for a given amount of purified LPG were calculated by the equation 5.1.

$$q = \frac{(C_o - C_e) \times V_p}{1000} \tag{5.1}$$

where C_o is the initial sulfur concentration in LPG (mg S/L), C_e is the sulfur concentration in the effluent (mg S/L), and V_p is the volume of purified the LPG per gram adsorbent at the breakthrough point (mL/g).

5.2.4 Characterization of adsorbents

Elemental composition of the adsorbent was determined by inductively coupled plasma (ICP) analysis (Thermo Scientific XSERIES 2) after microwave assisted acid digestion. The crystalline structures were analyzed by X-ray diffraction (XRD) (Mini Flex Rikagu) with Cu Kα radiation in the 2θ range of 5-50°. The adsorption mechanism between the sulfur compounds and adsorbent was determined by Fourier transform infrared (FT-IR) spectra recorded at room temperature on a Perkin-Elmer FT-IR spectrometer. The type and relative amounts of surface acidic sites of the adsorbents were also measured via FT-IR spectroscopy using pyridine as the probe molecule. 10 mg adsorbent samples were pressed into self-supporting wafers (diameter: 13 mm) and then were exposed to pyridine adsorption. IR spectra of samples were recorded after desorption at 200 °C and 400 °C for 30 min. The Raman spectra analyzes were conducted on a Horiba Jobin Yvon LabRAM HR 800 spectrometer using 633 nm red excitation from a He-Ne laser. The laser power on the sample surface was 3 mW. The Raman scattered light was detected perpendicular to the laser beam with an air-cooled CCD detector, and the spectral resolution was 1 cm^{-1} in all measurements. Surface area, pore volume and pore size of the adsorbents were determined by using a Micromeritics ASAP 2020 analyzer and the data were analyzed based on the Brunaeur, Emmert and Teller (BET) method. Pore size distribution was analyzed by using the Horvath-Kawazoe method. The surface morphological details obtained at a magnification of 10.000 times and Energy Dispersive X-ray (EDX) micro-analysis of adsorbents were studied by Zeiss Ultra Plus field emission scanning electron microscope (SEM).

5.2.5 Regeneration of adsorbents

One of the main criteria in adsorbent selection for industrial applications is reusability of the adsorbent to make desulfurization process economical and environmentally friendly. Adsorbents are needed to be reused for several times to reduce operational and supply costs. In order to evaluate the reusability of Cu-Y adsorbent, thermal regeneration tests were also carried out following the dynamic removal of DMDS and

TP experiments. The effect of the regeneration temperature and regeneration cycle on adsorption capacity were investigated. The sulfur-adsorbed samples were first calcined in air atmosphere for 3 h, in order to let sulfur compounds to leave the active sites of zeolites in the oxidized form. Then the samples were activated under nitrogen atmosphere for 3 h. The regenerated adsorbents were then reused in dynamic tests with LPG containing 196 mg S/L at LHSV = 5 h^{-1} and their performance were compared with fresh adsorbent.

5.3 Results and Discussion

5.3.1 Chemical composition of the adsorbents

The chemical compositions of the original and the Cu-ion exchanged NaY (Cu-Y) zeolites were determined by ICP analysis. Table 5.1 presents that weight percentage of Na ions in zeolite decreases after the ion-exchange while the amount of Cu ions increases, as expected. However, the amount of Si and Al ions remained almost unchanged after ion-exchange. While the concentration of $Cu(NO_3)_2$ solution increases from 0.1 to 0.5 M, the amount of Cu ion incorporated on zeolite changes in the range of 3 to 9 wt.%. The Cu^{2+} amount of zeolite increases rapidly with $Cu(NO_3)_2$ solution increasing up to 0.3 M, then increase rate in wt.% decreases. This shows that the ion-exchange rate finally becomes stable above certain concentrations.

The Cu/Al molar ratios of Cu-Y zeolites increased from 0.13 to 0.43 with increasing $Cu(NO_3)_2$ concentration from 0.1 to 0.5 M. This reveals that ion-exchange ratio of zeolite was changed between 26 and 86% [109]. As calculated from Table 5.1, the molar ratio $(2Cu^{2+}+ Na^{+})/(Al)$ calculated for ion-exchanged zeolite varied in the range of 1.03-1.04 which were comparable to Na/Al ratio (1.02) of the original NaY zeolite. These results suggest that the charge balance between the cations in the zeolite structure was still maintained after the ion-exchange which proceeded almost stoichiometrically.

Table 5.1 : Elemental compositions of the NaY and ion-exchanged Cu-Y zeolites.

Zeolite*	Chemical composition (wt.%)				Molar ratio		
	Si	Al	Na	Cu	Si/Al	Na/Al	Cu/Al
NaY	37.32	9.28	8.10		3.86	1.02	
Cu-Y(0.1)	37.24	9.26	6.02	2.83	3.86	0.77	0.13
Cu-Y(0.2)	37.16	9.24	4.16	5.27	3.86	0.53	0.25
Cu-Y(0.3)	37.10	9.22	2.73	7.44	3.87	0.33	0.35
Cu-Y(0.4)	37.03	9.20	1.93	8.42	3.87	0.25	0.39
Cu-Y(0.5)	36.97	9.19	1.40	9.32	3.87	0.18	0.43

* () : the concentration of $Cu(NO_3)_2$ solution used in the ion-exchanging.

5.3.2 Effect of calcination temperature on the adsorption performance

To investigate the effect of calcination temperature on the adsorption capacity of the adsorbents, NaY zeolite was loaded with 9 wt.% Cu^{2+} ion and then calcined at different temperatures in the range of 350-750 ºC with intervals of 100 ºC. The prepared adsorbents were labeled as Cu-Y(T-9), where T is the calcination temperature. The breakthrough curves of original and Cu ion-exchanged zeolites for removal of DMDS and TP from LPG are shown in Figure 5.1 in which the amount of sulfur in the effluent is plotted as a function of the cumulative volume of the purified LPG.

All modified zeolites adsorbed more sulfur, thus desulfurize more LPG, than the original NaY irrespective of the type of sulfur compound and calcination temperature. At breakthrough point (C_S = 0.28 mg S/L LPG) the sulfur adsorption capacity of the original NaY was 34.8 mg S/g adsorbent and 15.5 mg S/g adsorbent for DMDS and TP, respectively, while the capacities of the Cu-Y(T-9) adsorbents were higher and changed in the range of 39.9-67.3 and 16.4-24.2 mg S/g adsorbent, respectively. This indicates that addition of Cu improved the adsorption capacity of the zeolite up to 15-93% for DMDS and 6-60% for TP.

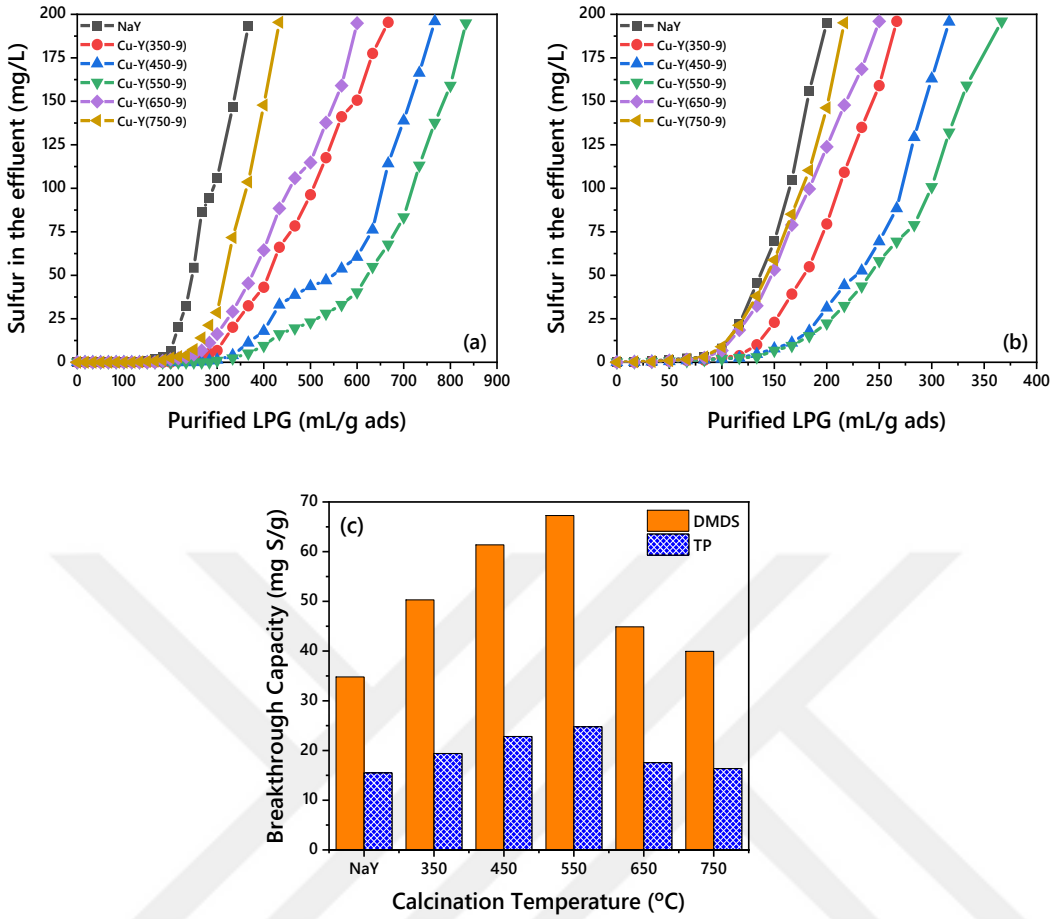

Figure 5.1 : Effect of calcination temperature on desulfurization performance for (a) DMDS and (b) TP removal breakthrough curves, (c) Breakthrough point capacity of adsorbent.

It is clearly seen from the breakthrough curves that the sulfur adsorption capacity of the Cu-Y(T-9) adsorbents is affected by the calcination temperature. The best adsorption performance for both sulfur compounds was obtained for the Cu-Y adsorbent calcined at 550 ºC, Cu-Y(550-9). The sulfur adsorption capacity of Cu-Y(550-9) was 67.3 mg S/g adsorbent for DMDS and completely desulfurized about 283 mL LPG per gram (Figure 5.1(a)). The cumulative amount of DMDS containing desulfurized LPG at the breakthrough point for this adsorbent was about 348 mL. Cu-Y(550-9) also displayed the highest activity with respect to desulfurization of LPG containing TP (Figure 5.1(b)). At breakthrough point, it attained an adsorption capacity of 24.2 mg S/g adsorbent and purified about 128 mL LPG per gram adsorbent.

The breakthrough adsorption results revealed that the desulfurization performance of Cu-Y(T-9) adsorbent improved with increasing calcination temperature up to 550 °C. This may be attributed to the fact that as the calcination temperature increases,

Brønsted acid sites in the zeolite are transformed into Lewis acid sites [209]. Therefore, DMDS and TP, which are Lewis base compounds, could be reacted with Lewis acid sites more easily. Hence, the affinity to the sulfur compounds and adsorption capacity of the zeolites increased. However, efficiency decreased at calcination temperatures higher than 550 ℃. Our findings are compatible with Yi et al. [118] who tested the effect of calcination temperature ranging from 150 ℃ to 650 ℃ over Cu-Y zeolite in a model fuel. They reported that the optimal calcination temperature was 450 ℃ and both the capacity and the crystallinity of the adsorbents decreased remarkably at 650 ℃.

The original NaY and Cu-Y(T-9) adsorbents were characterized by XRD to investigate the crystal structure of zeolites. Figure 5.2 shows the diffraction patterns of the Cu-Y(T-9) zeolites with characteristic peaks positioned at about 2θ = 10.20º, 15.85º, 20.50º, 23.80º and 31.60º which were in line with the patterns of the original NaY zeolite. The comparative examination of XRD patterns of Cu-Y(T-9) do not reveal any disruption in the crystal structures of the adsorbent due to the increase in the calcination temperature. The intensity of the characteristic diffraction peaks, however, decreased at temperatures above 550 ℃. That was consistent with the results of performance analysis which showed a decrease in the capacity at temperatures above 550 ℃. At high temperature the crystallinity of the zeolite structure may deteriorate and partially collapse resulting in a decrease in desulfurization performance.

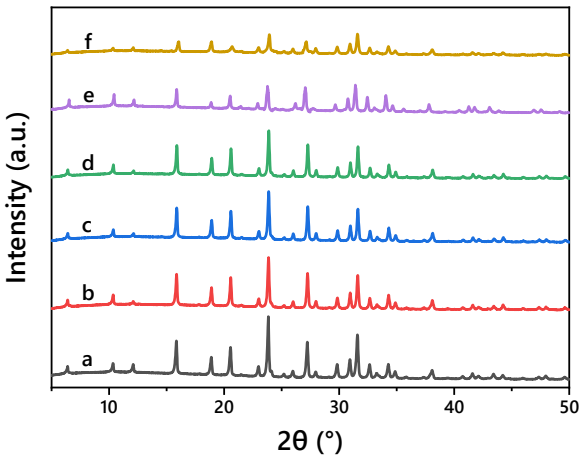

Figure 5.2 : XRD patterns of original NaY and the calcined Cu-Y zeolites: a) NaY, b) Cu-Y(350-9), c) Cu-Y(450-9), d) Cu-Y(550-9), e) Cu-Y(650-9), f) Cu-Y(750-9).

Figure 5.1(c) shows the effect of calcination temperature on the breakthrough adsorption capacity of the adsorbent. The breakthrough DMDS and TP removal capacities of Cu-Y(T-9) adsorbents varied in the decreasing order of Cu-Y(550-9) > Cu-Y(450-9) > Cu-Y(350-9) > Cu-Y(650-9) > Cu-Y(750-9). These results indicated that the calcination temperature could considerably influence desulfurization capacity of the Cu-modified NaY zeolites. The optimum calcination temperature as appeared to be 550 ℃. Table 5.2 summarizes the breakthrough adsorption capacities of the Cu-Y adsorbent under different conditions.

5.3.3 Effect of ion concentration on the adsorption performance

A set of adsorbents loaded with different Cu^{2+} concentration ranging from 3 to 9 wt.% was prepared by liquid phase ion exchange and then calcined at 550 ℃. The resulting adsorbents, with different ion concentrations, were labeled as Cu-Y(550-C), where C indicates the weight percentage of Cu^{2+} in the adsorbents. The copper ion contents of the adsorbents are given in Table 5.1. The adsorbents were tested to determine the effect of Cu concentration on their performance in desulfurization of LPG containing DMDS or TP. Results are presented in Figure 5.3.

The breakthrough curves of original zeolite and Cu-Y(550-C) adsorbents in Figure 5.3(a) and (b) indicate that the LPG desulfurization performance of the adsorbents can be affected by the amount of Cu for both DMDS and TP. The removal of DMDS, however, appeared to be more prone to the effect of Cu concentration as seen in Figure 5.3(a). The breakthrough curves of both sulfur compounds are increasingly shifted to right which indicates an improved performance as the concentration of Cu increased from 3 to 9 wt.% and then moved to the left at higher concentrations. As shown in Figure 5.3, Cu-Y(550-7) adsorbent exhibited the highest adsorption performance for both sulfur compounds. This adsorbent completely desulfurized about 300 mL LPG containing DMDS and desulfurized 390 mL LPG per gram before the breakpoint point was reached. Similar trend was observed for removal of TP from LPG, where up to 143 ml LPG was desulfurized per gram of adsorbent at breakthrough point (Figure 5.3(b)). Overall, the adsorption capacity of zeolite increased up to 27-117% for DMDS and 20-78% for TP after addition of copper ions.

The breakthrough point (C_S = 0.28 mg S/L) sulfur adsorption capacities are plotted as function of Cu concentration in Figure 5.3(c).

The breakthrough DMDS and TP removal capacities of ion-exchanged zeolites were in the order of Cu-Y(550-7) > Cu-Y(550-8) > Cu-Y(550-9) > Cu-Y(550-5) > Cu-Y(550-3). Among all ion-exchanged zeolites, Cu-Y(550-7) exhibited the highest breakthrough adsorption capacity of 75.4 mg S/g and 27.6 mg S/g for DMDS and TP, respectively. It is evident that introducing metal ions into the zeolite structure remarkably increased the number of active sites, which directly affected the adsorption performance of zeolites. While the ion concentration in the solution increased, the ion exchange rate in the zeolite also increased. The desulfurization performance of zeolites increased with the increasing metal solution concentration. However, adsorption capacity decreased slightly at the concentrations above 7 wt.%. Probably, the redundant ions may block the pores and channels of adsorbent that cause decrease in desulfurization performance. Cu-Y(550-7) was determined as the best adsorbent with the highest sulfur removal capacity according to performance analysis results.

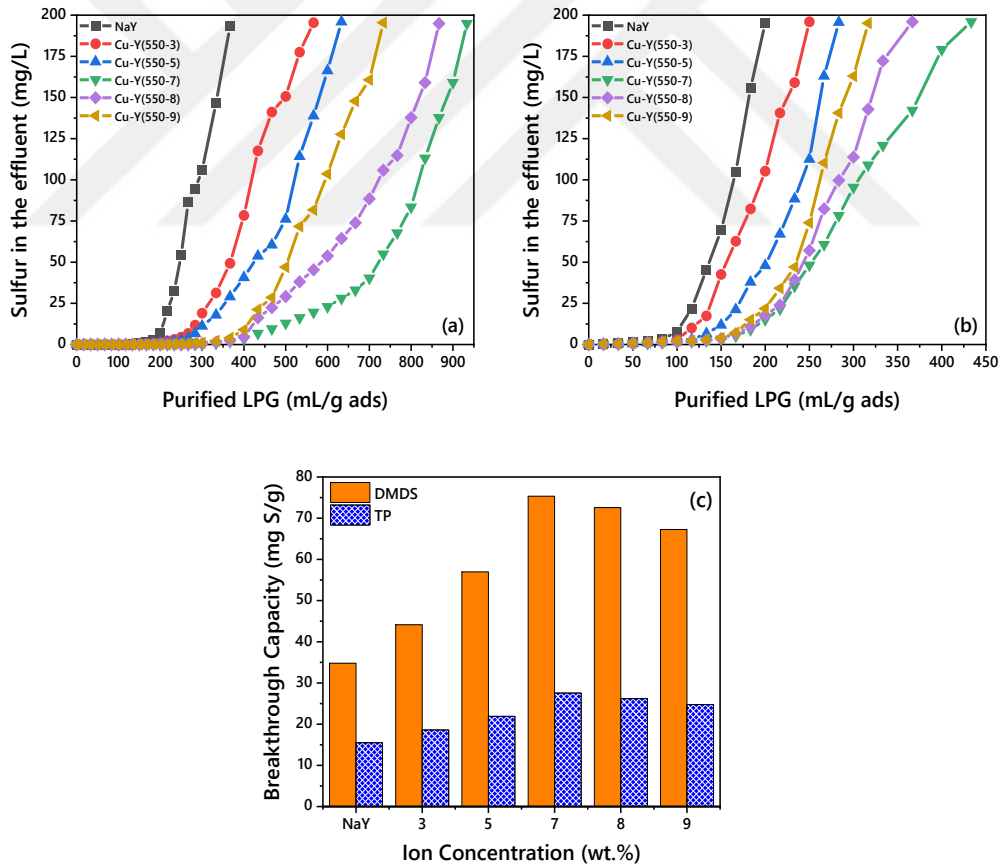

Figure 5.3 : Effect of Cu concentration on the desulfurization performance for (a) DMDS and (b) TP removal breakthrough curves, (c) Breakthrough point sulfur adsorption capacity of the adsorbent.

Table 5.2 : Breakthrough sulfur capacity of Cu-Y under different conditions.

Calcination Temperature (°C)	Breakthrough Capacity (mg S/g) [a]		Ion Concentration (wt.%)	Breakthrough Capacity (mg S/g) [b]		Initial Sulfur Concentration (mg/L)	Breakthrough Capacity (mg S/g) [c]		LPG Flow Rate (h^{-1})	Breakthrough Capacity (mg S/g) [d]	
	DMDS	TP		DMDS	TP		DMDS	TP		DMDS	TP
350	50.3	19.4	3	44.1	18.6	28	15.8	8.7	5	75.4	27.6
450	61.4	22.8	5	57.0	21.9	84	35.7	17.0	7.5	69.3	24.8
550	67.3	24.8	7	75.4	27.6	140	56.3	22.2	10	61.4	22.0
650	44.9	17.6	8	72.6	26.2	196	75.4	27.6	15	55.4	19.3
750	39.9	16.4	9	67.3	24.8	252	88.8	31.3			
						308	97.1	33.1			

[a] Ion concentration:9 wt.%, Initial sulfur concentration: 196 mg/L, LPG flow rate:5 h^{-1}.
[b] Calcination temperature: 550 °C, Initial sulfur concentration: 196 mg/L, LPG flow rate:5 h^{-1}.
[c] Calcination temperature: 550 °C, Ion concentration:7 wt.%, LPG flow rate:5 h^{-1}.
[d] Calcination temperature: 550 °C, Ion concentration:7 wt.%, Initial sulfur concentration: 196 mg/L.

5.3.4 Acidity investigation

The type and amount of surface acidic sites of the adsorbents were determined by pyridine-FT-IR analysis method in order to explore the relationship between adsorption performance and acidic properties of the adsorbents. Adsorbent containing 7 wt.% Cu^{2+} and calcined at 350 ℃, 450 ℃, 550 ℃ were analyzed. Results are presented in Figure 5.4. The vibrations of pyridine adsorbed on the Lewis and the Brønsted acid sites were observed at 1450 cm^{-1} and 1540 cm^{-1} characteristic bands, respectively. The band seen at 1490 cm^{-1} is due to the overlapping signals resulting from the contributions of both Lewis and Brønsted acid sites to pyridine adsorption [186].

The FT-IR patterns of total acid sites recorded at 200 ℃ in Figure 5.4 revealed a considerable increase in the intensity of bands at 1450 cm^{-1} and 1540 cm^{-1} after ion-exchange. As seen in Figure 5.4, NaY has very low Lewis acidity. On the other hand, the characteristic peaks at 1540 cm^{-1} attached to the Brønsted acid sites are not seen in the spectrum. Table 5.3 shows that the total acidity of Cu-exchanged zeolites is higher than the original one. The total acidity of Cu-Y zeolites is nearly 5.5-6.5 fold higher than that of NaY. The IR spectra of strong acid sites of adsorbents were obtained after desorption at 400 ℃, as shown in Figure 5.4. As the desorption temperature increased from 200 ℃ to 400 ℃, the intensity of the bands decreased dramatically due to the weak bonding of pyridine at these sites.

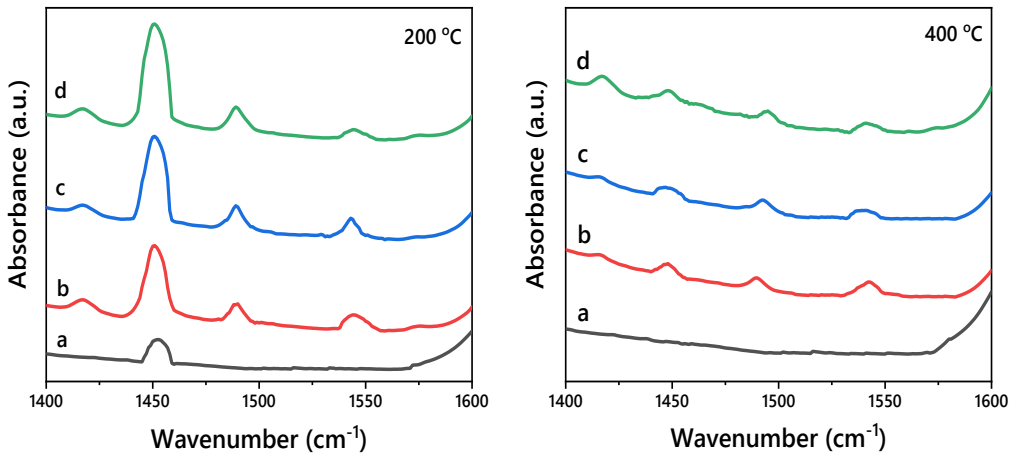

Figure 5.4 : Pyridine-FT-IR spectra of adsorbents at 200 °C and 400 °C. (a) NaY, (b) Cu-Y(350-7), (c) Cu-Y(450-7) and (d) Cu-Y(550-7).

Table 5.3 : Type and amount of surface acidic sites of adsorbents* (μmol/g).

Adsorbent	Total acidity	Total Brønsted	Total Lewis	Strong Brønsted	Strong Lewis	Weak Brønsted	Weak Lewis
NaY	78.17	0	78.17	0	0	0	78.17
Cu-Y(350-7)	501.86	40.51	461.35	32.57	23.31	7.94	438.04
Cu-Y(450-7)	543.16	34.00	509.16	29.39	16.73	4.61	492.42
Cu-Y(550-7)	570.38	26.20	544.18	23.83	15.54	2.37	528.64

*Acidity values were calculated based on the methods reported by Emeis [188].

Table 5.3 shows that Cu-Y(550-7) adsorbent had the highest amount of the Lewis acid sites. The total and Lewis acidity of the adsorbents increased whereas the amount of Brønsted acid sites decreased with increasing calcination temperature from 350 ℃ to 550 ℃. It appears that the Brønsted acid sites were gradually transformed into Lewis acid sites as the calcination temperature increases.

Results suggest that the inclusion of Cu ions improved mainly the Lewis acid centers. Similar results were found by Song et al. [119] who reported that Cu ions are electron acceptors, thus higher Lewis acidity enhances the adsorption of sulfur which is an electron donor element. Comparison of the desulfurization performances and acidity properties of adsorbents (Figure 5.1 and Table 5.3) reveals that the weak Lewis acid sites enhance the interaction between the zeolite and the sulfur compounds. These findings also suggest that NaY zeolite is nearly non-acidic, but its acidity can be enhanced by liquid-phase ion-exchange.

5.3.5 Adsorption mechanism

Cu-Y(550-7) adsorbent was characterized by FT-IR analysis to understand the nature of the interaction between sulfur compounds and the adsorbent. Various adsorption mechanisms are proposed to control the sulfur selectivity of adsorbents. The π-complexation and direct S-M interaction between metal cations and sulfur compounds are considered as the main mechanisms that are responsible for adsorptive desulfurization.

DMDS, an aliphatic sulfur compound, can be selectively removed by adsorption through direct sulfur-metal interaction. On the other hand, two different adsorption mechanisms are likely to be involved in the adsorption of thiophene.

Thiophene has two pairs of electrons attached to the S atom. One pair is in the six-electron π system and the other is in the ring plane. As a result, thiophene can act as

an n-type donor by donating the lone electron pair of the sulfur atom to the metal (direct S-M bond) or as a π-type donor using the displaced electrons of the aromatic ring (π complexation with metal ion) [85]. This suggests that thiophenic sulfur compounds can be removed from fuels either by direct S-M interaction or π-complexation. In addition, Cu metal sites of the adsorbent act as Lewis acid and contribute to binding with the basic sulfur atoms of DMDS and TP compounds [36].

The FT-IR spectra of Cu-Y(550-7) adsorbent recorded before and after DMDS and TP adsorption are shown in Figure 5.5(a). A clear distinction was observed between the fresh and used adsorbents. New peaks seen in the used adsorbents are obviously related to sulfur adsorption. The bands at the 1416 cm^{-1} and 1431 cm^{-1} formed after DMDS adsorption can be attributed to the δas(CH_3) mode of the CH_3–S–S–CH_3 molecule [118, 122]. The selective interaction between metal ion and sulfur is responsible for this adsorption.

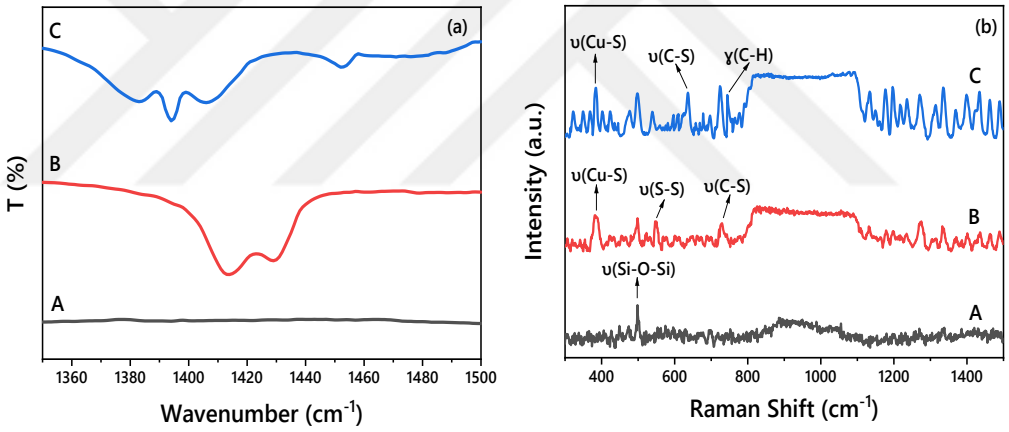

Figure 5.5 : The (a) IR and (b) Raman spectrum of the adsorbents: (A) Fresh Cu-Y(550-7), (B) Cu-Y(550-7) used in DMDS removal, (C) Cu-Y(550-7) used in TP removal.

The fundamental thiophene ring has a peak at 1409 cm^{-1} which is attributed to the perturbed symmetrical C=C stretching vibration [107]. In the IR spectra of the Cu-Y(550-7) zeolite after TP adsorption (Figure 5.5(a)), the peak is seen at 1396 cm^{-1} that is shifted about 13 cm^{-1} to lower wavenumbers compared to fundamental thiophene ring. This shift, caused by a decrease in the electron density of the entire thiophene ring, implies that the ring of the adsorbed thiophene molecule is parallel to the surface of the adsorbent [194]. That may happen when TP ring is adsorbed through π electronic interaction.

The peak at 1452 cm^{-1}, on the other hand, indicates that the symmetrical C=C vibrations are shifted to higher frequencies. It is due to the increased electron density within the C=C–C=C fragment when thiophene is coordinated via an S atom. These results suggest that thiophene compound may be adsorbed on Cu-Y(550-7) adsorbent by both direct S-M interaction and π-complexation. The acidity and performance analysis revealed that Lewis acid sites may improve the S-M interaction between metal cation and sulfur atoms of DMDS and TP.

Raman analysis was conducted for the Cu-Y(550-7) adsorbent before and after DMDS and TP adsorption to investigate the characteristic Cu-S bonds. Figure 5.5(b) presents the analysis results. The peak observed at about 500 cm^{-1} before and after adsorption indicate υ(Si-O-Si) bonding of adsorbent. The peak at 383 cm^{-1} seen after sulfur adsorption presents characteristic Cu-S stretching vibrations and indicates that υ(Cu-S) bond is established in the adsorbent structure [210]. The peaks at 725 cm^{-1} indicate the presence of υ(C-S) bond in the adsorbent after sulfur adsorption. The peaks at 546 cm^{-1} belong to the characteristic disulfide υ(S-S) bond of DMDS [118]. On the other hand, the bands at 637 cm^{-1} and 742 cm^{-1} originated from the υ(C-S) and the ɣ(C-H) bonds of the thiophene ring, respectively [211]. Results indicated that the sulfur atoms of DMDS and TP compounds formed interactions with Cu ions after adsorption.

5.3.6 Effect of liquid hourly space velocity on the adsorption performance

The effect of LPG flow rate on desulfurization performance of Cu-Y(550-7) was investigated under different liquid hourly space velocity (LHSV) varied from 5 to 15 h^{-1}. Figure 5.6 shows the effect of LHSV on the adsorption capacity of the Cu-Y(550-7) adsorbent. The contact time between the adsorbent and LPG decreases with increasing LHSV, resulting in a reduced sulfur adsorption capacity. Increasing LHSV from 5 to 15 h^{-1}, resulted in a decrease of about 26% and 30% in the DMDS and TP adsorption capacity of Cu-Y(550-7) adsorbent, respectively. This is related to the mass transfer phenomenon between the zeolite surface and the LPG stream [122]. Thus, mass transfer takes place more effectively.

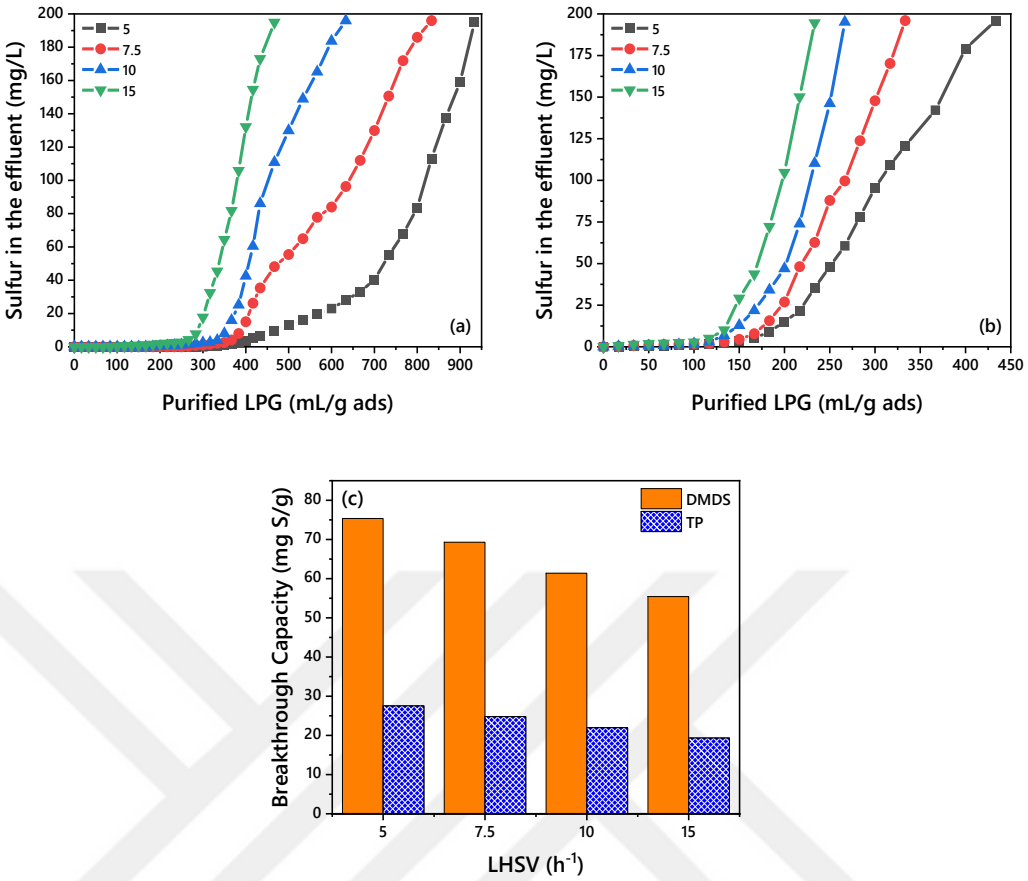

Figure 5.6 : Effect of LHSV on the LPG desulfurization performance for (a) DMDS and (b) TP removal breakthrough curves, (c) Breakthrough sulfur adsorption capacity of Cu-Y(550-7).

5.3.7 Effect of competitive adsorption on the performance

The commercial LPG may contain various sulfur compounds such as dimethyl disulfide and thiophene depending on its supplying source. Therefore, in the course of desulfurization of LPG containing both of these compounds, a competitive adsorption phenomenon may likely take place. In order to investigate the competitive adsorption effect dynamic LPG desulfurization experiments were conducted with LPG containing both single and binary sulfur components for the Cu-Y(550-7) adsorbent. The concentrations of both DMDS and TP in LPG were 196 mg/L in all experiments which were carried out at LHSV = 5 h^{-1} and ceased after the breakthrough point (C_S = 0.28 mg S/L) was reached. The breakthrough point DMDS and TP removal capacities of the Cu-Y(550-7) adsorbent in single and binary systems are shown in Figure 5.7.

The adsorption capacity of the adsorbent for DMDS was higher than that for TP in both cases. Being a refractory aromatic sulfur compound, it is more difficult for

thiophene to interact with the adsorbent and be removed from fuels due to its chemical structure [190]. The sulfur adsorption capacity of the adsorbent decreased for both compounds in binary adsorption, with a far more extent for TP. Compared to the single system adsorption, a drop of about 10% and 43% was observed in the adsorbent capacity for DMDS and TP, respectively. This indicates that Cu-exchanged Y zeolite has higher selectivity for DMDS compound than for TP. The stronger interaction between DMDS and Cu-Y(550-7) might be an important factor leading to the poor selectivity of TP.

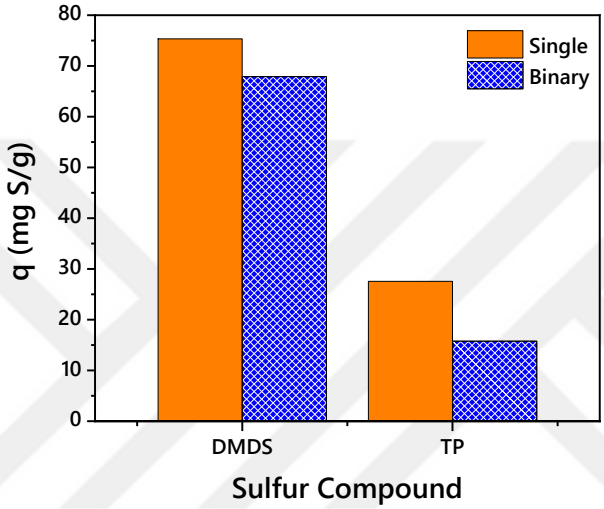

Figure 5.7 : Adsorption capacity of Cu-Y(550-7) in single and binary systems.

5.3.8 Effect of initial sulfur concentration on the adsorption performance

In order to understand the effect of initial sulfur concentration on the adsorbent capacity, Cu-Y(550-7) zeolite was tested with LPG containing sulfur in the range of 28 mg/L to 308 mg/L concentration. Figure 5.8(a) and (b) exhibits the breakthrough curves of Cu-Y(550-7) for removal of DMDS and TP from LPG with varying sulfur concentration.

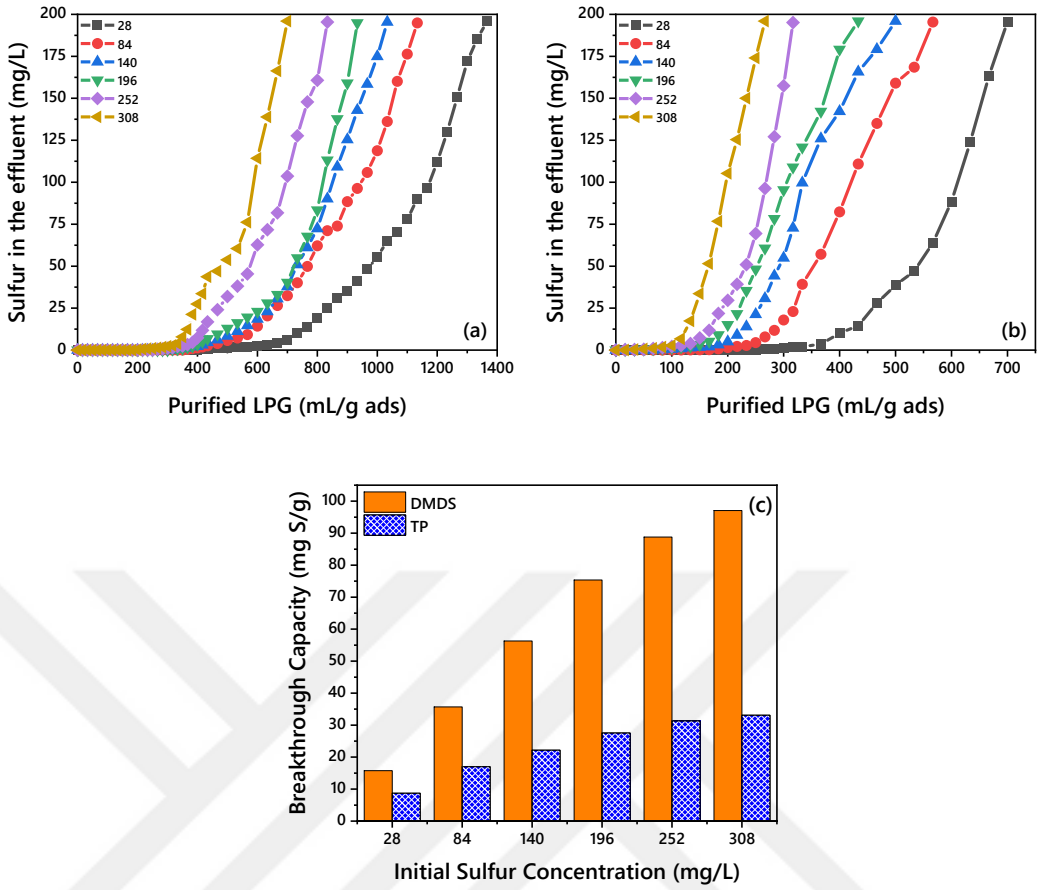

Figure 5.8 : Effect of initial LPG sulfur concentration on desulfurization performance for (a) DMDS and (b) TP removal breakthrough curves, (c) Breakthrough sulfur adsorption capacity of Cu-Y(550-7).

The time needed to reach the breakthrough point sulfur level in the adsorber effluent became longer with decreasing sulfur concentration in LPG. This leaded to an increased amount of desulfurized LPG up to breakthrough point. For an initial 28 mg/L sulfur concentration, about 400 mL DMDS and 183 mL TP was purified per gram of adsorbent at the breakthrough point. The cumulative volume of purified LPG at the breakthrough point decreased approximately 49% and 67% for DMDS and TP, respectively, when initial sulfur concentration increases from 28 mg/L to 308 mg/L. Figure 5.8(c) indicates that adsorption capacity of the adsorbent for both compounds considerably enhanced with increasing initial sulfur concentration in LPG. The breakthrough DMDS and TP adsorption capacities of Cu-Y(550-7) increased about 5 fold and 3 fold, respectively, as the initial concentrations increased from 28 mg/L to 308 mg/L. Obviously, the enhanced mass transfer driving force between the adsorbent and LPG as LPG sulfur concentration increased, led to a substantial improvement in

the adsorbent performance, but to considerably different extents for the two sulfur compounds. However, the rate of adsorption capacity slowed down at higher initial sulfur concentrations likely due to the change in rates of mass transfer and surface adsorption phenomena. Our findings are compatible with that of Lv et al. [122] who studied removal of DMDS (containing 1000 ppmw S) from model LPG. Although no study is reported in the literature regarding the removal of thiophene from LPG, our results are also in line with that of Yang et al. [113] who studied the removal of thiophenic sulfur compounds from commercial gasoline fuel by using Cu ion-exchanged NaY zeolite and reported a breakthrough (~0.28 ppmw) adsorption capacity of 4.48 mg S/g adsorbent slightly lower than our result of 5.88 mg S/g. It should be noted that, the performance of adsorbent materials may be affected by various parameters and experimental conditions of different work in the literature may vary. Therefore, comparison done here can only provide a general perspective about consistency or inconsistency of results and should be considered cautiously.

5.3.9 Regeneration of adsorbents

Cu-Y(550-7) adsorbent was tested in a temperature range of 150-550 ℃ for its regeneration ability in single adsorption-regeneration cycle. Figure 5.9 shows the effect of regeneration temperature on the performance of Cu-Y(550-7) adsorbent where the regeneration degree was determined based on breakthrough adsorbent capacity (q). The breakthrough sulfur adsorption capacity of the adsorbent was considerably affected by the regeneration temperature. The regeneration percentages of the adsorbent were the lowest at 150 ℃, 43% and 39% for DMDS and TP, respectively. Better adsorbent regeneration degrees, however, were attained at higher temperatures for both sulfur compounds. The regeneration degree of adsorbent loaded with DMDS increased from 43% at 150 ℃ to 80% at 550 ℃. A similar trend was also observed in case of TP where adsorbent regeneration was slightly lower but increasing from 39% to 73% in the same temperature range. A better oxidation of the adsorbed sulfur likely take place at higher temperatures which results in higher adsorption capacity and regeneration degrees.

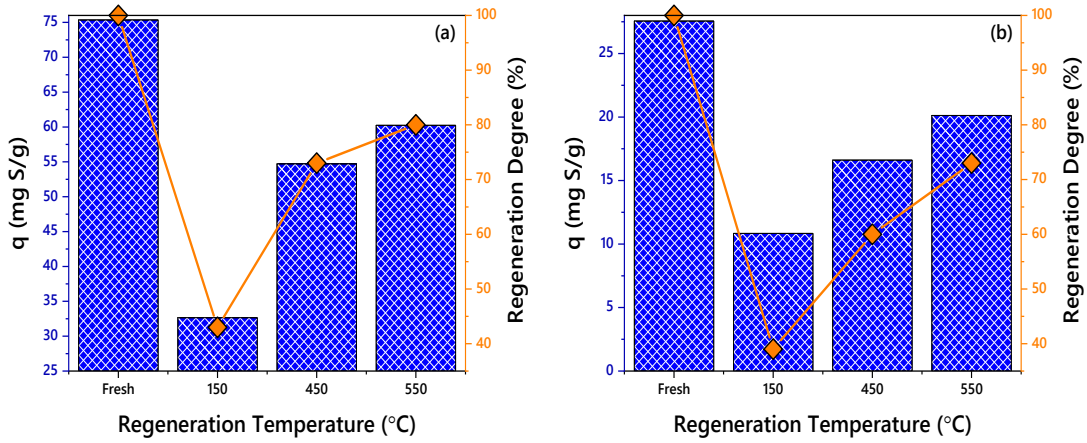

Figure 5.9 : Effect of regeneration temperature on the adsorption capacity and regeneration degree of Cu-Y(550-7) in single adsorption-regeneration cycle (a) DMDS removal and (b) TP removal.

SEM analysis was performed to determine the effect of regeneration process on surface morphology of the adsorbent. SEM patterns of NaY, fresh Cu-Y(550-7) and regenerated Cu-Y(550-7) at 550 °C are shown in Figure 5.10. The homogeneity of the particles, their shape and the spaces between the particles provide information about the structure of the adsorbents. From Figure 5.10(a) and (b), it is seen that the shape and the particle size of NaY and the used Cu-Y(550-7) adsorbent are similar. Although slightly agglomerated particles formed on the surface of the adsorbent after regeneration, especially for TP case, regeneration did not result in a noticeable change in the structure of adsorbent surface (Figure 5.10(c) and (d)).

SEM-EDX analysis was performed for the fresh Cu-Y(550-7), Cu-Y(550-7) used for TP adsorption and Cu-Y(550-7) regenerated at 550 °C after TP adsorption. The surface images and the elemental compositions of the adsorbents are presented in Figure 5.11. Trace amount of sulfur was determined in the fresh adsorbent structure, while a significant amount of sulfur was measured in the used adsorbent after TP adsorption, as expected. The regenerated adsorbent still contains certain amount of sulfur which indicates that TP could not be completely removed by the regeneration process. These results are in line with that in Figure 5.9 and confirm incomplete regeneration of adsorbent even at temperatures as high as 550 °C.

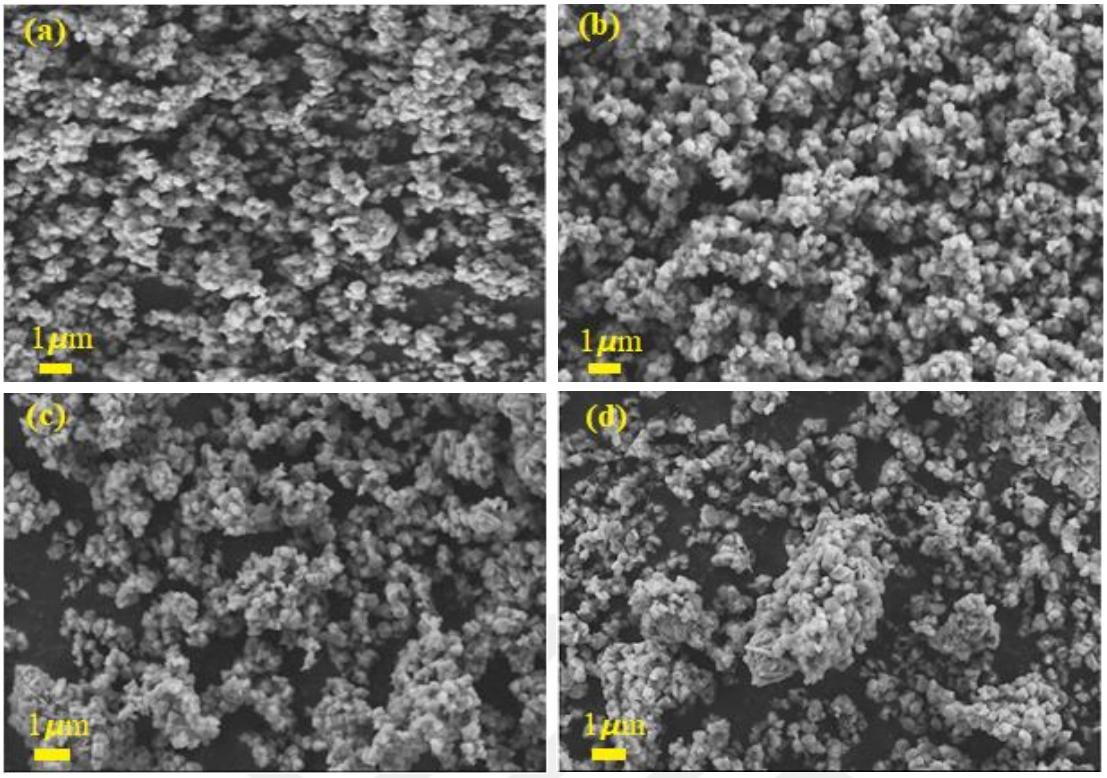

Figure 5.10 : SEM images of adsorbents: (a) NaY, (b) Fresh Cu-Y(550-7), (c) Regenerated Cu-Y(550-7) (DMDS), (d) Regenerated Cu-Y(550-7) (TP).

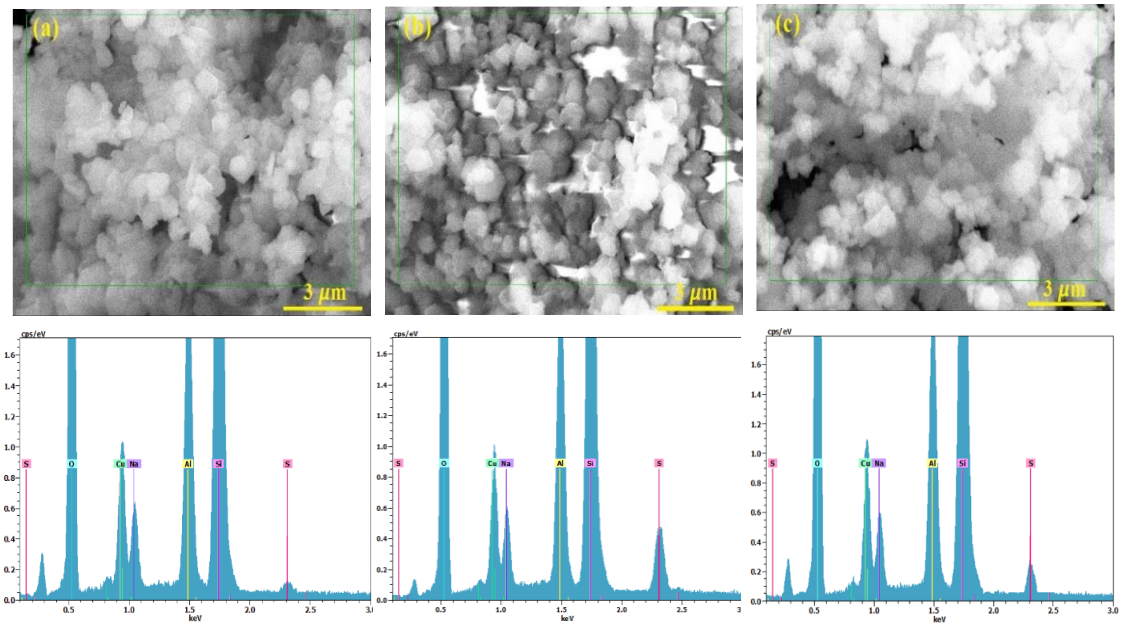

Figure 5.11 : SEM-EDX analysis of adsorbents: (a) Fresh Cu-Y(550-7), (b) Used Cu-Y(550-7) for TP adsorption, (c) Regenerated Cu-Y(550-7) after TP adsorption.

The effect of regeneration cycle on the capacity of the Cu-Y(550-7) adsorbent was studied for up to 3 adsorption-regeneration cycles. Regeneration was performed at 550 °C. Results presented in Figure 5.12 indicate that the breakthrough capacity (q) of the adsorbent diminishes with increasing regeneration cycle for both DMDS and TP. The decrease in the capacity was comparatively high in the first cycle but became rather slower in the following cycles. After the first regeneration cycle, the breakthrough capacity of the adsorbent for DMDS and TP decreased up to 20% and 27%, respectively. After the third cycle, the adsorbent still kept about 70% of its DMDS and 61% of its TP removal capacity. This may stem to some extent from decreasing surface area and pore volume of the adsorbent due to agglomeration occurred during the course of regeneration as confirmed by SEM analysis. The results of the BET analysis in Table 5.4 showed that the surface area and pore volume of the fresh Cu-Y(550-7) adsorbent steadily dropped with increasing adsorption-regeneration cycles. The sulfur remained in the adsorbent structure may contribute to the decrease of adsorption capacity by occupying the active pores.

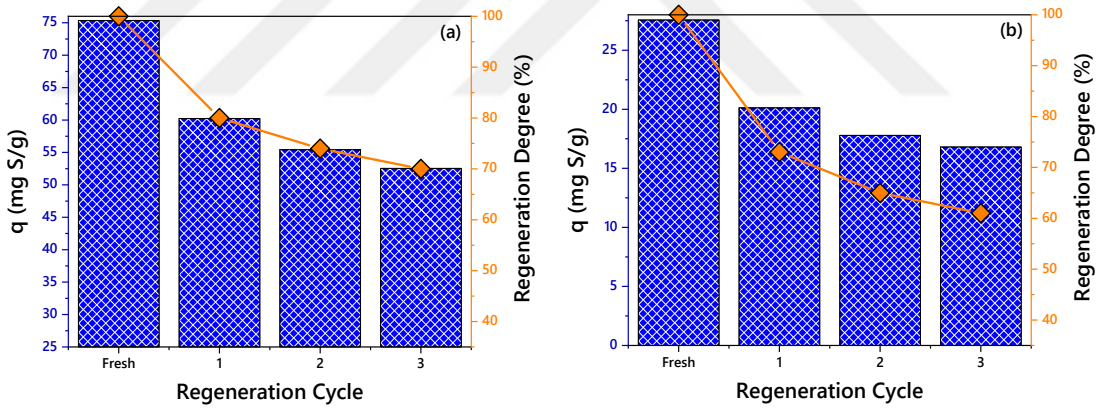

Figure 5.12 : Effect of regeneration cycle on the adsorption capacity and regeneration degree of Cu-Y(550-7) adsorbent (a) DMDS removal and (b) TP removal.

BET analysis was performed to investigate the surface area, pore volume and pore diameter of NaY, used Cu-Y(550-7), and regenerated Cu-Y(550-7) adsorbents (Table 5.4). The textural properties of NaY zeolite worsened after the modification process. Incorporation of copper ions reduced the surface area, pore volume and pore size by 6.9%, 5.6%, and 3.0%, respectively. However, Cu ions increased the number of active sites and consequently improved the adsorption ability of the zeolite. Thus, Cu-Y(550-7) with slightly smaller surface area exhibited higher adsorption capacity than NaY.

Table 5.4 also indicates that the surface area, pore volume and pore diameter of zeolites decreased by regeneration and kept decreasing with increasing number of regeneration cycles. These are consistent with the performance results in Figure 5.12 which displays the reduction in both DMDS and TP adsorption capacities after regeneration. Despite a decrease in the capacity, it is clear that Cu-Y(550-7) adsorbent has a good thermal stability and can be reused efficiently up to 3 cycles without a substantial loss in performance. This makes Cu-Y(550-7) adsorbent highly beneficial for practical use.

Table 5.4 : Surface area, pore volume, and pore diameter of adsorbents through regeneration cycles.

Adsorbent	Surface area (m^2/g)	Pore volume (cm^3/g)	Pore diameter (nm)
NaY	659	0.36	0.99
Fresh Cu-Y(550-7)	615	0.34	0.96
Used Cu-Y(550-7)-R1*(DMDS)	552	0.32	0.93
Used Cu-Y(550-7)-R1(TP)	543	0.32	0.91
Used Cu-Y(550-7)-R2(DMDS)	484	0.31	0.89
Used Cu-Y(550-7)-R2(TP)	465	0.30	0.86
Used Cu-Y(550-7)-R3(DMDS)	427	0.30	0.85
Used Cu-Y(550-7)-R3(TP)	414	0.29	0.79

* R indicates regeneration. The number following R indicates number of regeneration cycles.

5.4 Summary

In this study, the removal of DMDS and TP from real LPG by ion-exchanged NaY zeolite was investigated. Copper ions were successfully dispersed in the zeolite structure by ion-exchange. Cu-ion exchanged adsorbents (Cu-Y) with different Cu loadings were prepared by liquid phase ion-exchange of NaY zeolite. Adsorbents were investigated for their sulfur removal performance through dynamic adsorption tests and the effect of different parameters on adsorption capacity was systematically studied. The adsorbent with the best performance was also exposed to regeneration tests in order to explore its performance in multi-cycle adsorption-regeneration process to explore its full potential. A detailed characterization was carried out to determine the structure-performance relationships. Adsorbent performances were evaluated based on pre-set breakthrough point of 0.28 mg S/L sulfur concentration.

The incorporation of Cu ion to NaY increased its sulfur removal capacity for both DMDS and TP but to different extents. Cu-Y adsorbent containing 7 wt.% Cu^{2+} and

calcined at 550 ℃, Cu-Y(550-7), attained the best sulfur uptake capacity. Its breakthrough point DMDS (75.4 mg S/g adsorbent) and TP (27.6 mg S/g adsorbent) adsorption capacities was about 2.2 and 1.8 times higher, respectively, than that of the NaY zeolite.

DMDS was attached to Cu-Y(550-7) adsorbent by direct sulfur-metal (S-M) interaction while both direct S-M interaction and π-complexation took place in TP adsorption. Results showed that the characteristic Cu-S bond was established in the adsorbent structure after sulfur adsorption. The amount of Lewis acid sites of Cu-Y(550-7) which contributed to the adsorption of sulfur compounds increased by increasing calcination temperature. Calcination at temperatures higher than 550 ℃, however, had a negative impact on the relative crystallinity and performance of the zeolite.

Adsorption-regeneration cycles decreased the surface area and pore volume of Cu-Y(550-7) and caused some agglomeration which resulted in a decrease in adsorption capacity. However, Cu-Y(550-7) has good thermal stability and can be reused efficiently up to 3 cycles by keeping about 70% of its DMDS and 61% of its TP removal capacity. The Cu-Y(550-7) adsorbent proved to be highly beneficial for practical use and efficient for deep desulfurization of LPG.

6. CONCLUSIONS

6.1 Summary and Conclusions

Adsorptive desulfurization is regarded as simple, effective and safe technique that has become of interest to produce cleaner fuels due to its relatively low cost, operation at ambient conditions and environmentally friendly nature. It is important to determine the most suitable adsorbent with high capacity and selectivity for the target sulfur compounds. In this dissertation, different kind of commercial adsorbents were examined in terms of their adsorption capacity towards DMDS and TP compounds. The work adresses three types of commercial adsorbents namely, NaX, NaY and Cu-BTC MOF.

The type of adsorbent material is a crucial factor to determine the adsorption performance. The textural, structural and chemical properties are critical to evaluate the adsorption mechanism. The impacts of these properties on performance are aimed to be understood as the factors that affect the capacity and selectivity of the adsorbent. Hence, specific emphasis was given to detailed characterization of original and modified adsorbents in order to see the relations with performance.

Several modified zeolites were successfully prepared using liquid phase ion-exchange (LPIE) method, which is practical and industrially applicable, in order to improve the adsorption capacity and selectivity of adsorbents. Firstly, modified adsorbents were prepared by loading Cu^{2+}, Zn^{2+} and Cu^{2+}-Zn^{2+} ions into NaX and NaY zeolites. The characterization analyzes of adsorbents were carried out to determine their crystal structure, surface area, surface acidity, ion-exchange rate, and adsorption mechanism, and their desulfurization performance were tested under both static and dynamic adsorption conditions. The performance results of original and modified zeolites obtained from static adsorption experiments were compared with commercial Cu-BTC adsorbent. The equilibrium isotherms and kinetics for adsorption of DMDS and TP

from LPG over modified zeolites were also investigated for the first time in the literature.

Ion-exchange studies revealed that NaX zeolite with lower Si/Al ratio showed a superior ion-exchange capacity in comparison to NaY for both ion types. The affinity of both zeolites towards Cu^{2+} ion was higher than Zn^{2+}. However, the ion-exchange capacity of the zeolites decreased in binary ion solutions due to the competitive effect between ions. Characterization results showed that the zeolite crystal structure remained stable after modification process which pointed that ions were successfully dispersed in the zeolites. However, the textural properties of both zeolites decreased when Na^{+} ion was exchanged.

Performance analysis indicated that incorporation of copper and zinc ions improved the LPG desulfurization performance of the zeolites in the order of Cu > CuZn > Zn for DMDS and TP under both static and dynamic conditions. Among the prepared zeolites, Cu-Y displayed the highest sulfur removal capacity in both desulfurization tests. The Cu-Y zeolite proved to be a strong alternative to Cu-BTC with its cost-benefit advantage. On the other hand, the dynamic adsorption capacity of Cu-Y measured at 2.8 mg/L (5 ppmw) breakthrough point for DMDS (50.3 mg S/g adsorbent) and TP (19.4 mg S/g adsorbent) was 45% and 25% higher compared to original NaY zeolite, respectively.

The relationship between adsorption performance and acidic properties of the zeolites was explored by investigating the surface acidic sites of the adsorbents. Results proved that the Cu ions improve mainly the Lewis acid sites of the zeolites and increase the sulfur adsorption capacity. A mechanistic investigation on the interaction between the sulfur molecules and adsorbent revealed that DMDS compound is attached to Cu-X and Cu-Y adsorbents via direct sulfur-metal interaction while both direct sulfur-metal interaction and π-complexation play a role in the TP adsorption onto zeolites. The Cu-Y zeolite is considered as a promising adsorbent for industrial LPG desulfurization but still, it is necessary to study more deeply on Cu-Y zeolite to improve its performance. That is why we needed to carry out the following studies with Cu-Y.

In the second experimental part, the detailed research on the optimization of modification parameters, performance analysis, and adsorption mechanism was studied. The effects of calcination temperature, metal concentration and initial sulfur

concentration on the desulfurization were investigated by static adsorption method. Moreover, we systematically focused on the auto-thermal reduction of copper species, equilibrium isothermal adsorption and kinetics for both DMDS and TP compounds over Cu-Y zeolite in real LPG. The structural characterization of prepared zeolites was also examined to reveal their relationships with performance.

Cu-Y zeolite ion-exchanged with 0.3 M $Cu(NO_3)_2$ solution (loaded 7 wt.% Cu^{2+}) and calcined at 550 ℃ exhibited the highest equilibrium sulfur adsorption capacity. As comparison to original NaY zeolite, Cu-Y exhibited 91% and 62% higher equilibrium DMDS (54.8 mg S/g) and TP (22.4 mg S/g) removal capacities, respectively. The results of the performance analysis revealed that the calcination temperature has great influence on adsorption capacity. The formation of active Cu^{+} species, being softer acid with higher interaction to soft basic sulfur compounds, after the thermal treatment under N_2 flow was also confirmed. Results revealed that calcination at 550 °C leads to the auto-reduction of Cu^{2+} ions into Cu^{+} ones in higher amount than calcination at 350 °C, which noticeable increased the adsorbent efficiency.

The modification process decreased the surface area, pore volume and pore size of zeolite. It is clearly seen that the decline in textural properties increases with increasing metal ion concentration. Surface images showed that copper ions were successfully dispersed in the zeolite structure after modification. However, the metal loading over a certain amount caused agglomeration in some regions on zeolite structure and slightly increased the number of large particles, which supported the textural analysis and performance results.

The results of adsorption isotherm study indicated that Langmuir model was best fitted to the equilibrium adsorption of DMDS and TP onto Cu-Y. The overall kinetic analysis shows that the pseudo-second order model is suitable for kinetics of adsorptive desulfurization. In this model rate limiting step may be assumed as chemisorption and adsorption process of DMDS and TP involves more than one mechanism.

Studies carried out in this part proved that the equilibrium adsorption performance of Cu-Y zeolite can be improved by changing the modification conditions. Based on these results, the Cu-Y adsorbent can be reported to be efficiently used for adsorptive desulfurization of LPG. However, further research and development is required to convert the batch process into continuous system for the industrial applications of the

ADS process. Because operating in continuous system and upgrading to industrial scale would be easier and more economical for adsorptive desulfurization. Thus, we continued our studies in dynamic nature in the following part.

Apparently, new adsorbents with better performance, physical properties, and economical advantage should be developed for ADS. Furthermore, there is not any systematic and detailed study on desulfurization of LPG over zeolites. To close the gap in this area, we paid attention to adsorption interactions, performance-structure relations, and regeneration to explore its full potential in dynamic system. In order to improve the desulfurization efficiency, it is worth studying the optimization of adsorbent preparation and operational conditions. Therefore, the effect of calcination temperature, concentration of $Cu(NO_3)_2$ solution, initial sulfur concentration, competitive adsorption between sulfur compounds and LPG flow rate were studied. Cu-Y zeolite was characterized for its chemical composition, crystal structure, surface acidity, adsorption mechanism, textural properties and surface morphology.

Cu-Y zeolite loaded with 7 wt.% Cu^{2+} (70% ion-exchange degree) and calcined at 550 °C exhibited the best sulfur uptake capacity. The breakthrough DMDS (75.35 mg S/g adsorbent) and TP (27.56 mg S/g adsorbent) removal capacities of Cu-Y zeolite was 117% and 78% higher than those of the original NaY zeolite, respectively.

A detailed characterization was conducted to determine the adsorption mechanism. Results showed that Cu-Y binded DMDS by direct sulfur-metal (S-M) interaction while TP was adsorbed onto zeolite by both direct S-M interaction and π-complexation. The characteristic C-S, Cu-S and S-S bonds were established in the Cu-Y after sulfur adsorption. Acidity analysis showed that the amount of Lewis acid sites, which enhanced the sulfur adsorption, increased with the increasing calcination temperature. It was consisted with the results in previous part, which confirmed the auto-reduction of Cu^{2+} ions into Cu^{+} ones as calcination temperature increases. On the other hand, calcination temperatures above 550 °C caused decrease in both relative crystallinity and performance of zeolite.

Surface images showed that copper ions were successfully dispersed in the zeolite structure after modification. Adsorption-regeneration process caused reduction in textural properties and agglomeration in some regions on zeolite which results decrease in adsorption capacity. However, Cu-Y has good thermal stability and can be

reused efficiently up to 3 cycle that makes it highly beneficial and economical for the practical use. The Cu-Y adsorbent proved to be useful for deep desulfurization of LPG in industrial applications.

This thesis is a kind of university-industry collaboration study that develops solution for a problem of the fuel indusrty. Therefore, we considered not only the academical novelty of our study, but also its industrial applicability which requires adsorbents with high desulfurization performance as well as affordable cost.

With the success of this thesis, it will be possible to comply with the EN 589 standard in advance, to become independent from the LPG supply source, and to reduce the procurement cost, thus the import cost paid abroad. The process of removing sulfur from LPG with high-performance and economical modified adsorbents, which have not yet been used commercially in our country, is important and necessary in terms of reducing the foreign trade deficit and foreign dependency commercially.

6.2 Recommendations for Future Research

With the development of high-capacity, selective and reusable ion-exchanged zeolites, and confirming their potential use as adsorbent material, the adsorptive desulfurization process can be readily applied in industrial scale.

Adsorptive separation with zeolites has become a popular topic with a significant industrial prospect. The fundamental mechanism is guest-host interaction for the separation of target molecules. Different types of interactions like physisorption and chemisorption, which might be combined with non-equilibrium diffusion phenomena can take place on zeolite structure. The unique structure of zeolites can provide more possibilities in adsorptive separations but zeolite should be developed on a target basis in order to make separation process simple. The size of the sulfur compounds is effective in the ease of removal by the adsorbent and thus affects the performance of the adsorption process. For this purpose, improvement of modification techniques, and process conditions should be studied in detail to develop the most suitable adsorbents for specific sulfur compounds.

The development of selective and economical adsorbents is an ongoing research area. The adsorption performance of zeolites is strongly dependent on the structural, textural and acidic properties and the number of active sites present on the framework.

Modification of zeolites by incorporation of metal ions improves the physicochemical properties of the adsorbents. Additionally, the acidity properties of zeolites can be enhanced via ion-exchange which increases the number of active sites and makes zeolite structure more convenient for sulfur adsorption. The sulfur adsorption mechanisms on ion-exchanged zeolites seemed to depend on the type and the state of the cation, but this still awaits more investigation for clarification. Further research should focus on the increase in the number of Lewis acid sites in order to improve the S-M interaction and π-complexation for desulfurization.

Although one of the most studied challenges is to develop high capacity and selective adsorbents via ion-exchange process, the mechanism behind the adsorption phenomena is still needed to understand better. Thus, the research should be steered towards advanced characterization of the ion-exchanged zeolites as well as performance analysis. This would give more information about the mechanism of adsorption and how ion-exchange process affects the structure-performance relation.

Even though the high-capacity adsorbent materials are developed and process conditions being improved, more research on continuous systems with real feedstocks should be studied to enhance its chances to be successful in commercial scale. This is to account for the effects of other substances exist in the fuel. Because the real feedstock contains different compounds that may hinder adsorption of sulfur compounds through competitive adsorption and affects the performance of the whole adsorption process. In literature, very few reports are available on the adsorptive desulfurization of real fuels. Most of the studies done with model fuels show good removal performance, but not effective for real fuels. Hence, more emphasis are required to properly determine the efficiency of adsorbents in real fuels.

The studies on lab-scale indicate that modified zeolite-based adsorbents can be used for desulfurization of real LPG to produce ultra-low fuel, however, more effective ways are required to develop higher performance adsorbents especially for removal of aromatics. Thus, future studies can be directed to the development of new generation zeolites as immobilization of ionic liquids, which have been rarely studied for desulfurization.

Adsorptive desulfurization is practical and economical to operate but most of the studies has been in batch system and on lab-scales. The process parameters like contact

time in the column, initial sulfur concentration, flow rate of fuel, and operating temperature show significant impact on the success of the adsorption process. For the industrial application of the ADS process, continuous system studies should be scaled up and the process parameters should be optimized to mimic large scale applications.

Regeneration efficiency of the adsorbents plays a critical role on the capacity and the feasibility of the adsorption process. Although zeolites are excellent adsorbents due to their high surface area, porous structure and active sites, regeneration and reusability need to be addressed. The reusability of adsorbents makes adsorption process cost-effective in the industrial applications. Therefore, studies are much needed to develop adsorbents durable to different regeneration treatments and determine the ideal regeneration conditions for successful scale-up.

REFERENCES

[1] **World Health Organization** (2016). *A Report on ambient air pollution: A global assessment of exposure and burden of disease*. ISBN: 9789241511353.

[2] **Srivastava, V. C.** (2012). An evaluation of desulfurization technologies for sulfur removal from liquid fuels. *RSC Advances, 2*, 759-783.

[3] **Brannigan, C., Glenn E., Twisse F., Griffin A. & Hill N.** (2007). *EU Fuel Quality Monitoring - Summary Report*. United Kingdom.

[4] **Environmental Protection Agency** (2016). Highway and Nonroad, Locomotive, and Marine (NRLM) Diesel Fuel Sulfur Standards. *Office of Transportation and Air Quality,* EPA-420-B-16-005.

[5] **Environmental Protection Agency** (2014). Control of Air Pollution from Motor Vehicles: Tier 3 Motor Vehicle Emission and Fuel Standards; Final Rule. *Federal Register, 79,* 23414-23886.

[6] **EN 589:2018** (2018). *Automotive fuels - LPG - Requirements and test methods*.

[7] **Song, C. & Ma, X.** (2003). New design approaches to ultra-clean diesel fuels by deep desulfurization and deep dearomatization. *Applied Catalysis B: Environmental, 41 (1),* 207-238.

[8] **Klimov, O.V., Pashigreva, A.V., Fedotov, M.A,. Kochubey, D.I., Chesalov, Y.A., Bukhtiyarova, G.A. & Noskov A.S.** (2010). Co-Mo catalysts for ultra-deep HDS of diesel fuels prepared via synthesis of bimetallic surface compounds. *Journal of Molecular Catalysis A: Chemical, 322* 80-89.

[9] **Wu, G. Yin, Y. Chen, Xin, W. F. Lu, Y. Qin, K. Zhang, L. Song, Y. & Li, M.** (2020). Catalytic kinetics for ultra-deep hydrodesulfurization of diesel. *Chemical Engineering Science, 214,* 115446.

[10] **Zhoua, C., Wang, Y., Huang, X., Wu, Y. & Chen, J.** (2020). Optimization of ultrasonic-assisted oxidative desulfurization of gasoline and crude oil. *Chemical Engineering and Processing: Process Intensification, 147,* 107789.

[11] **Guo, W., Wang, C., Lin, P. & Lu, X.P.** (2011). Oxidative desulfurization of diesel with TBHP/isobutyl aldehyde/air oxidation system. *Applied Energy, 88,* 175-179.

[12] **Boniek, D., Figueiredo, D., Dos Santos, A.F.B. & De Resende Stoianoff, M.A.** (2015). Biodesulfurization: a mini review about the immediate search for the future technology. *Clean Technologies and Environmental Policy, 17,* 29-37.

[13] **Mohebali, G. & Ball, A.S.** (2016). Biodesulfurization of diesel fuels - Past, present and future perspectives. *International Biodeterioration & Biodegradation, 110,* 163-180.

[14] **Xu, L., Luo, Y., Liu, H., Yin, J., Li, H., Jiang, W., Zhu, W., Li, H. & H. Ji.** (2021). Extractive desulfurization of diesel fuel by amide-based type IV deep eutectic solvents. *Journal of Molecular Liquids, 338,* 1166200.

[15] **Dharaskar, S. & Sillanpaa, M.** (2018). Synthesis, characterization, and application of trihexyl(tetradecyl)phosphonium chloride as promising solvent for extractive desulfurization of liquid fuel. *Chemical Engineering Research and Design, 133,* 388-397.

[16] **Yoosuk, B., Silajan, A. & Prasassarakich, P.** (2020). Deep adsorptive desulfurization over ion-exchanged zeolites: Individual and simultaneous effect of aromatic and nitrogen compounds. *Journal of Cleaner Production, 248,* 119291.

[17] **Saleh, T.A.** (2018). Simultaneous adsorptive desulfurization of diesel fuel over bimetallic nanoparticles loaded on activated carbon. *Journal of Cleaner Production, 172,* 2123-2132.

[18] **Ganiyu, S.A. & Lateef, S.A.** (2021). Review of adsorptive desulfurization process: Overview of the non-carbonaceous materials, mechanism and synthesis strategies. *Fuel, 294,* 120273.

[19] **Martyr, A. J. & Plint, M. A.** (2012). Engine Testing, The Design, Building, Modification and Use of Powertrain Test Facilities, (4 ed.). Elsevier.

[20] **Bahadori, A.** (2014). Natural Gas Processing Technology and Engineering Design, (1st ed.). Elsevier.

[21] **European LPG Association** (2009). *The LPG Industry Roadmap*.

[22] **Elvers, B.** (2008). *Handbook of fuels*. Wiley-VCH: Weinheim.

[23] **Obobisa, E. S.** (2022). Achieving 1.5 °C and net-zero emissions target: The role of renewable energy and financial development. *Renewable Energy, 188,* 967-985.

[24] **Lee, K., Tsilomelekis, X. & Valla, G. J. A.** (2018). Removal of benzothiophene and dibenzothiophene from hydrocarbon fuels using CuCe mesoporous Y zeolites in the presence of aromatics. *Applied Catalysis B: Environmental, 234,* 130-142.

[25] **World LPG Association and Argus Media** (2021). Statistical Review of Global LPG.

[26] **European LPG Association** (2013). *Autogas in Europe, The Sustainable Alternative an LPG Industry Roadmap*.

[27] **URL-1** <*http://www.lpg-apps.org*>, date retrieved 26.10.2022.

[28] **Lampert, J.** (2004). Selective catalytic oxidation: a new catalytic approach to the desulfurization of natural gas and liquid petroleum gas for fuel cell reformer applications. *Journal of Power Sources, 131 (1),* 27-34.

[29] **Wild, P. J., Nyqvist, R. G., de Bruijn, F. A. & Stobbe, E. R.** (2006). Removal of sulphur-containing odorants from fuel gases for fuel cell-based combined heat and power applications. *Journal of Power Sources, 159 (2),* 995-1004.

[30] **Takatsu, K., Takegoshi, G., Katsuno, H., Kawashima, Y. & Matsumoto, H.** (2007). Room Temperature Sulfur Removal from LPG with Adsorbent for Fuel Cell Applicatio-Adsorption Behavior of Sulfur Compounds. *Journal of the Japan Petroleum Institute, 50 (4),* 200-207.

[31] **Silva, P. P., Ferreira, R. A., Nunes, J. F., Sousa, J. A., Romanielo, L. L., Noronha, F. B. & Hori, C. E.** (2015). Production of Hydrogen from the Steam and Oxidative Reforming of Lpg: Thermodynamic and Experimental Study. *Brazilian Journal of Chemical Engineering, 32,* 647-662.

[32] **Lee, K. X. & Valla, J. A.** (2017). Investigation of metal-exchanged mesoporous Y zeolites for the adsorptive desulfurization of liquid fuels. *Applied Catalysis B: Environmental, 201,* 359-369.

[33] **Ding, R.-d., Zu, Y., Zhou, C.-h., Wang, H., Mo, Z.-s., Qin, Y.-c., Sun, Z.-l. & Song, L.-j.** (2018). Insight into the correlation between the effective adsorption sites and adsorption desulfurization performance of CuNaY zeolite. *Journal of Fuel Chemistry and Technology, 46 (4),* 451-458.

[34] **Astle, M. A., Rance, G. A., Loughlin, H. J., Peters, T. D. & Khlobystov, A. N.** (2019). Molybdenum Dioxide in Carbon Nanoreactors as a Catalytic Nanosponge for the Efficient Desulfurization of Liquid Fuels. *Advanced Functional Materials, 29 (17),* 1808092.

[35] **Lateef, S.A., Ajumobi, O.O. & Onaizi, S.A.** (2019). Enzymatic desulfurization of crude oil and its fractions: a mini review on the recent progresses and challenges. *Arabian Journal for Science and Engineering, (44),* 5181-5193.

[36] **Saha, B., Vedachalam, S. & Dalai, A. K.** (2021). Review on recent advances in adsorptive desulfurization. *Fuel Processing Technology, 214,* 106685.

[37] **Ibrahim, M. H., Hayyan, M., Hashim, M. A. & Hayyan, A.** (2017). The role of ionic liquids in desulfurization of fuels: A review. *Renewable and Sustainable Energy Reviews, 76,* 1534-1549.

[38] **Yue, B., Liu, S., Chai, Y., Wua, G., Guan, N. & Li, L.** (2022). Zeolites for separation: Fundamental and application. *Journal of Energy Chemistry 71,* 288-303.

[39] **Lei, J., Ding, R. & Zhang, J.** (2021). Study on seepage and adsorption characteristics of porous media containing adsorbent based on lattice Boltzmann. *AIP Advances 11,* 045126.

[40] **Dąbrowski, A.** (2001). Adsorption–from theory to practice. *Advances in Colloid and Interface Science, 93 (1),* 135-224.

[41] **Dehghan, R. & Anbia, M.** (2017). Zeolites for adsorptive desulfurization from fuels: A review. *Fuel Processing Technology, 167,* 99-116.

[42] **Hernández-Maldonado, A. J., Yang, F. H., Qi, G. & Yang, R. T.** (2005). Desulfurization of transportation fuels by π-complexation sorbents: Cu(I)-, Ni(II)-, and Zn(II)-zeolites. *Applied Catalysis B: Environmental, 56 (1),* 111-126.

[43] **Song, C.** (2003). An overview of new approaches to deep desulfurization for ultra-clean gasoline, diesel fuel and jet fuel. *Catalysis Today, 86 (1),* 211-263.

[44] **Velu, S., Ma, X. & Song, C.** (2003). Mechanistic investigations on the adsorption of organic sulfur compounds over solid adsorbents in the adsorptive desulfurization of transportation fuels. *ACS Division of Fuel Chemistry, Preprints, 48,* 693-694.

[45] **Khan, N. A., Kim, C. M. & Jhung, S. H.** (2017). Adsorptive desulfurization using Cu–Ce/metal–organic framework: Improved performance based on synergy between Cu and Ce. *Chemical Engineering Journal, 311,* 20-27.

[46] **Satokawa, S., Kobayashi, Y. & Fujiki, H.** (2005). Adsorptive removal of dimethylsulfide and t-butylmercaptan from pipeline natural gas fuel on Ag zeolites under ambient conditions. *Applied Catalysis B: Environmental, 56 (1),* 51-56.

[47] **Salem, A. B. S. H.** (1994). Naphtha desulfurization by adsorption. *Industrial & Engineering Chemistry Research, 33 (2),* 336-340.

[48] **Salem, A. B. S. H. & Hamid, H. S.** (1997). Removal of sulfur compounds from naphtha solutions using solid adsorbents. *Chemical Engineering & Technology, 20 (5),* 342-347.

[49] **Jiang, Z., Liu, Y., Sun, X., Tian, F., Sun, F., Liang, C., You, W., Han, C. & Li, C.** (2003). Activated Carbons Chemically Modified by Concentrated H2SO4 for the Adsorption of the Pollutants from Wastewater and the Dibenzothiophene from Fuel Oils. *Langmuir, 19 (3),* 731-736.

[50] **Yang, Y., Lu, H., Ying, P., Jiang, Z. & Li, C.** (2007). Selective dibenzothiophene adsorption on modified activated carbons. *Carbon, 45 (15),* 3042-3044.

[51] **Ania, C. O. & Bandosz, T. J.** (2005). Importance of Structural and Chemical Heterogeneity of Activated Carbon Surfaces for Adsorption of Dibenzothiophene. *Langmuir, 21 (17),* 7752-7759.

[52] **Ganiyu, S. A., Ajumobi, O. O., Lateef, S. A., Sulaiman, K. O., Bakare, I. A., Qamaruddin, M. & Alhooshani, K.** (2017). Boron-doped activated carbon as efficient and selective adsorbent for ultra-deep desulfurization of 4,6-dimethyldibenzothiophene. *Chemical Engineering Journal, 321,* 651-661.

[53] **Selvavathi, V., Chidambaram, V., Meenakshisundaram, A., Sairam, B. & Sivasankar, B.** (2009). Adsorptive desulfurization of diesel on activated carbon and nickel supported systems. *Catalysis Today, 141 (1),* 99-102.

[54] **Zhou, A., Ma, X. & Song, C.** (2009). Effects of oxidative modification of carbon surface on the adsorption of sulfur compounds in diesel fuel. *Applied Catalysis B: Environmental, 87 (3),* 190-199.

[55] **Yu, C., Fan, X., Yu, L., Bandosz, T. J., Zhao, Z. & Qiu, J.** (2013). Adsorptive Removal of Thiophenic Compounds from Oils by Activated Carbon Modified with Concentrated Nitric Acid. *Energy & Fuels, 27 (3),* 1499-1505.

[56] **Fallah, R. N. & Azizian, S.** (2012). Removal of thiophenic compounds from liquid fuel by different modified activated carbon cloths. *Fuel Processing Technology, 93 (1),* 45-52.

[57] **Kampouraki, Z. C., Giannakoudakis, D. A., Triantafyllidis, K. & Deliyanni, E.** (2019). Catalytic oxidative desulfurization of a 4,6-DMDBT containing model fuel by metal-free activated carbons: the key role of surface chemistry. *Green Chemistry, 21,* 6685-6698.

[58] **Saleh, T. A. & Danmaliki, G. I.** (2016). Influence of acidic and basic treatments of activated carbon derived from waste rubber tires on adsorptive desulfurization of thiophenes. *Journal of the Taiwan Institute of Chemical Engineers, 60,* 460-468.

[59] **Seredych, M., Hulicova-Jurcakova, D. & Bandosz, T. J.** (2010). Effect of the Incorporation of Nitrogen to a Carbon Matrix on the Selectivity and Capacity for Adsorption of Dibenzothiophenes from Model Diesel Fuel. *Langmuir, 26 (1),* 227-233.

[60] **Boudou, J. P., Chehimi, M., Broniek, E., Siemieniewska, T. & Bimer, J.** (2003). Adsorption of H_2S or SO_2 on an activated carbon cloth modified by ammonia treatment. *Carbon, 41 (10),* 1999-2007.

[61] **Yu, Z., Wang, X., Zhou, S., Yang, L., Zhao, Z. & Qiu, J.** (2016). A facile soft-template synthesis of nitrogen doped mesoporous carbons for hydrogen sulfide removal. *Adsorption, 22 (8),* 1075-1082.

[62] **Shi, Y., Liu, G., Wang, L. & Zhang, X.** (2015). Efficient adsorptive removal of dibenzothiophene from model fuel over heteroatom-doped porous carbons by carbonization of an organic salt. *Chemical Engineering Journal, 259,* 771-778.

[63] **Xiao, J., Bian, G., Zhang, W. & Li, Z.** (2010). Adsorption of Dibenzothiophene on Ag/Cu/Fe-Supported Activated Carbons Prepared by Ultrasonic-Assisted Impregnation. *Journal of Chemical & Engineering Data, 55 (12),* 5818-5823.

[64] **Tang, X.-l., Qian, W., Hu, A., Zhao, Y.-m., Fei, N.-n. & Shi, L.** (2011). Adsorption of Thiophene on Pt/Ag-Supported Activated Carbons Prepared by Ultrasonic-Assisted Impregnation. *Industrial & Engineering Chemistry Research, 50 (15),* 9363-9367.

[65] **Martins, A. V. P. R., Ramos, J. E. T., Coelho, J. A., Vidal, C. B., Cavalcante, C. L. & Azevedo, D. C. S.** (2014). Metal-impregnated carbon applied as adsorbent for removal of sulphur compounds using fixed-bed column technology. *Environmental Technology, 35 (11),* 1367-1377.

[66] **Li, W., Sun, X., Fan, J., Cui, A., Ma, Y. & Zhang, Z.** (2014). Adsorptive Removal of Thiophenic Sulfur Compounds Over Ag-Loaded Spherical Activated Carbon. *Asian Journal of Chemistry, 26,* 2588-2592.

[67] **Olajire, A. A., Abidemi, J. J., Lateef, A. & Benson, N. U.** (2017). Adsorptive desulphurization of model oil by Ag nanoparticles-modified activated carbon prepared from brewer's spent grains. *Journal of Environmental Chemical Engineering, 5 (1),* 147-159.

[68] **Wang, Y., Yang, F. H., Yang, R. T., Heinzel, J. M. & Nickens, A. D.** (2006). Desulfurization of High-Sulfur Jet Fuel by π-Complexation with Copper and Palladium Halide Sorbents. *Industrial & Engineering Chemistry Research, 45 (22),* 7649-7655.

[69] **Ma, L. & Yang, R. T.** (2007). Selective Adsorption of Sulfur Compounds: Isotherms, Heats, and Relationship between Adsorption from Vapor and Liquid Solution. *Industrial & Engineering Chemistry Research, 46 (9),* 2760-2768.

[70] **Wang, Y. & Yang, R. T.** (2007). Desulfurization of Liquid Fuels by Adsorption on Carbon-Based Sorbents and Ultrasound-Assisted Sorbent Regeneration. *Langmuir, 23 (7),* 3825-3831.

[71] **Vilarrasa-García, E., Infantes-Molina, A., Moreno-Tost, R., Rodríguez-Castellón, E., Jiménez-López, A., Cavalcante, C. L. & Azevedo, D. C. S.** (2010). Thiophene Adsorption on Microporous Activated Carbons Impregnated with $PdCl_2$. *Energy & Fuels, 24 (6),* 3436-3442.

[72] **Khan, N. A., Hasan, Z., Min, K. S., Paek, S.-M. & Jhung, S. H.** (2013). Facile introduction of Cu+ on activated carbon at ambient conditions and adsorption of benzothiophene over Cu^{+}/activated carbon. *Fuel Processing Technology, 116,* 265-270.

[73] **Jiang, X., Xu, W., Liu, W., Yue, M., Zhu, Y. & Yang, M.** (2019). Facile preparation of cuprous oxide decorated mesoporous carbon by one-step reductive decomposition for deep desulfurization. *Fuel, 241,* 777-785.

[74] **Safieh, K. A. A., Al-Degs, Y. S., Sunjuk, M. S., Saleh, A. I. & Al-Ghouti, M. A.** (2015). Selective removal of dibenzothiophene from commercial diesel using manganese dioxide-modified activated carbon: a kinetic study. *Environmental Technology, 36 (1),* 98-105.

[75] **Saleh, T. A., Sulaiman, K. O., Al-Hammadi, S. A., Dafalla, H. & Danmaliki, G. I.** (2017). Adsorptive desulfurization of thiophene, benzothiophene and dibenzothiophene over activated carbon manganese oxide nanocomposite: with column system evaluation. *Journal of Cleaner Production, 154,* 401-412.

[76] **Al. Swat, A. A., Saleh, T. A., Ganiyu, S. A., Siddiqui, M. N. & Alhooshani, K. R.** (2017). Preparation of activated carbon, zinc oxide and nickel oxide composites for potential application in the desulfurization of model diesel fuels. *Journal of Analytical and Applied Pyrolysis, 128,* 246-256.

[77] **Velo-Gala, I., López-Peñalver, J. J., Sánchez-Polo, M. & Rivera-Utrilla, J.** (2014). Surface modifications of activated carbon by gamma irradiation. *Carbon, 67,* 236-249.

[78] **Abdulrasheed, A. A., Jalil, A. A., Triwahyono, S., Zaini, M. A. A., Gambo, Y. & Ibrahim, M.** (2018). Surface modification of activated carbon for adsorption of SO_2 and NO_X: A review of existing and emerging technologies. *Renewable and Sustainable Energy Reviews, 94,* 1067-1085.

[79] **Shafeeyan, M. S., Daud, W. M. A. W., Houshmand, A. & Shamiri, A.** (2010). A review on surface modification of activated carbon for carbon dioxide adsorption. *Journal of Analytical and Applied Pyrolysis, 89 (2),* 143-151.

[80] **Triantafyllidis, K. S. & Deliyanni, E. A.** (2014). Desulfurization of diesel fuels: Adsorption of 4,6-DMDBT on different origin and surface chemistry nanoporous activated carbons. *Chemical Engineering Journal, 236,* 406-414.

[81] **Al-Zuhair, S., Khalil, A., Hassan, M., Abdulrazak, A., Basel, K. & Fardoun, A.** (2015). Performance evaluation of LPG desulfurization by adsorption for hydrogen production. *Journal of Energy Chemistry, 24 (4),* 477-484.

[82] **Broclawik, E., Kozyra, P., Mitoraj, M., Radoń, M. & Rejmak, P.** (2021). Zeolites at the Molecular Level: What Can Be Learned from Molecular Modeling, *Molecules, 26(6),* 1511.

[83] **Yang, R. T., Hernández-Maldonado, A. J. & Yang, F. H.** (2003). Desulfurization of Transportation Fuels with Zeolites Under Ambient Conditions. *Science, 301 (5629),* 79-81.

[84] **Hernández-Maldonado, A. J. & Yang, R. T.** (2004). Desulfurization of Diesel Fuels by Adsorption via π-Complexation with Vapor-Phase Exchanged Cu(I)−Y Zeolites. *Journal of the American Chemical Society, 126 (4),* 992-993.

[85] **Velu, S., Ma, X. & Song, C.** (2003). Selective Adsorption for Removing Sulfur from Jet Fuel over Zeolite-Based Adsorbents. *Industrial & Engineering Chemistry Research, 42 (21),* 5293-5304.

[86] **Song, H., Cui, X.-H., Song, H.-L., Gao, H.-J. & Li, F.** (2014). Characteristic and Adsorption Desulfurization Performance of Ag–Ce Bimetal Ion-Exchanged Y Zeolite. *Industrial & Engineering Chemistry Research, 53 (37),* 14552-14557.

[87] **Crandall, B. S., Zhang, J., Stavila, V., Allendorf, M. D. & Li, Z.** (2019). Desulfurization of Liquid Hydrocarbon Fuels with Microporous and Mesoporous Materials: Metal-Organic Frameworks, Zeolites, and Mesoporous Silicas. *Industrial & Engineering Chemistry Research, 58 (42),* 19322-19352.

[88] **Lee, K. X. Valla, & J. A.** (2019). Adsorptive desulfurization of liquid hydrocarbons using zeolite-based sorbents: a comprehensive review. *Reaction Chemistry & Engineering, 4 (8),* 1357-1386.

[89] **Mahmoudi, R. & Falamaki, C.** (2016). Ni^{2+}-ion-exchanged dealuminated clinoptilolite: A superior adsorbent for deep desulfurization. *Fuel, 173,* 277-284.

[90] **Moradi, M., Karimzadeh, R. & Moosavi, E. S.** (2018). Modified and ion exchanged clinoptilolite for the adsorptive removal of sulfur compounds in a model fuel: New adsorbents for desulfurization. *Fuel, 217,* 467-477.

[91] **Tang, X.-l., Meng, X. & Shi, L.** (2011). Desulfurization of Model Gasoline on Modified Bentonite. *Industrial & Engineering Chemistry Research, 50 (12),* 7527-7533.

[92] **Huang, H., Yi, D., Lu, Y., Wu, X., Bai, Y., Meng, X. & Shi, L.** (2013). Study on the adsorption behavior and mechanism of dimethyl sulfide on silver modified bentonite by in situ FTIR and temperature-programmed desorption. *Chemical Engineering Journal, 225,* 447-455.

[93] **Mustafa, F., Al-Ghouti, M. A., Khalili, F. I. & Al-Degs, Y. S.** (2010). Characteristics of organosulphur compounds adsorption onto Jordanian zeolitic tuff from diesel fuel. *Journal of Hazardous Materials, 182 (1),* 97-107.

[94] **Kulprathipanja, S.** (2010). *Zeolites in Industrial Separation and Catalysis*. Wiley Online Library.

[95] **Sun, H.-Y., Sun, L.-P., Li, F. & Zhang, L.** (2015). Adsorption of benzothiophene from fuels on modified NaY zeolites. *Fuel Processing Technology, 134,* 284-289.

[96] **Xiang, H., Zhang, H., Liu, P. & Yan, Y.** (2016). Preparation of high purity propane from liquefied petroleum gas in a fixed bed by removal of sulfur and butanes. *Chemical Engineering Journal, 284,* 224-232.

[97] **Fu, H., Wang, Y., Zhang, T., Yang, C. & Shan, H.** (2017). Adsorption and Separation Mechanism of Thiophene/Benzene in MFI Zeolite: A GCMC Study. *The Journal of Physical Chemistry C, 121 (46),* 25818-25826.

[98] **Zeng, Y., Moghadam, P. Z. & Snurr, R. Q.** (2015). Pore Size Dependence of Adsorption and Separation of Thiophene/Benzene Mixtures in Zeolites. *The Journal of Physical Chemistry C, 119 (27),* 15263-15273.

[99] **Chica, A., Strohmaier, K. & Iglesia, E.** (2004). Adsorption, Desorption, and Conversion of Thiophene on H-ZSM5. *Langmuir, 20 (25),* 10982-10991.

[100] **Gong, Y., Dou, T., Kang, S., Li, Q. & Hu, Y.** (2009). Deep desulfurization of gasoline using ion-exchange zeolites: Cu(I)- and Ag(I)-beta. *Fuel Processing Technology, 90 (1),* 122-129.

[101] **Tian, F., Yang, X., Shi, Y., Jia, C. & Chen, Y.** (2012). Adsorptive desulfurization over hierarchical beta zeolite by alkaline treatment. *Journal of Natural Gas Chemistry, 21 (6),* 647-652.

[102] **Laborde-Boutet, C., Joly, G., Nicolaos, A., Thomas, M. & Magnoux, P.** (2006). Selectivity of Thiophene/Toluene Competitive Adsorptions onto NaY and NaX Zeolites. *Industrial & Engineering Chemistry Research, 45 (20),* 6758-6764.

[103] **Miao, T., Ju, S. & Xue, F.** (2012). Selectivity adsorption of thiophene alkylated derivatives over modified Cu^{+}-13X zeolite. *Journal of Rare Earths, 30 (8),* 807-813.

[104] **Chen, X., Shen, B., Sun, H. & Zhan, G.** (2018). Ion-exchange modified zeolites X for selective adsorption desulfurization from Claus tail gas: Experimental and computational investigations. *Microporous and Mesoporous Materials, 261,* 227-236.

[105] **Yongping, Z., Shengui, J., Weihong, X. & Changlin, C.** (2008). Adsorption of mercaptan from model gasoline on 13X loaded with Zn^{2+}. *The Canadian Journal of Chemical Engineering, 86 (2),* 186-191.

[106] **Lin, L., Zhang, Y., Zhang, H. & Lu, F.** (2011). Adsorption and solvent desorption behavior of ion-exchanged modified Y zeolites for sulfur removal and for fuel cell applications. *Journal of Colloid and Interface Science, 360 (2),* 753-759.

[107] **Tian, F., Wu, W., Jiang, Z., Liang, C., Yang, Y., Ying, P., Sun, X., Cai, T. & Li, C.** (2006). The study of thiophene adsorption onto La(III)-exchanged zeolite NaY by FT-IR spectroscopy. *Journal of Colloid and Interface Science, 301 (2),* 395-401.

[108] **Zhang, Z. Y., Shi, T. B., Jia, C. Z., Ji, W.J., Chen, Y. & He, M. Y.** (2008). Adsorptive removal of aromatic organosulfur compounds over the modified Na-Y zeolites. *Applied Catalysis B: Environmental, 82,* 1-10.

[109] **Wang, J., Xu, F., Xie, W.-j., Mei, Z.-j., Zhang, Q.-z., Cai, J. & Cai, W.-m.** (2009). The enhanced adsorption of dibenzothiophene onto cerium/nickel-exchanged zeolite Y. *Journal of Hazardous Materials, 163 (2),* 538-543.

[110] **Duan, L., Gao, X., Meng, X., Zhang, H., Wang, Q., Qin, Y., Zhang, X. & Song, L.** (2012). Adsorption, Co-adsorption, and Reactions of Sulfur Compounds, Aromatics, Olefins over Ce-Exchanged Y Zeolite. *The Journal of Physical Chemistry C, 116 (49),* 25748-25756.

[111] **Shi, Y., Zhang, W., Zhang, H., Tian, F., Jia, C. & Chen, Y.** (2013). Effect of cyclohexene on thiophene adsorption over NaY and LaNaY zeolites. *Fuel Processing Technology, 110,* 24-32.

[112] **Hernández-Maldonado, A. J. & Yang, R. T.** (2003). Desulfurization of Liquid Fuels by Adsorption via π Complexation with Cu(I)−Y and Ag−Y Zeolites. *Industrial & Engineering Chemistry Research, 42 (1),* 123-129.

[113] **Hernández-Maldonado, A. J. & Yang, R. T.** (2003). Desulfurization of Commercial Liquid Fuels by Selective Adsorption via π-Complexation with Cu(I)−Y Zeolite. *Industrial & Engineering Chemistry Research, 42 (13),* 3103-3110.

[114] **Hernández-Maldonado, A. J., Stamatis, S. D., Yang, R. T., He, A. Z. & Cannella, W.** (2004). New Sorbents for Desulfurization of Diesel Fuels via π Complexation: Layered Beds and Regeneration. *Industrial & Engineering Chemistry Research, 43 (3),* 769-776.

[115] **Hernández-Maldonado, A. J. & Yang, R. T.** (2004). Desulfurization of Diesel Fuels via π-Complexation with Nickel(II)-Exchanged X- and Y-Zeolites. *Industrial & Engineering Chemistry Research, 43 (4),* 1081-1089.

[116] **Hernández-Maldonado, A. J. & Yang, R. T.** (2004). Desulfurization of Transportation Fuels by Adsorption. *Catalysis Reviews, 46 (2),* 111-150.

[117] **Xue, M., Chitrakar, R., Sakane, K., Hirotsu, T., Ooi, K., Yoshimura, Y., Feng, Q. & Sumida, N.** (2005). Selective adsorption of thiophene and 1-benzothiophene on metal-ion-exchanged zeolites in organic medium. *Journal of Colloid and Interface Science, 285 (2),* 487-492.

[118] **Yi, D., Huang, H., Meng, X. & Shi, L.** (2014). Adsorption–desorption behavior and mechanism of dimethyl disulfide in liquid hydrocarbon streams on modified Y zeolites. *Applied Catalysis B: Environmental, 148-149,* 377-386.

[119] **Song, H., Wan, X., Dai, M., Zhang, J., Li, F. & Song, H.** (2013). Deep desulfurization of model gasoline by selective adsorption over Cu–Ce bimetal ion-exchanged Y zeolite. *Fuel Processing Technology, 116,* 52-62.

[120] **Song, H., Chang, Y., Wan, X., Dai, M., Song, H. & Jin, Z.** (2014). Equilibrium, Kinetic, and Thermodynamic Studies on Adsorptive Desulfurization onto CuICeIVY Zeolite. *Industrial & Engineering Chemistry Research, 53 (14),* 5701-5708.

[121] **Jung, S. Y., Moon, J. M., Lee, S. C., Paik, S. C., Park, K. S. & Kim, J. C.** (2014). The adsorption properties of organic sulfur compounds on zeolite-based sorbents impregnated with rare-earth metals. *Adsorption, 20 (2),* 341-348.

[122] **Lv, L., Zhang, J., Huang, C., Lei, Z. & Chen, B.** (2014). Adsorptive separation of dimethyl disulfide from liquefied petroleum gas by different zeolites and selectivity study via FT-IR. *Separation and Purification Technology, 125,* 247-255.

[123] **Zhang, Q., Shi, L. & Meng, X.** (2016). Deep adsorption desulfurization of liquid petroleum gas by copper-modified bentonite. *RSC Advances, 6 (12),* 9589-9597.

[124] **Li, J.-R., Kuppler, R. J. & Zhou, H.-C**. (2009). Selective gas adsorption and separation in metal–organic frameworks. *Chemical Society Reviews, 38 (5),* 1477-1504.

[125] **Calero, S. & Gómez-Álvarez, P.** (2015). Insights into the Adsorption of Water and Small Alcohols on the Open-Metal Sites of Cu–BTC via Molecular Simulation. *The Journal of Physical Chemistry C, 119 (1),* 467-472.

[126] **Bai, Y., Dou, Y., Xie, L.-H., Rutledge, W., Li, J.-R. & Zhou, H.-C.** (2016). Zr-based metal–organic frameworks: design, synthesis, structure, and applications. *Chemical Society Reviews, 45 (8),* 2327-2367.

[127] **Falcaro, P., Ricco, R., Doherty, C. M., Liang, K., Hill, A. J. & Styles, M. J.** (2014). MOF positioning technology and device fabrication. *Chemical Society Reviews, 43 (16),* 5513-5560.

[128] **URL-2** *<http://theconversation.com/mof-the-chart-why-a-record-breaking-surface-area-matters-9915>,* date retrieved 28.10.2022.

[129] **Furukawa, H., Cordova, K. E., O'Keeffe, M. & Yaghi, O. M.** (2013). The Chemistry and Applications of Metal-Organic Frameworks. *Science, 341 (6149),* 1230444.

[130] **Chen, Z., Ling, L., Wang, B., Fan, H., Shangguan, J. & Mi, J.** (2016). Adsorptive desulfurization with metal-organic frameworks: A density functional theory investigation. *Applied Surface Science, 387,* 483-490.

[131] **Wu, L., Xiao, J., Wu, Y., Xian, S., Miao, G., Wang, H. & Li, Z.** (2014). A Combined Experimental/Computational Study on the Adsorption of Organosulfur Compounds over Metal-Organic Frameworks from Fuels. *Langmuir, 30 (4),* 1080-1088.

[132] **Ban, S., Long, K., Xie, J., Sun, H. & Zhou, H.** (2018). Thiophene Separation with Silver-Doped Cu-BTC Metal-Organic Framework for Deep Desulfurization. *Industrial & Engineering Chemistry Research, 57 (8),* 2956-2966.

[133] **Wei, W., Zhang, K., Qiao, Z. & Jiang, J.** (2019). Functional UiO-66 for the removal of sulfur-containing compounds in gas and liquid mixtures: A molecular simulation study. *Chemical Engineering Journal, 356,* 737-745.

[134] **Zeng, Y., Zhu, X., Yuan, Y., Zhang, X. & Ju, S.** (2012). Molecular simulations for adsorption and separation of thiophene and benzene in Cu-BTC and IRMOF-1 metal-organic frameworks. *Separation and Purification Technology, 95,* 149-156.

[135] **Yang, K., Yan, Y., Chen, W., Kang, H., Han, Y., Zhang, W., Fan, Y. & Li, Z.** (2018). The high performance and mechanism of metal-organic frameworks and their composites in adsorptive desulfurization. *Polyhedron, 152,* 202-215.

[136] **Cychosz, K. A., Wong-Foy, A. G. & Matzger, A. J.** (2008). Liquid Phase Adsorption by Microporous Coordination Polymers: Removal of Organosulfur Compounds. *Journal of the American Chemical Society, 130 (22),* 6938-6939.

[137] **Britt, D., Tranchemontagne, D. & Yaghi, O. M.** (2008). Metal-organic frameworks with high capacity and selectivity for harmful gases. *Proceedings of the National Academy of Sciences, 105 (33),* 11623-11627.

[138] **Achmann, S., Hagen, G., Hämmerle, M., Malkowsky, I. M., Kiener, C. & Moos, R.** (2010). Sulfur Removal from Low-Sulfur Gasoline and Diesel Fuel by Metal-Organic Frameworks. *Chemical Engineering & Technology, 33 (2),* 275-280.

[139] **Tian, F., Fu, Z., Zhang, H., Zhang, J., Chen, Y. & Jia, C.** (2015). Thiophene adsorption onto metal–organic framework HKUST-1 in the presence of toluene and cyclohexene. *Fuel, 158,* 200-206.

[140] **Liu, B., Zhu, Y., Liu, S. & Mao, J.** (2012). Adsorption Equilibrium of Thiophenic Sulfur Compounds on the Cu-BTC Metal-Organic Framework. *Journal of Chemical & Engineering Data, 57 (4),* 1326-1330.

[141] **Peralta, D., Chaplais, G., Simon-Masseron, A., Barthelet, K. & Pirngruber, G. D.** (2012). Metal-Organic Framework Materials for Desulfurization by Adsorption. *Energy & Fuels, 26 (8),* 4953-4960.

[142] **Hamon, L., Serre, C., Devic, T., Loiseau, T., Millange, F., Férey, G. & Weireld, G. D.** (2009). Comparative Study of Hydrogen Sulfide Adsorption in the MIL-53(Al, Cr, Fe), MIL-47(V), MIL-100(Cr), and MIL-101(Cr) Metal−Organic Frameworks at Room Temperature. *Journal of the American Chemical Society, 131 (25),* 8775-8777.

[143] **Wang, X.-L., Fan, H.-L., Tian, Z., He, E.-Y., Li, Y. & Shangguan, J.** (2014). Adsorptive removal of sulfur compounds using IRMOF-3 at ambient temperature. *Applied Surface Science, 289,* 107-113.

[144] **Li, Y., Wang, L.-J., Fan, H.-L., Shangguan, J., Wang, H. & Mi, J.** (2015). Removal of Sulfur Compounds by a Copper-Based Metal Organic Framework under Ambient Conditions. *Energy & Fuels, 29 (1),* 298-304.

[145] **Blanco-Brieva, G., Campos-Martin, J. M., Al-Zahrani, S. M. & Fierro, J. L. G.** (2011). Effectiveness of metal-organic frameworks for removal of refractory organo-sulfur compound present in liquid fuels. *Fuel, 90 (1),* 190-197.

[146] **Zhang, H.-X., Huang, H.-L., Li, C.-X., Meng, H., Lu, Y.-Z., Zhong, C.-L., Liu, D.-H. & Yang, Q.-Y.** (2021). Adsorption Behavior of Metal–Organic Frameworks for Thiophenic Sulfur from Diesel Oil. *Industrial & Engineering Chemistry Research, 51 (38),* 12449-12455.

[147] **Li, S.-L., Lan, Y.-Q., Sakurai, H. & Xu, Q.** (2012). Unusual Regenerable Porous Metal–Organic Framework Based on a New Triple Helical Molecular Necklace for Separating Organosulfur Compounds. Chemistry – *A European Journal, 18 (51),* 16302-16309.

[148] **Liu, X., Wang, J., Li, Q., Jiang, S., Zhang, T. & Ji, S.** (2014). Synthesis of rare earth metal-organic frameworks (Ln-MOFs) and their properties of adsorption desulfurization. *Journal of Rare Earths 2014, 32 (2),* 189-194.

[149] **Liu, B., Peng, Y. & Chen, Q.** (2016). Adsorption of N/S-Heteroaromatic Compounds from Fuels by Functionalized MIL-101(Cr) Metal-Organic Frameworks: The Impact of Surface Functional Groups. *Energy & Fuels, 30 (7),* 5593-5600.

[150] **Shi, R.-H., Zhang, Z.-R., Fan, H.-L., Zhen, T., Shangguan, J. & Mi, J.** (2017). Cu-based metal–organic framework/activated carbon composites for sulfur compounds removal. *Applied Surface Science, 394,* 394-402.

[151] **Petit, C., Mendoza, B. & Bandosz, T. J.** (2010). Hydrogen Sulfide Adsorption on MOFs and MOF/Graphite Oxide Composites. *ChemPhysChem, 11 (17),* 3678-3684.

[152] **Bhoria, N., Basina, G., Pokhrel, J., Kumar Reddy, K. S., Anastasiou, S., Balasubramanian, V. V., AlWahedi, Y. F. & Karanikolos, G. N.** (2020). Functionalization effects on HKUST-1 and HKUST-1/graphene oxide hybrid adsorbents for hydrogen sulfide removal. *Journal of Hazardous Materials, 394,* 122565.

[153] **Zhu, L., Jia, X., Bian, H., Huo, T., Duan, Z., Xiang, Y. & Xia, D.** (2018). Structure and adsorptive desulfurization performance of the composite material MOF-5@AC. *New Journal of Chemistry, 42 (5),* 3840-3850.

[154] **Shi, F., Hammoud, M. & Thompson, L. T.** (2011). Selective adsorption of dibenzothiophene by functionalized metal organic framework sorbents. *Applied Catalysis B: Environmental, 103 (3),* 261-265.

[155] **Matloob, A. M., El-Hafiz, D. R. A., Saad, L., Mikhail, S. & Guirguis, D.** (2019). Metal organic framework-graphene nano-composites for high adsorption removal of DBT as hazard material in liquid fuel. *Journal of Hazardous Materials, 373,* 447-458.

[156] **Qin, L., Zhou, Y., Li, D., Zhang, L., Zhao, Z., Zuhra, Z. & Mu, C.** (2016). Highly Dispersed HKUST-1 on Milimeter-Sized Mesoporous γ-Al_2O_3 Beads for Highly Effective Adsorptive Desulfurization. *Industrial & Engineering Chemistry Research, 55 (27),* 7249-7258.

[157] **Tan, P., Xie, X.-Y., Liu, X.-Q., Pan, T., Gu, C., Chen, P.-F., Zhou, J.-Y., Pan, Y. & Sun, L.-B.** (2017). Fabrication of magnetically responsive HKUST-1/Fe_3O_4 composites by dry gel conversion for deep desulfurization and denitrogenation. *Journal of Hazardous Materials, 321,* 344-352.

[158] **Khan, N. A. & Jhung, S. H.** (2013). Effect of central metal ions of analogous metal-organic frameworks on the adsorptive removal of benzothiophene from a model fuel. *Journal of Hazardous Materials, 260,* 1050-1056.

[159] **Khan, N. A. & Jhung, S. H.** (2012). Low-temperature loading of Cu^+ species over porous metal-organic frameworks (MOFs) and adsorptive desulfurization with Cu^+-loaded MOFs. *Journal of Hazardous Materials, 237-238,* 180-185.

[160] **Guan, X., Wang, Y. & Cai, W.** (2019). A composite metal-organic framework material with high selective adsorption for dibenzothiophene. *Chinese Chemical Letters, 30 (6),* 1310-1314.

[161] **Valdes, M. D. C., Vega, M. A. S., Cely, M. J., Pinto, Pinilla, A. M., Antolínez, J. V. A., Rojas, M. F. & Carreno, A.** (2018). Effect of the BMIM BF4 immobilization on oxidized activated carbon in fuel desulfurization. *Advanced Materials Letters, 9,* 488-493.

[162] **Wen, L.-j., Tian, J.-p., Lv, Y.-k. Li, B.-z & Ma, Y.** (2012). Adsorption Performance of Ionic Liquid [BPy]Br Immobilized on Activated Carbon to SO_2. *The Chinese Journal of Process Engineering, 12,* 223-226.

[163] **Shirani, M., Semnani, A., Habibollahi, S., Haddadi, H. & Narimani, M.** (2016). Synthesis and application of magnetic NaY zeolite composite immobilized with ionic liquid for adsorption desulfurization of fuel using response surface methodology. *Journal of Porous Materials, 23 (3),* 701-712.

[164] **Ding, W., Zhu, W., Xiong, J., Yang, L., Wei, A., Zhang, M. & Li, H.** (2015). Novel heterogeneous iron-based redox ionic liquid supported on SBA-15 for deep oxidative desulfurization of fuels. *Chemical Engineering Journal, 266,* 213-221.

[165] **Zhang, M., Zhu, W., Li, H., Xun, S., Ding, W., Liu, J., Zhao, Z. & Wang, Q.** (2014). One-pot synthesis, characterization and desulfurization of functional mesoporous W-MCM-41 from POM-based ionic liquids. *Chemical Engineering Journal, 243,* 386-393.

[166] **Khan, N. A., Hasan, Z. & Jhung, S. H.** (2014). Ionic Liquids Supported on Metal-Organic Frameworks: Remarkable Adsorbents for Adsorptive Desulfurization. *Chemistry – A European Journal, 20 (2),* 376-380.

[167] **Khan, N. A., Hasan, Z. & Jhung, S. H.** (2016). Ionic liquid@MIL-101 prepared via the ship-in-bottle technique: remarkable adsorbents for the removal of benzothiophene from liquid fuel. *Chemical Communications, 52 (12),* 2561-2564.

[168] **Khan, N. A., Bhadra, B. N. & Jhung, S. H.** (2018). Heteropoly acid-loaded ionic liquid@metal-organic frameworks: Effective and reusable adsorbents for the desulfurization of a liquid model fuel. *Chemical Engineering Journal, 334,* 2215-2221.

[169] **Ahmed, I., Panja, T., Khan, N. A., Sarker, M., Yu, J.-S. & Jhung, S. H.** (2017). Nitrogen-Doped Porous Carbons from Ionic Liquids@MOF: Remarkable Adsorbents for Both Aqueous and Nonaqueous Media. *ACS Applied Materials & Interfaces, 9 (11),* 10276-10285.

[170] **Qi, Z., Qiu, T., Wang, H. & Ye, C.** (2020). Synthesis of ionic-liquid-functionalized UiO-66 framework by post-synthetic ligand exchange for the ultra-deep desulfurization. *Fuel, 268,* 117336.

[171] **Abro, R., Kiran, N., Ahmed, S., Muhammad, A., Jatoi, A. S., Mazari, S. A., Salma, U. & Plechkova, N. V.** (2022). Extractive desulfurization of fuel oils using deep eutectic solvents – A comprehensive review. *Journal of Environmental Chemical Engineering, 10,* 107369.

[172] **Liu, Y., Xue, J., Zhou, X., Cui, Y. & Yin, J.** (2021). Deep desulfurization performance of thiophene with deep eutectic solvents loaded carbon nanotube composites. *Royal Society Open Science, 8,* 201736.

[173] **Arcibar-Orozco, J. A., Rangel-Mendez, J. R. & Bandosz, T. J.** (2013). Desulfurization of Model Diesel Fuel on Activated Carbon Modified with Iron Oxyhydroxide Nanoparticles: Effect of tert-Butylbenzene and Naphthalene Concentrations. *Energy & Fuels, 27 (9),* 5380-5387.

[174] **Wang, L., Sun, B., Yang, F. H. & Yang, R. T.** (2012). Effects of aromatics on desulfurization of liquid fuel by π-complexation and carbon adsorbents. *Chemical Engineering Science, 73,* 208-217.

[175] **Aslam, S., Subhan, F., Yan, Z., Etim, U. J. & Zeng, J.** (2017). Dispersion of nickel nanoparticles in the cages of metal-organic framework: An efficient sorbent for adsorptive removal of thiophene. *Chemical Engineering Journal, 315,* 469-480.

[176] **Dai, W., Hu, J., Zhou, L., Li, S., Hu, X. & Huang, H.** (2013). Removal of Dibenzothiophene with Composite Adsorbent MOF-5/Cu(I). *Energy & Fuels, 27 (2),* 816-821.

[177] **Song, H., Gao, H., Song, H., Yang, G. & Li, X.** (2016). Effects of Si/Al Ratio on Adsorptive Removal of Thiophene and Benzothiophene over Ion-Exchanged AgCeY Zeolites. *Industrial & Engineering Chemistry Research, 55 (13),* 3813-3822.

[178] **Girardon, P.** (2019). Propellant Gases for Aerosols Containers, in: Cachon, R., Girardon, P., Voilley, A. (Eds.), *Gases in Agro-Food Processes* (pp. 479-482).

[179] **Malaibari, Z.O., Amin, A., Croiset, E. & Epling, W.** (2014). Performance characteristics of Mo-Ni/Al_2O_3 catalysts in LPG oxidative steam reforming for hydrogen production. *International Journal of Hydrogen Energy, 39,* 10061-10073.

[180] **Yi, Z., Ma, X., Song, J., Yang, X. & Tang, Q.** (2019). Investigations in enhancement biodesulfurization of model compounds by ultrasound pre-oxidation. *Ultrasonics Sonochemistry, 54,* 110-120.

[181] **Kühl, G. H.** (1999). Modification of Zeolites, in: Weitkamp J., Puppe L. (Eds.) *Catalysis and Zeolites* (pp. 81-197).

[182] **Hattori, H. & Ono, Y.** (2018). Catalysts and catalysis for acid-base reactions, in: *Metal Oxides in Heterogeneous Catalysis* (pp. 133-209).

[183] **Kinraide, T.B. & Yermiyahu, U.** (2007). A scale of metal ion binding strengths correlating with ionic charge, Pauling electronegativity, toxicity, and other physiological effects. *Journal of Inorganic Biochemistry, 101,* 1201-1213.

[184] **Sdiri, A., Higashi, T., Chaabouni, R. & Jamoussi, F.** (2012). Competitive removal of heavy metals from aqueous solutions by montmorillonitic and calcareous clays. *Water, Air and Soil Pollution,. 223,* 1191-1204.

[185] **Treacy, M. M. J. & Higgins, J. B.** (2001). *Collection of Simulated XRD Powder Patterns for Zeolites,* fourth revised edition, Elsevier.

[186] **Zholobenko, V., Freitas, C., Jendrlin, M., Bazin, P., Travert, A. & Thibault-Starzyk, F.** (2020). Probing the acid sites of zeolites with pyridine: Quantitative AGIR measurements of the molar absorption coefficients. *Journal of Catalysis, 385,* 52-60.

[187] **Verdoliva, V., Saviano, M. & Luca, S. D.** (2019). Zeolites as Acid/Basic Solid Catalysts: Recent Synthetic Developments. *Catalysts, 9,* 248.

[188] **Emeis, C. A.** (1993). Determination of Integrated Molar Extinction Coefficients for Infrared Absorption Bands of Pyridine Adsorbed on Solid Acid Catalysts. *Journal of Catalysis, 141,* 347-354.

[189] **Minkin, V.I.** (1999). Glossary of terms used in theoretical organic chemistry. *Pure and Applied Chemistry, 71,* 1919-1981.

[190] **Ng, F.T.T., Rahman, A., Ohasi, T. & Jiang, M.** (2005). A study of the adsorption of thiophenic sulfur compounds using flow calorimetry. *Applied Catalysis B: Environmental, 56,* 127-136.

[191] **Rashidi, S., Nikou, M. R. K. & Anvaripour, B.** (2015). Adsorptive desulfurization and denitrogenation of model fuel using HPW and NiO-HPW modified aluminosilicate mesostructures. *Microporous and Mesoporous Materials, 211,* 134-141.

[192] **Nejad, N. F., Shams, E., Amini, M. K. & Bennett, J. C.** (2013). Ordered mesoporous carbon CMK-5 as a potential sorbent for fuel desulfurization: Application to the removal of dibenzothiophene and comparison with CMK-3. *Microporous and Mesoporous Materials, 168,* 239-246.

[193] **Fallah, R. N., Azizian, S., Reggers, G., Carleer, R., Schreurs, S., Ahenach, J., Meynen, V. & Yperman, J.** (2014). Effect of aromatics on the adsorption of thiophenic sulfur compounds from model diesel fuel by activated carbon cloth. *Fuel Processing Technology, 119,* 278-285.

[194] **Garcia, C. L. & Lercher, J. A.** (1992). Adsorption and surface reactions of thiophene on ZSM 5 zeolites. *Journal of Physical Chemistry, 96,* 2669-2675.

[195] **Wang, H., Song, L. Jiang, H. Xu, J., Jin, L., Zhang, X. & Sun, Z.** (2009). Effects of olefin on adsorptive desulfurization of gasoline over Ce(IV)Y zeolites. *Fuel Processing Technology, 90,* 835-838.

[196] **Velu, S., Song, C., Engelhard, M. H. & Chin, Y.-H.** (2005). Adsorptive Removal of Organic Sulfur Compounds from Jet Fuel over K-Exchanged NiY Zeolites Prepared by Impregnation and Ion Exchange. *Industrial and Engineering Chemistry Research, 44 (15),* 5740-5749.

[197] **Bulut, B., Isbilen, E., Atakül, H. & Tantekin-Ersolmaz, S. B.** (2022). Adsorptive removal of dimethyl disulfide and thiophene from liquefied petroleum gas by zeolite-based adsorbents. *Microporous and Mesoporous Materials, 337,* 111924.

[198] **Yang, R. T.** (2003). *Adsorbents: Fundamentals and Applications*. John Wiley & Sons, Inc., ISBN 0-471-29741-0.

[199] **Gaudin, P., Fioux, P., Dorge, S., Nouali, H., Vierling, M., Fiani, E., Molière, M., Brilhac, J.-F. & Patarin, J.** (2016). Formation and role of Cu^{+} species on highly dispersed CuO/SBA-15 mesoporous materials for SOx removal: An XPS study. *Fuel Processing Technology, 153,* 129-136.

[200] **Iwamoto, M., Yahiro, H. Tanda, K. Mizuno, N. Mine, Y. & Kagawa, S.** (1991). Removal of Nitrogen Monoxide through a Novel Catalytic Process: 1. Decomposition on Excessively Copper Ion-Exchanged ZSM-5 Zeolites. *Journal of Physical Chemistry, 95,* 3727-3730.

[201] **Sarkany, J., Ditri, J. L. & Sachtler, W. M. H.** (1992). Redox Chemistry in Excessively Ion-Exchanged Cu/Na-ZSM-5. *Catalysis Letters, 16,* 241.

[202] **Valyon, J., & Hall, W. K.** (1993). Effects of Reduction and Reoxidation on the Infrared-Spectra from Cu-Y and Cu-ZSM-5 Zeolites. *Journal of Physical Chemistry, 97,* 7054.

[203] **Larsen, S. C., Aylor, A., Bell, A. T. & Reimer, J. A.** (1994). Electron Paramagnetic Resonance Studies of Copper Ion-Exchanged ZSM-5. *Journal of Physical Chemistry, 98,* 11533.

[204] **Takahashi, A., Yang, R. T., Munson, C. L. & Chinn, D.** (2001). Cu(I)-Y-Zeolite as a Superior Adsorbent for Diene/Olefin Separation. *Langmuir, 17,* 8405.

[205] **Hernández-Maldonado, A. J. & Yang, R. T.** (2004). New Sorbents for Desulfurization of Diesel Fuels via-Complexation. *American Institute of Chemical Engineers, 50,* 791-801.

[206] **Amano, F., Tanaka, T. & Funabiki, T.** (2004). Auto-reduction of Cu(II) species supported on Al_2O_3 to Cu(I) by thermovacuum treatment. *Journal of Molecular Catalysis A: Chemical, 221,* 89-95.

[207] **Liu, L., Luo, X.-B., Ding, L. & Luo, S.-L.** (2019). Application of Nanotechnology in the Removal of Heavy Metal from Water, in: *Nanomaterials for the Removal of Pollutants and Resource Reutilization,* pp. 83-147.

[208] **Montazerolghaem, M., Rahimi, A. & Seyedeyn-Azad, F.** (2010). Equilibrium and kinetic modeling of adsorptive sulfur removal from gasoline by synthesized Ce–Y zeolite. *Applied Surface Science, 257,* 603-609.

[209] **Liao, J., Wang, W., Xie, Y., Zhang, Y., Chang, L. & Bao, W.** (2012). Adsorptive removal of thiophene from benzene by NaY zeolite ion-exchanged with Ce(IV). *Separation Science and Technology, 47,* 1880-1885.

[210] **Andrew, C. R., Yeom, H., Valentine, J. S., Karlsson, B. G., Bonander, N., Pouderoyen, G., Canters, G. W., Loehr, T. M. & Loeh, J. S.** (1994). Raman Spectroscopy as an Indicator of Cu-S Bond Length in Type 1 and Type 2 Copper Cysteinate Proteins. *Journal of the American Chemical Society, 116,* 11489-11498.

[211] **Magdaline, J. D. & Chithambarathanu, T.** (2015). Vibrational Spectra (FT-IR, FT-Raman), NBO and HOMO, LUMO Studies of 2-Thiophene Carboxylic Acid Based on Density Functional Method. *IOSR Journal of Applied Chemistry, 8,* 06-14.

CURRICULUM VITAE

Name Surname **:** Betül BULUT

EDUCATION:

- **Ph.D.** **:** Istanbul Technical University (2013-)
  Material Science and Engineering
- **M.Sc.** **:** Istanbul Technical University (2011-2013)
  Chemical Engineering
- **B.Sc.** **:** Hacettepe University (2005-2010)
  Chemical Engineering

PROFESSIONAL EXPERIENCE:

- **AYGAZ A.Ş.** (2018-)
  R&D Specialist
- **Ak-Kim Kimya** (2014-2017)
  R&D Researcher
- **Arçelik A.Ş.** (2012-2013)
  R&D Engineer

PUBLICATIONS, PRESENTATIONS AND PATENTS ON THE THESIS:

- **Bulut, B.,** Isbilen, E., Atakül, H. & Tantekin-Ersolmaz, S. B. (2022). Adsorptive removal of dimethyl disulfide and thiophene from liquefied petroleum gas by zeolite-based adsorbents. *Microporous and Mesoporous Materials, 337,* 111924.
- **Bulut, B.,** Atakül, H., Aksoylu, A. E. & Tantekin-Ersolmaz, S. B., Deep Adsorptive Desulfurization of Liquefied Petroleum Gas Over Cu Ion-Exchanged Y Zeolite. (in preparation)
- **Bulut, B.,** Atakül, H., Aksoylu, A. E. & Tantekin-Ersolmaz, S. B., Modification of Zeolite Y for Adsorptive Desulfurization of Liquefied Petroleum Gas. (in preparation)

- **Bulut, B.,** Velioğlu, S., Atakül, H., & Tantekin-Ersolmaz, S. B., Review: A Materials Roadmap for Adsorptive Desulfurization of Liquified Petroleum Gas. (in preparation)
- **Bulut, B.,** Atakül, H., & Tantekin-Ersolmaz, S. B. (2020). Development of Modified Zeolite Based Adsorbents for High-Performance Desulfurization, 5th Global Conference On Material Sciences, Istanbul, Turkey. (Oral Presentation)

OTHER PUBLICATIONS, PRESENTATIONS AND PATENTS:

- **Bulut, B.** (2016). Removal of Hardness Ions by Nanofiltration and Reverse Osmosis, 16th Aachener Membran Kolloquium (AMK), Aachen, Germany. (Poster Presentation)
- Kasap, F. & **Bulut, B.** (2014). *Patent, WO2014180691 (A1).* A Washing Machine Comprising A Filtration Unit.
- Kasap, F., **Bulut, B.,** Efe, S. & Erdem, İ. (2014). *Patent, WO2014101959 (A1*). A Washing Machine Having An Improved Nanofiltration System And Method Thereof.
- **Bulut, B.,** Kasap, F., Tantekin-Ersolmaz, B. (2013). Removal of Hardness Ions by Nanofiltration and Reverse Osmosis for Water Softening, International Conference on Environmental Science and Technology (ICOEST), Cappadocia, Turkey. (Oral Presentation)